Enhancing the Spontaneous Imbibition Process in Naturally Fractured Reservoirs through Wettability Alteration Using Surfactants: Mechanistic Study and Feasibility of Using Biosurfactants Produced from Agriculture Waste Streams

By

Mehdi Salehi

Submitted to the graduate degree program in Chemical & Petroleum Engineering and the Graduate Faculty of the University of Kansas School of Engineering in partial fulfillment of the requirements for the degree of Doctor of Philosophy.

Committee members

_____
Jenn-Tai Liang
(Chairperson)

_____
D. W. Green

_____
G. P. Willhite

_____
C. S. McCool

_____
C. D. McElwee

_____
S. J. Johnson

Date defended: _____

The Dissertation Committee for Mehdi Salehi certifies

that this is the approved version of the following dissertation:

Enhancing the Spontaneous Imbibition Process in Naturally Fractured Reservoirs through Wettability Alteration Using Surfactants: Mechanistic Study and Feasibility of Using Biosurfactants Produced from Agriculture Waste Streams

Committee:

_____
Jenn-Tai Liang
(Chairperson)

_____
D. W. Green

_____
G. P. Willhite

_____
C. S. McCool

_____
C. D. McElwee

_____
S. J. Johnson

Date approved: _____

Abstract

Naturally fractured reservoirs are characterized by having low-permeability matrix blocks surrounded with fractures of high hydraulic conductivity. Waterflooding process in such reservoirs is successful if the matrix blocks holding the dominant fraction of the reservoir porosity are able to imbibe the injected water (water-wet) and expel the oil into the fracture system and finally to the production well. This mechanism referred to as spontaneous imbibition of water into the matrix blocks is an efficient method to increase oil recovery from fractured reservoirs. However, most naturally fractured reservoir rocks are mixed- to oil-wet and do not imbibe the injected water, which translates into low-efficiency waterflood recovery. To enhance the spontaneous imbibition process, low concentration of surfactants is dissolved into the injected water to induce wettability alteration of the reservoir rock by changing the wettability of the rock toward a more water-wet state. This is the main subject of this research study. The first part of this study was devoted to evaluating and comparing the effectiveness of using a biosurfactant (surfactin) produced from agriculture waste streams against a benchmark chemical surfactant in mediating the wettability of oil-wet rocks. The ability of surfactants to enhance the spontaneous imbibition process in cleaned and crude oil-aged reservoir core plugs was tested. One of the other factors that needs to be considered is the estimation of the loss of surfactants due to adsorption onto the reservoir rock, because for the process to be effective, the injected surfactant solution should be able to penetrate deep into the

reservoir. So, in this work, static and dynamic adsorption isotherms for both biosurfactant and benchmark chemical surfactants on crushed reservoir rocks and reservoir core plugs were generated and compared. The second part of the study focused on the mechanistic study of wettability alteration by surfactants. There are two main mechanisms proposed for the wettability alteration process, but none have been verified. This study is focused on investigating the wettability alteration mechanisms though experimental observations. The results of the work will provide better guidelines in designing and improving water flood performance in naturally fractured reservoirs. It was verified that wettability alteration is caused by either surfactant adsorption or the ion-pair formation between the surfactant monomer and the material adsorbed on the reservoir rock from exposure to crude oil. It was further demonstrated that the ion-pair process can be improved by increasing the charge density of the head-group in the surfactant molecule.

Acknowledgments

First of all, I want to express my sincere gratitude to my advisor Dr. Jenn-Tai Liang for his invaluable guidance, counsel and support throughout my research.

I am particularly indebted to Dr. Stephen J. Johnson for his insightful comments and criticisms on my weekly reports. I learned a lot from him. He provided comments on my writing, and I gratefully acknowledge that.

I would also like to extend my appreciation to Dr. G. Paul Willhite, Dr. Don W. Green, and Dr. Carl D. McElwee, and Dr. C. Stanley McCool for serving on my dissertation committee.

I greatly appreciate Mr. Alan Byrnes from Kansas Geological Survey for providing the reservoir core materials used in this work. Mr. Greg Bala and Ms. Sandra Fox from Idaho National Lab are greatly appreciated for providing surfactin samples. Special thanks go to Mr. Jim Pilch and Mr. Scott Ramskill for their assistance in construction and operating laboratory equipment and procuring supplies. I would also like to thank Dr. Mike Michnick for his suggestions. Help from Ms. Maxine Younes and Ms. Mayumi Crider are also appreciated. I also thank all the other TORP staff members and my fellow students for their help and friendship.

I appreciate the financial support provided by the US Department of Energy and the Tertiary Oil Recovery Project, University of Kansas.

Finally, I would like to express my deepest gratitude to my wife, for her faith, love, understanding and support.

Table of Content

List of Figures

List of Tables

Symbols and Abbreviations

Symbols

σ: IFT (mN/m)

σ_{OS} : Oil-solid IFT (N/m)

σ_{OW} : Oil-water IFT (N/m)

σ_{WS} : Water-solid IFT (N/m)

θ : contact angle (degree)

Γ: amount adsorbed (mg/g)

Γ_{max} : maximum amount adsorbed (monolayer adsorption)

λ : dispersion coefficient

ϕ : porosity

ρ_r : porous medium density

μ: viscosity (cp)

ρ: density of fluid saturating the core, g/cm^3

a_λ: wavelength-dependent absorptivity coefficient

ΔH_A: characteristic heat of adsorption

ΔH_L: heat of condensation of the vapor in system

$\Delta\rho$: density difference between the two immiscible phases (g/cm^3)

ΔP: pressure drop (atm)

Abbreviations

A: area per molecule of the adsorbed gas

A : cross sectional area

A_w: area under the secondary water drainage curve

A_o: area under the imbibition curve falling below the zero-P_c axis

A_s: specific surface area

$a = bC_r^*$: constant in Langmuir equation (ml/mg)

$b = \frac{K_1}{K_2}$: constant in Langmuir equation (ml/mg)

C : surfactant concentration (mg/ml)

c: constant in Eq. 2.12

C_r : amount adsorbed surfactant per gram of solid (mg/g)

C_r^* : maximum equilibrium adsorption of surfactant per gram of solid (mg/g)

C_i^α : concentration of component *i* in phase α

C_i^β : concentration of component *i* in phase β

C_B: normalized tracer concentration

C_B^*: measured tracer concentration

C_{Bi}: injected or maximum tracer concentration

C_{B0}: initial concentration of fluid B in the system

C: ring circumference (cm)

C_i: initial surfactant concentration (mg/l)

C_f: final (residual) surfactant concentration (mg/l)

C_s: concentration of surfactant (mmol/l)

C: constant related to the pore geometry (*C*=0.4 for cylindrical capillaries)

c: analyte concentration

C_h: concentration of hyamine (mmol/l)

D : diffusion coefficient

d_v: dead volume

D: density of the lower phase (g/cm^3)

D: density of the upper phase (g/cm^3)

g: gravitational acceleration (cm/s^2)

h: length of the core (cm)

I_w: water wettability index

I_o: oil wettability index

$I_{A\text{-}H}$: Amott-Harvey index

k_H, and k_F: constants in units of L/m^2

k_L: Langmuir constant

K_1: kinetic constant for adsorption (ml/g.hr)

K_2: kinetic constant for desorption (ml/g.hr)

k_1 and k_2: kinetic constants k_1 and k_2

K: permeability (Darcies)

L: length (cm)

L: circumference of the ring (cm)

M: mass of weight used (g)

M_s: mass of surfactant solution (mg)

M_R: mass of crushed rock (g)

M_v: molar volume of gas, 22.4 L at standard temperature and pressure (STP)

m_1 and m_2: monolayer coverage

N_a: Avogadro's number

n_i: total amount of component *i* in solution

n_i^σ: surface excess amount of component *i*

P: partial pressure of the adsorbate

p_o: saturation vapor pressure of the adsorbate

PV: pore volume, cm^3

P: dial reading for apparent surface tension

q: flow rate (cm^3/s)

R: radius of the ring (cm)

r: radius of the wire (cm)

S: apparent IFT (dynes/cm)

S: selectivity

S_{iw}: initial water saturation

S_{ws}: water saturation after spontaneous imbibition of aqueous phase

S_{wf}: water saturation after forced imbibition of aqueous phase

S_{or}: residual oil saturation

S_{os}: oil saturation after spontaneous imbibition of oil phase

S_{of} : oil saturation after forced imbibition of oil phase

t : time

t_{50}: time normalized concentration equals 0.5

t_o: time tracer begun

t_{eq}: time equal area reached

V: volume of adsorbed vapor at standard temperature and pressure

V_α: volumes of phase α

V_β: volumes of phase β

V_m: monolayer capacity at standard temperature and pressure

V_m: monolayer capacity

V_s: volume of surfactant (ml)

V_h: volume of hyamine 1622 (ml) at the inflection point

W_s: saturated core weight

W_d: dry core weight

1 Introduction

Most of the world's oil reservoirs are found in carbonate rocks, many of which contain fractures with high hydraulic conductivity surrounding low-permeability matrix blocks. Evaluation of the wetting state for different reservoirs from all over the world indicates that most carbonate reservoirs seem to be mixed to oil-wet (Treiber, Archer et al. 1972; Chilingar and Yen 1983; Roehl and Choquette 1985; Allan and Sun 2003). After the primary production period, waterflooding is usually performed to recover more oil from reservoirs. However, waterflooding recoveries are low from naturally fractured carbonate reservoirs, due in part to these reservoirs being mixed to oil-wet. In such reservoirs, production depends on spontaneous imbibition of water to expel the oil from the matrix into the fracture system, but this is only efficient when the matrix blocks are water-wet. Wettability is an important parameter controlling the capillary pressure (Parsons and Chaney 1966; Zhou, Torsaeter et al. 1993), which is in turn the driving force for the spontaneous imbibition process. The imbibition process is also affected by many other factors including matrix permeability (Mattax and Kyte 1962), size and shape (Cuiec, Bourbiaux et al. 1994; Zhang, Morrow et al. 1995; Ma, Morrow et al. 1997), heterogeneity (Parsons and Chaney 1966; Torsaeter 1984), and boundary conditions (Bourbiaux and Kalaydjian 1990; Cuiec, Bourbiaux et al. 1994). Fluid properties such as viscosities of the phases and interfacial tensions (IFT) also play a role in capillary imbibition recovery rate (Schechter, Zhou et al. 1991; Babadagli 2000).

Naturally fractured reservoirs are good candidates for enhanced oil recovery (EOR) processes since the matrix part of the reservoir may contain a large amount of oil. Chemical EOR methods such as surfactant flooding are used to improve the recovery from reservoirs. Surfactants can act in several ways to enhance the oil production: lowering the IFT between residual oil and injected water, changing the wettability of the surface, forming emulsions, etc. To enhance the spontaneous imbibition process in fractured reservoirs, surfactants are used as wettability alteration agents to modify the wettability of the reservoir rock. Several mechanisms are proposed in the literature for wettability alteration using surfactants, but none have been verified experimentally. Knowledge of the mechanisms behind wettability alteration could help to improve the performance of the process and also aid in identification of alternative surfactants for use in field applications.

This research study can be divided into two parts. The first part was devoted to evaluating and comparing the effectiveness of using a biosurfactant (surfactin) produced from agriculture waste streams against a benchmark chemical surfactant in mediating the wettability of oil-wet rocks. The ability of surfactants to enhance the spontaneous imbibition process in cleaned and crude oil-aged reservoir core plugs was tested. One of the other factors that needs to be considered is the estimation of the loss of surfactants due to adsorption onto the reservoir rock, because for the process to be effective, the injected surfactant solution should be able to penetrate deep into the reservoir. So, in this work, static and dynamic adsorption isotherms for both biosurfactant and benchmark chemical surfactants on crushed reservoir rocks

and reservoir core plugs were generated and compared. The second part of the work investigated the proposed mechanisms for wettability alteration experimentally. In this part, the proposed mechanisms were tested experimentally through observations of surfactant adsorption isotherms and Amott-Harvey wettability indices in oil-wet synthetic and crude oil-aged sandstone core plugs. The following chapter presents the available background related to this research. Chapter 3 introduces the experimental materials, equipments and procedures used. In Chapter 4 experimental results are presented and discussed. Chapter 5 lists the conclusions drawn from this study.

2 Background and Literature Review

This chapter reviews the literature related to the study of surfactant systems and the wettability alteration mechanisms. First a general introduction to wettability is given, followed by a review of the development of oil-wetness on reservoir rocks. Surfactants and their properties, and methods of measuring their adsorption are introduced in the next section. Finally the proposed mechanisms for wettability alteration using surfactants are discussed in last section.

2.1 Background

Historically, oil production from oil reservoirs has been divided into three phases. Initially, oil is produced by the native energy of the reservoir (such as the dissolved gas drive, or the natural water-drive aquifer) and this period is called primary production. Primary production results in 5-30 % OOIP recovery (Farouq-Ali and Stahl 1970). As the reservoir loses its energy, a fluid needs to be injected into the reservoir to keep its energy and extend its lifetime. Since water is the cheapest fluid available, waterflooding is used to increase the oil production beyond that of primary production and this stage is called secondary production. The water pushes the oil in front of it toward the production wells and helps to increase the total recovery to 40-60 % OOIP. The process continues until the water-oil ratio at the production wells becomes very high and reaches the economic level where the oil production is not cost-effective anymore. At this stage there is a significant amount of oil (40-60 % OOIP) still left in the reservoir due to many factors including unfavorable wettability

conditions, heterogeneity of reservoir rock (existence of high permeability zones, fractures, vugs, and impermeable layers) and capillary-trapped oil. In order to recover this residual oil and increase the ultimate oil recovery of the reservoir, Enhanced Oil Recovery (EOR) methods are utilized. Since these methods often follow the secondary production, they are sometimes called tertiary oil recovery methods. The EOR processes can be divided into three main categories (Marle 1991): chemical, miscible, and thermal methods. The processes are intended to either increase the sweep efficiency of the injected fluid (macroscopic) by contacting the untouched areas of the reservoir or increase the displacement efficiency at the pore level (microscopic) in areas previously swept by water and decrease the residual oil saturation.

In chemical EOR methods, an agent that is not normally present in the reservoir is injected to enhance the oil displacement. Examples of the chemical processes are gel-polymer and polymer flooding aimed to shut-off the high-permeability areas of the reservoir (Seright and Liang 1994; Sydansk and Southwell 1998), and to increase the viscosity of the injected water to increase the sweep areas in the reservoir (Chauveteau and Sorbie 1991) , and alkaline and surfactant flooding to create low oil-water interfacial tension (IFT) and hence remobilizing the trapped oil (Foster 1973; Adams and Schievelbein 1987; Olsen, Hicks et al. 1990; Austad, Matre et al. 1998; Ashayer, Grattoni et al. 2000; Chen, Lucas et al. 2000). It is also possible to enhance the oil production through wettability alteration of the reservoir rock during a surfactant flooding and this is the main subject of this work (See Section 2.6)

(Wagner and Leach 1959; Austad and Milter 1997; Austad, Matre et al. 1998; Chen, Lucas et al. 2000; Spinler, Zornes et al. 2000B).

Fractured carbonate reservoirs are a class of reservoirs characterized by high conductivity fractures surrounding low permeability matrix blocks. In these reservoirs, the production relies on the suction of the injected water by the matrix blocks which expel the oil toward the fracture network and thence to the production wells. This capillary suction of water by matrix and expelling the oil simultaneously is a mechanism called spontaneous imbibition of water. Water will imbibe into the matrix blocks if the reservoir rock is water-wet. However, the results of two comprehensive studies (Treiber, Archer et al. 1972; Chilingar and Yen 1983) show that most carbonate reservoir are mixed- to oil-wet. As a result, the recovery from waterflooding of fractured carbonate reservoirs is low. To make the process more effective, dilute solutions of surfactants have been dissolved in the injected water and injected into the reservoir with the aim of changing the wettability of the reservoirs to a more water-wet state hence enhancing the spontaneous imbibition process and higher oil recovery. It should be noted that in this study the purpose of the surfactant flooding is not to create ultra-low IFT values, but to induce wettability alteration.

2.2 Wettability

Wettability is one the most important parameters affecting the fluid distribution in reservoirs and has a strong influence on the spontaneous imbibition process (Morrow

1990). Its definition, methods of measurement, its effect on fluids distribution, waterflooding performance, and capillary pressure are summarized in this section.

2.2.1 Definition

Wettability is defined as "the tendency of one fluid to spread on, or adhere to a solid surface in the presence of other immiscible fluids" (Anderson 1986a). The fluid with the higher affinity toward the solid surface is called the wetting phase, the other fluid is called non-wetting. Wettability is a very important concept in oil recovery processes and has a strong impact on distribution, location and flow of oil and water in reservoir during production (Anderson 1986b; Anderson 1987a; Anderson 1987b; Anderson 1987c; Morrow 1990; Cuiec 1991). In a water-wet system, water will occupy the narrowest pores and will be present as a film on the pores wall while oil will reside as oil droplets in the middle of the pores. The reverse fluid distribution will exist in the case of an oil-wet reservoir (See **Figure 2-1**)

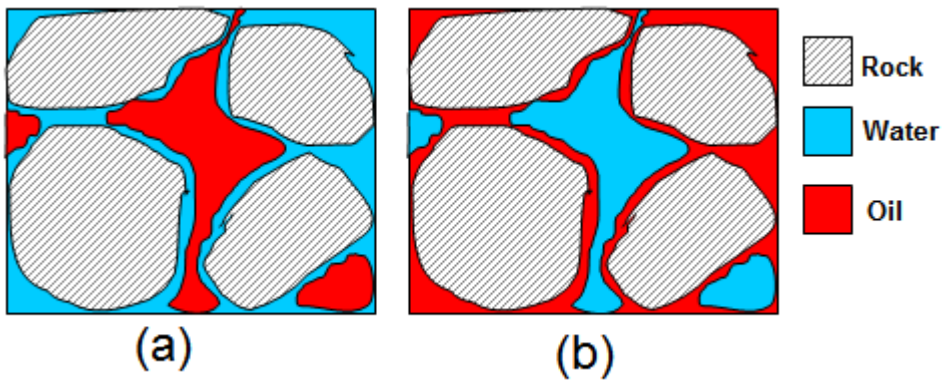

Figure 2-1 Fluid distribution in (a) water-wet and (b) oil-wet rock

A core sample which imbibes only water spontaneously is said to be water-wet; one that imbibes oil spontaneously is called oil-wet. Samples imbibing neither water nor oil are said to be neutral wet. It is also recognized that wettability of porous rocks may not necessarily be uniform. Local chemical heterogeneities in the mineral composition and complexities of the pore system can generate non-uniform wettability. Fractional wettability is characterized by isolated areas being water and oil-wet. Mixed-wettability is a special type of fractional wettability where water and oil-wet areas are assumed to be inter-connected (Salathiel 1973). When performing waterflood in water-wet porous media, the injected water will tend to flow close to the walls of porous media while pushing the oil in to the larger pores and in to the middle of the pore space. Oil will be trapped by snap-off, where water films over the pore walls grow and reach to each other. Most of the mobile oil will be produced by the time the water front reaches the production well and after breakthrough little more oil will be produced (**Figure 2-2**.A). The production profile looks very sharp. Waterflooding an oil-wet reservoir will result in the water occupying the center of the pore space and oil will continue to produce even after water breakthrough from the oil film on the pores wall. The production profile will have a long tail in this case. These situations are shown in **Figure 2-2**.

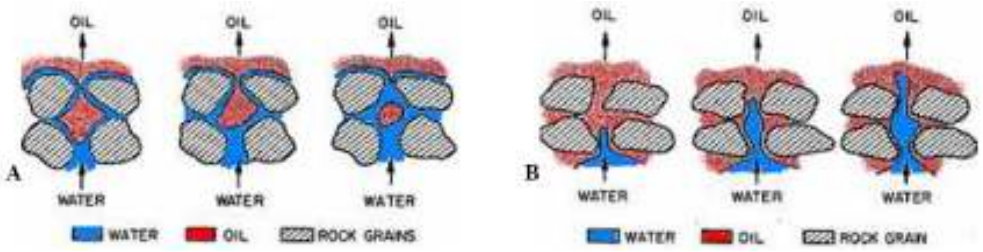

Figure 2-2 Wettability effect on waterflooding (A) water-wet porous media (B) oil-wet porous media (Anderson 1987b)

Wettability also affects the capillary pressure curves. In a water-wet core plug, because of existence of high positive capillary pressure, oil is produced as soon as the core is exposed to water and production will stop when the capillary pressure reaches zero. As was mentioned previously, little more oil is produced by flooding the core with water. The capillary pressure curve looks like curve A in **Figure 2-3**. In the case of an oil-wet core, the capillary pressure is very close to zero or negative and most oil is produced by forced imbibition of water. Not much oil is expected to produce by water spontaneous imbibition. The expected capillary pressure curve is shown in **Figure 2-3** as curve B. A mixed-wet core has the same tendency for both oil and water phases and the capillary curve looks like the curve C in **Figure 2-3**.

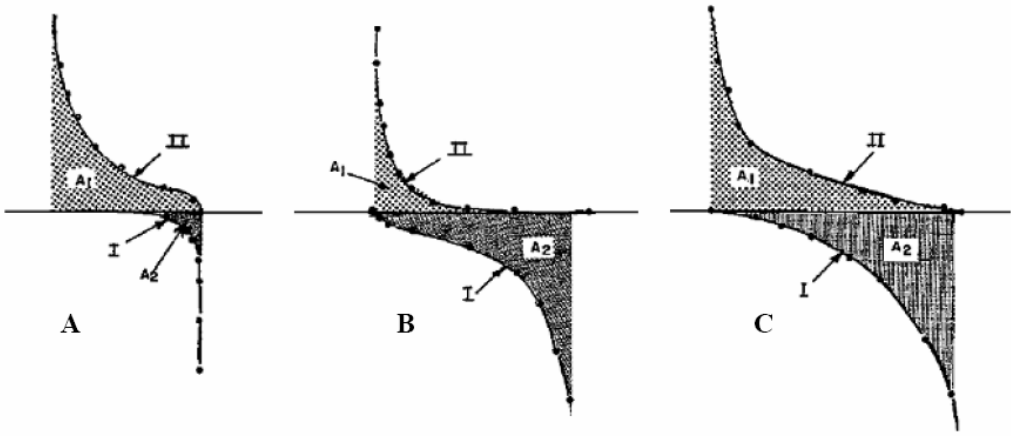

Figure 2-3 Wettability effect on capillary pressure curve: (A) Water-wet core (B) Oil-wet core (C) Mixed-wet core (Morrow 1976)

2.2.2 Measurement

The wettability of a reservoir is not a simply defined property and quantifying the wettability is not an easy task. Various procedures for measuring the wettability have been proposed, both quantitative and qualitative. Contact angle is the most universal measure of the wettability of flat surfaces (Morrow 1991). The most common methods of quantifying the wettability of porous media are the modified Amott test and the USBM test. Both rely on the rock/brine/oil displacement behavior. Each method depends on water saturation measurements and related capillary pressure of flow conditions to define a wettability scale. The wettability of the rock can be also assessed qualitatively by rate of spontaneous imbibition of water and the amount of water imbibed.

2.2.2.1 Contact Angle

Contact angle is the most universal measure of the wettability of flat surfaces. For a system consisting of two pure immiscible fluids placed on a smooth homogeneous

solid surface (**Figure 2-4**) there exists an angle θ called "contact angle" which can be described by Young's equation (Young 1805). It can be regarded as a mechanical force balance for the interfacial/surface tensions involved (Morrow 1970).

$$\sigma_{OS} = \sigma_{WS} + \sigma_{OW}.\cos\theta \qquad (2.1)$$

where

σ_{OS} : Oil-solid IFT (N/m)

σ_{OW} : Oil-water IFT (N/m)

σ_{WS} : Water-solid IFT (N/m)

θ: contact angle (degree)

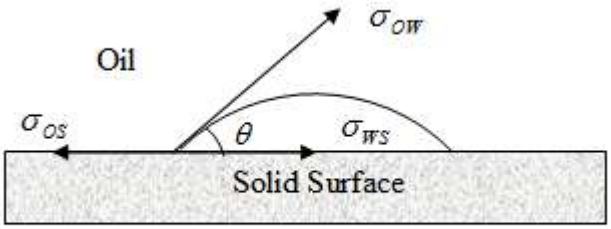

Figure 2-4 Contact angle and its relation to interfacial tensions (water drop on a water-wet surface)

θ is measured through the water phase and can change from 0 to 180°. A value below 90° indicates a water-wet surface with higher affinity for water than oil. If the contact angle value is greater than 90°, the surface has a higher affinity toward the oil phase and is oil-wet. In the case where the surface shows a same affinity for both phases, the surface is called neutral-wet and the angle is close to 90°. There are some drawbacks when quantifying the wettability of porous media. Since contact angle is

measured on a flat surface, it cannot be measured on porous media. Representing the carbonate rock by calcite plates with the same mineral composition and using glass surfaces to represent sandstone rock solved the issue (Wagner and Leach 1959; Morrow 1990; Sharma 1995). However, parameters such as surface roughness, heterogeneity of mineral and pore structure are not taken into account.

2.2.2.2 Amott –Harvey Test

The Amott-Harvey test (Anderson 1986b) is an extension of the wettability test introduced by Amott (Amott 1959). In the Amott-Harvey test, the core sample is first brought to S_{iw} by oil displacement of water by centrifuge or by use of a high flowing pressure gradient. The time and the pressure level to reach to S_{iw} are somewhat arbitrary. The core at S_{iw} is then immersed in water to allow the spontaneous imbibition of water. After the spontaneous imbibition of water ceases at a S_{ws} saturation, further oil is recovered by forced displacement through flowing water at a high pressure gradient or centrifuge to a final water saturation of S_{wf}. An advantage of this method is that both reservoir cores and fluids can be used in the determination of wettability.

This method, after establishing the initial water saturation (S_{iw}) consists of the following steps (**Figure 2-5**):

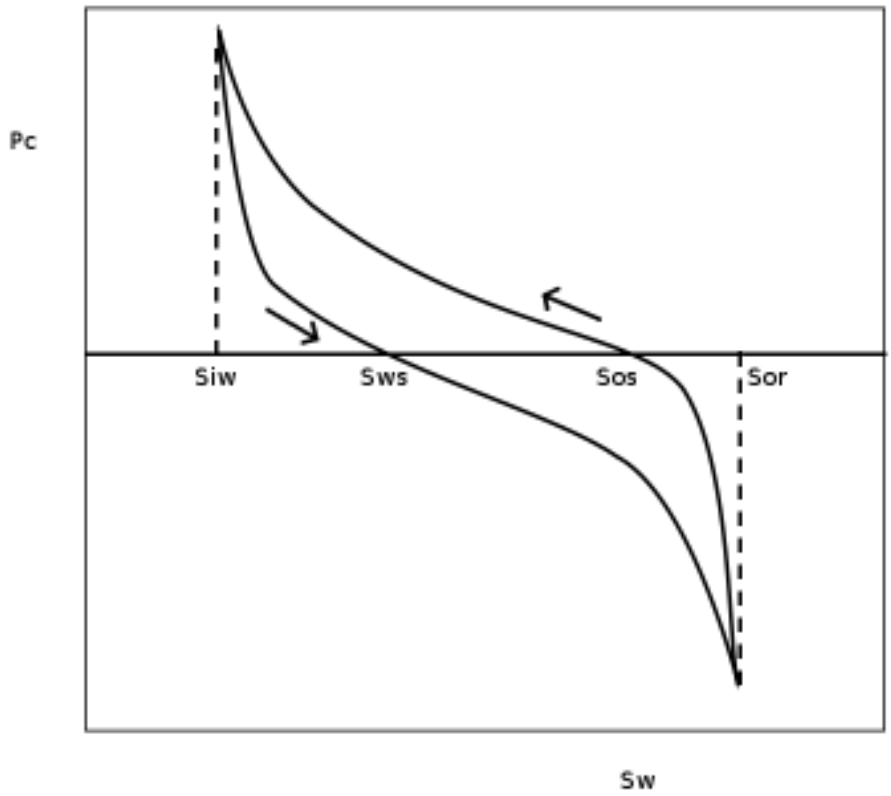

Figure 2-5 Capillary pressure curve illustrating the steps needed in calculating the I_{A-H} wettability index (Standnes 2001)

1. Spontaneous imbibition of water to reach S_{ws}
2. Flooding the core with water (forced imbibition) to reach residual oil saturation S_{or}
3. Spontaneous imbibition of oil to reach S_{os}
4. Flooding the core with oil to reach initial water saturation, S_{iw}

The water wettability index, I_w, The oil wettability index, I_o, and the relative displacement index (Amott-Harvey) I_{A-H} can then be defined as:

$$I_w = \frac{S_{ws} - S_{iw}}{S_{wf} - S_{iw}} \qquad (2.2)$$

$$I_o = \frac{S_{os} - S_{or}}{S_{of} - S_{or}} \qquad (2.3)$$

$$I_{A-H} = I_W - I_O \qquad (2.4)$$

where:

S_{iw} = initial water saturation

S_{ws} = water saturation after spontaneous imbibition of aqueous phase

S_{wf} = water saturation after forced imbibition of aqueous phase

S_{or} = residual oil saturation

S_{os} = oil saturation after spontaneous imbibition of oil phase

S_{of} = oil saturation after forced imbibition of oil phase

I_{A-H} varies between +1 for strongly water-wet systems and -1 for strongly oil-wet systems. Cuiec (Cuiec 1984) considers a system as water-wet when $+0.3 \le I_{A-H} \le +1$, intermediate for $-0.3 \le I_{A-H} \le +0.3$, and oil-wet for $-1 \le I_{A-H} \le -0.3$.

2.2.2.3 USBM Method

In this method drainage and imbibition capillary pressures are measured through centrifuge tests. Compared to Amott test, it is more sensitive near neutral wettability. This method is also less time consuming, but is restricted to the use of plug-size core samples, since samples must be used in a centrifuge. USBM method compares the

work necessary for one fluid to displace the other. The required work is proportional to the area under the capillary pressure curve and the wettability number is defined as (Donaldson, Thomas et al. 1969) (See **Figure 2-6**):

$$N_W = \log(\frac{A_w}{A_o}) \qquad (2.5)$$

where:

A_w= area under the secondary water drainage curve (drainage started from residual oil)

A_o= area under the imbibition curve falling below the zero-P_c axis

The main advantages of this method are the speed and simplicity of procedure.

In the modified version of the test, both Amott-Harvey index and USBM number is measured.

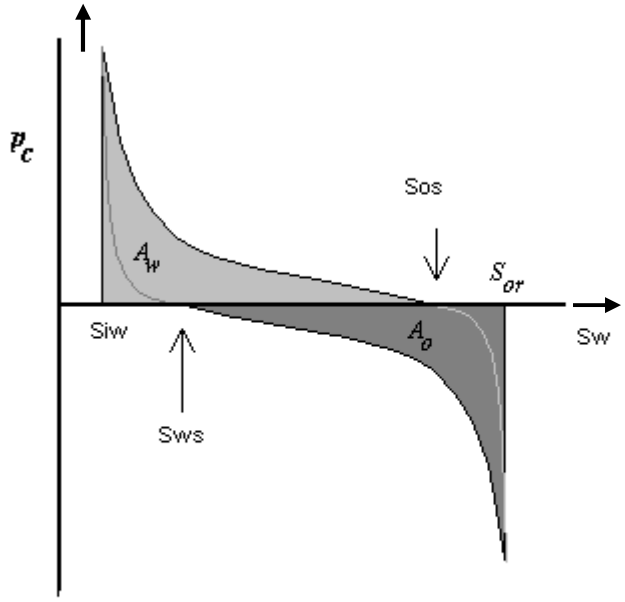

Figure 2-6 Wettability measurement by USBM method (Morrow 1976)

2.2.2.4 Imbibition Rates

Measuring the spontaneous imbibition of water into a core sample is a qualitative measure of wettability of the rock (Morrow 1990). Capillary pressure is the driving force behind the spontaneous imbibition and hence imbibition rate is proportional to the imbibition capillary pressure. So, measurements of spontaneous imbibition rate could be considered as a useful supplement to Amott indices and USBM wettability number. Both the rate and amount of water imbibed will decrease as the wettability of the rock changes from strongly water-wet to neutral-wet conditions. These measurements could be of special value as a sensitive measure of wettability in the

range where the Amott index is close to unity. Measurements of imbibition rates also provide information on dynamic IFT and wetting phenomena that may be important in reservoir but are not reflected by Amott or USBM wettability test (Morrow 1990). Bobek *et al.* (1958) believed that porous media wettability should be measured by methods related to capillary pressure measurement, since imbibition depends mainly on the water-wetness of the porous media, rather than the viscosities of the fluids involved and the pore structure.

2.3 Wetting Alteration by Crude Oil

Polar components present in crude oils were first identified by Benner and Bartell (1942) as being surface active and capable of altering the wetting state of high-energy mineral surfaces. These components can adsorb on mineral surfaces and alter their wetting properties. Understanding the whole nature and the extent of interactions between solid surfaces and oil components in porous media is difficult because all three phases in crude oil/brine/rock (COBR) are mixtures of many components themselves. Many factors such as the composition of the crude oil, brine composition and saturation, rock surface mineralogy, pore roughness, etc. can affect the interactions in a COBR system (Marsden and Nikias 1962; Buckley, Bousseau et al. 1995; Xie, Morrow et al. 2000). Other factors such as temperature and pressure also control the interactions in a crude oil/rock/brine system. Among these factors, oil composition is the most prominent (Buckley, Bousseau et al. 1995). It is widely believed that asphaltenes and other high molecular weight polar components of crude

oil are responsible for altering the wetting of reservoir rocks. The concentration of asphaltenes in oil is not necessarily a good predictor of oil/rock interaction. However, it was shown by Buckley *et al.* (1998) that as crude oils became poorer asphaltene solvents through hydrocarbon additives, they induce greater alteration. Most oil reservoirs are located in sedimentary rocks consisting of either sandstone or carbonate. These minerals are water-wet before exposure to crude oil. It is generally considered that oil reservoirs were created by accumulation of hydrocarbons in a rock originally filled with water, and therefore it was assumed that rock surface in all oil reservoirs are water-wet (Benner and Bartell 1942; Morrow 1990; Morrow 1991; Chernicoff 1999), because the connate water would prevent the invading crude oil from touching the rock surface. However, observations from wettability tests on cores from different reservoirs indicated that some reservoir rocks are oil-wet (Treiber, Archer et al. 1972; Wardlaw, Chilingarian et al. 1996). Experiments have shown that certain components in the crude oil under certain conditions were able to alter the wettability of the original water-wet rock toward a more oil-wet state, despite the presence of a water film.

It has been recognized by many authors that certain components, mainly the heavy asphaltene and resin fractions of crude oil are able to alter the wettability of the original water-wet rock by adsorption to the rock surface (Benner and Bartell 1942; Reisberg and Doscher 1956; Bobek, Mattax et al. 1958; Denekas, Mattax et al. 1959; Marsden and Nikias 1962; Clementz 1982; Collins and Melrose 1983; Anderson 1986a; Crocker and Marchin 1988; Dubey and Waxman 1989; Xie and Morrow

2000). This asphaltene/resin induced wettability alteration is now generally accepted. Asphaltenes are large complex molecules, somewhat polar, with molecular weights in the range 600-300000 (Collins and Melrose 1983). They are defined as the components that precipitate from crude oil when diluting with large excess of n-pentane, n-hexane or n-heptane. Resins are smaller molecules than asphaltenes, but have in general higher content of the polar elements: nitrogen, sulfur and oxygen and are more polar than asphaltenes. Although asphaltenes are related to the wetting state of oil reservoirs, observations have shown that a smaller group of components from the asphaltene/resin fraction are more important regarding wettability alteration. The most important components are those carrying a charged group such as an acid or base (Cuiec 1984; Anderson 1986b; Crocker and Marchin 1988). These compounds are more or less present in all crude oils, and include components such as phenols, carboxylic acids, sulfur components (sulfides, polysulfides) and nitrogen components (amides, pyridines)(Reisberg and Doscher 1956; Anderson 1986a). Many of these components have been shown to act as wettability modifiers when adsorbed on clean water-wet minerals (Benner and Bartell 1942; Wagner and Leach 1959; Cuiec 1977; Thomas, Clouse et al. 1993a; Madsen, Gron et al. 1996; Legens, Palermo et al. 1998a; Standal 1999). There also seem to be a difference in the way sandstone and carbonate rocks respond to acidic and basic components in crude oil (Denekas, Mattax et al. 1959; Buckley and Liu 1998). Carbonate rocks have a higher affinity toward the acidic components in crude oil (Cuiec 1977; Thomas, Clouse et al. 1993a; Madsen, Gron et al. 1996), whereas sandstone rocks became more oil-wet after being aged in

oils with higher basic components (Benner and Bartell 1942; Wagner and Leach 1959; Cuiec 1977; Skauge, Standal et al. 1999). These may be explained by the difference in the surface charge of these two types of rocks. Sandstone is negatively charged above pH=2 (Buckley and Morrow 1990; Skauge, Standal et al. 1999) and therefore sensitive to positively charged components. Carbonates are in general positively charged below pH 8 to 9 and are therefore able to adsorb the negatively charged acidic groups. A schematic representation of oil-wetness development is shown in **Figure 2-7**.

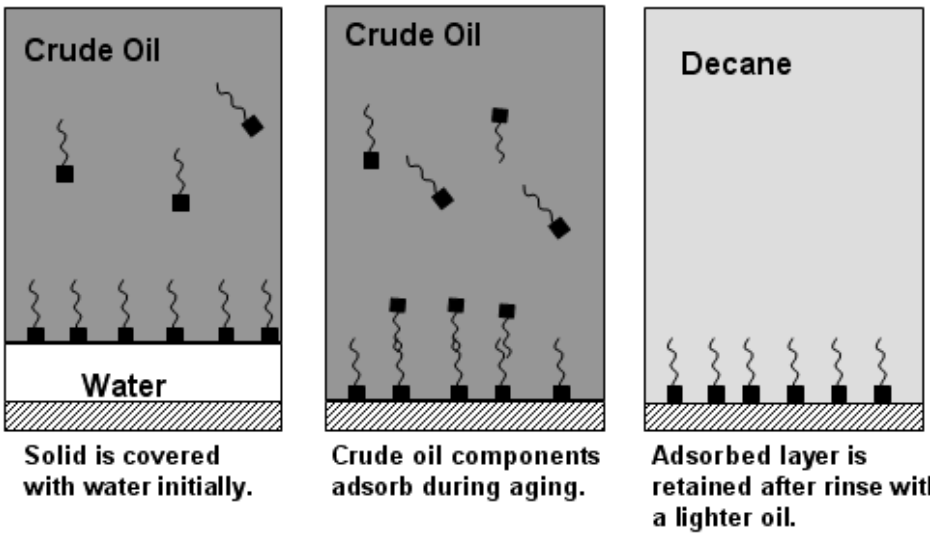

Figure 2-7 Oil-wetness development. Squares are charged/polar organic materials from crude oil (Buckley, Liu et al. 1998)

Polar groups are responsible for wettability alteration from water-wet to oil-wet in oil reservoirs. Besides the amount of these components in the crude oil, there are other parameters shown to be related to the degree of wettability alteration such as:

- Mineral composition and surface charge of the rock (Anderson 1986a; Dubey and Waxman 1989; Buckley and Liu 1998)
- Brine salinity and composition, concentration of divalent and other multivalent ions (Buckley, Liu et al. 1996; Morrow, Tang et al. 1998; Xie and Morrow 2000)
- Capillary pressure and thin film forces (Melrose 1982; Hirasaki 1991)
- Water solubility of polar oil components (Anderson 1986a; Kaminsky and Radke 1998)
- The solvent power of oil for its heavy components (Buckley 1993; Cimino, Correra et al. 1995; Buckley, Hirasaki et al. 1998; Al-Maamari and Buckley 2000; Buckley and Wang 2000)
- Temperature, pressure, initial water saturation (Jadhunandan and Morrow 1995; Al-Maamari and Buckley 2000; Zhou, Morrow et al. 2000b)

Buckley (1998; 1998) proposed four different mechanisms by which polar components from crude oil are adsorbed to mineral surfaces :

- Polar interactions, which can only happen when there is no water present in the system and is likely to happen between polar surface sites and polar components

- Surface precipitation of asphaltenes when the oil is a poor solvent for the heavy fraction
- Acid/base interactions, which take place between sites of opposite electrical charge
- Ion binding, which divalent or multivalent ions in the brine can bridge the mineral surface to oil/brine interface

2.4 Surfactants

2.4.1 Chemistry and Classifications

Surface **act**ive **a**g**ents** (surfactants) are amphiphilic materials with a characteristic chemical structure consists of one molecular component that will have little attraction (solubility) for the surrounding phase (solvent), normally called lyophobic group, and a chemical component that have a strong attraction (solubility) for the surrounding phase, the lyophilic group (Myers 1999). In the standard surfactant terminology, the soluble component lyophilic is called "head" group and the lyophobic group called "tail". A schematic of a surfactant molecule structure is shown in **Figure 2-8**.

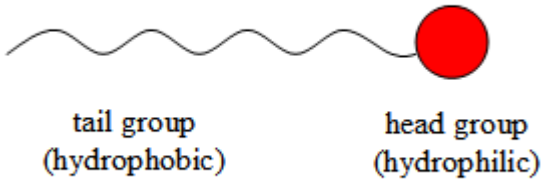

Figure 2-8 Structure of a surfactant molecule

Since most of the literature is concerned with aqueous systems the term hydrophobic is used instead of the more general term lyophobic; analogously, hydrophilic is used instead of lyophilic. In these aqueous systems, the hydrophobic group is usually a long-chain hydrocarbon and the hydrophilic group is an ionic or polar group that gives some water solubility to the molecule. The simplest classification of surfactants is determined by the nature of the hydrophilic group, and the subgroups are based on the nature of the hydrophobic groups. Myers (1999) classified surfactants into four general groups:

1. *Anionic*, where the hydrophilic group carries a negative charge such as carboxyl ($RCOO^-M^+$), sulfonate ($RSO_3^-M^+$), or sulfate ($ROSO_3^-M^+$), or phosphate ($ROPO_3^-M^+$)
2. *Cationic*, with the hydrophilic group bearing a positive charge, such as the quaternary ammonium halides ($R_4N^+X^-$)
3. *Nonionic*, where the hydrophilic group has no net charge but gets its water solubility from highly polar groups such as polyoxyethylene (POE or R-OCH_2CH_2O-), sugars or similar groups
4. *Amphoteric* (or zwitterionic), where the molecule contains both a negative and a positive charge on the principal chain such as the sulfobetaines, $RN^+(CH_3)_2CH_2CH_2SO_3^-$.

These materials have a tendency to concentrate (adsorb) at the interfaces of a system, or to form aggregates in solution at very low molar concentrations as shown in **Figure 2-9**.

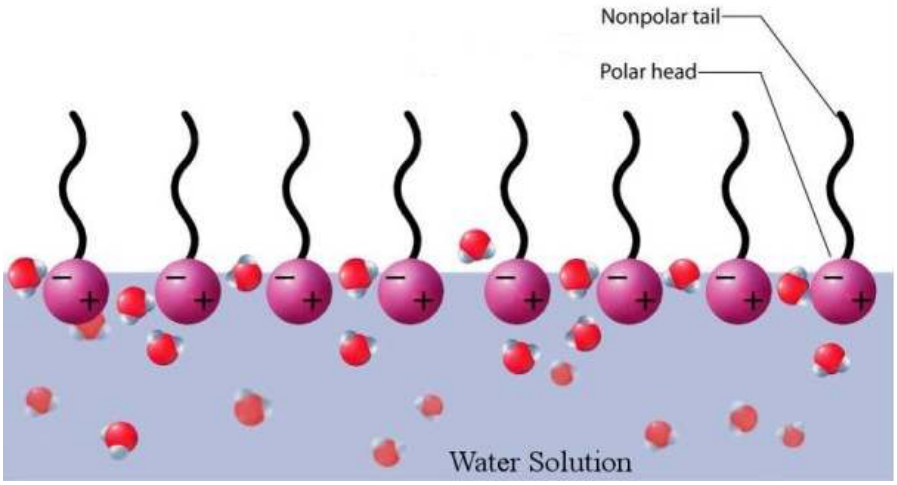

Figure 2-9 Adsorption of surfactant molecules at an air-water interface surface (Web Page)

This surfactant adsorption at the interface can be explained in the following way. When a surfactant is dissolved in a solvent (water), the hydrophobic group causes an unfavorable distortion (ordering) of the liquid structure and the result would be an increase in the overall free energy of the system and a decrease in the overall entropy of the system as shown in **Figure 2-10**. This entropy of the system can be regained when surfactant molecules are transferred to an interface and the associated water molecules are released. Therefore, the surfactant will adsorb or it may undergo some other process like micelle formation to lower the energy of the system. On the other hand, the presence of surfactant molecules at the interface decreases the amount of

work required to increase the interfacial area, resulting in a decrease of surface or interfacial tensions.

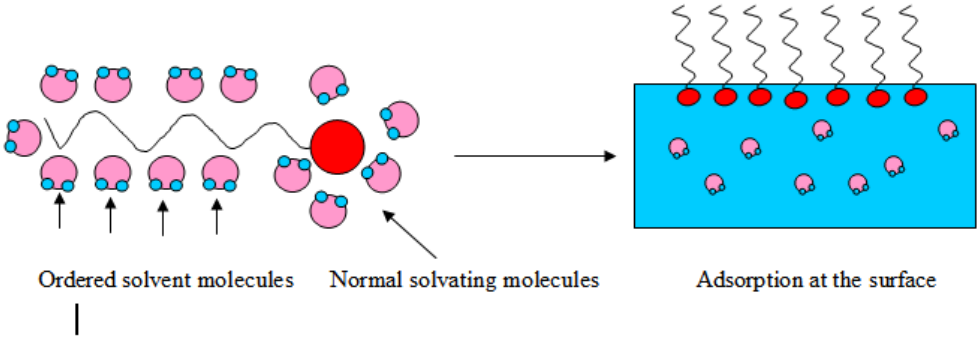

Figure 2-10 Surfactant adsorption process at interface (Myers 1999)

2.4.2 Different Options for Surfactants in Solution

Surfactant molecules have a tendency to adsorb at different interfaces available to them in order to reduce the free energy of the system. However, when all the available interfaces are occupied, the overall energy reduction continuous through other mechanisms shown in **Figure 2-11**. One of the most important mechanisms is the precipitation of the surfactant from solution, i.e., bulk-phase separation. Another mechanism is the formation of molecular aggregates or micelles. Micelles are thermodynamically stable dispersed species in solution with different properties from those of monomers.

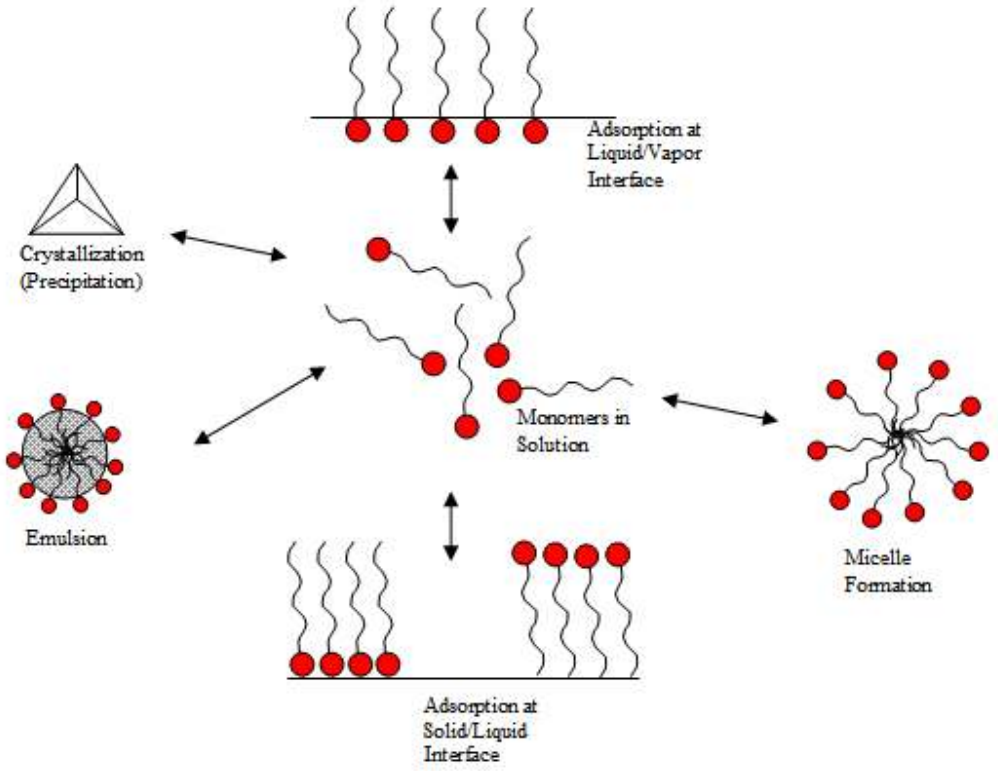

Figure 2-11 Different options for surfactant in solution (Myers 1999)

2.4.3 Surfactant Critical Micelle Concentration (CMC)

Study of the properties of solutions containing surface-active materials has shown that the bulk solution properties can change dramatically over small changes in concentration of surface-active materials. The graph of bulk solution properties (**Figure 2-12**) such as surface tension, electrical conductivity, or light scattering as a function of surfactant concentration exhibits sharp discontinuities at low concentrations.

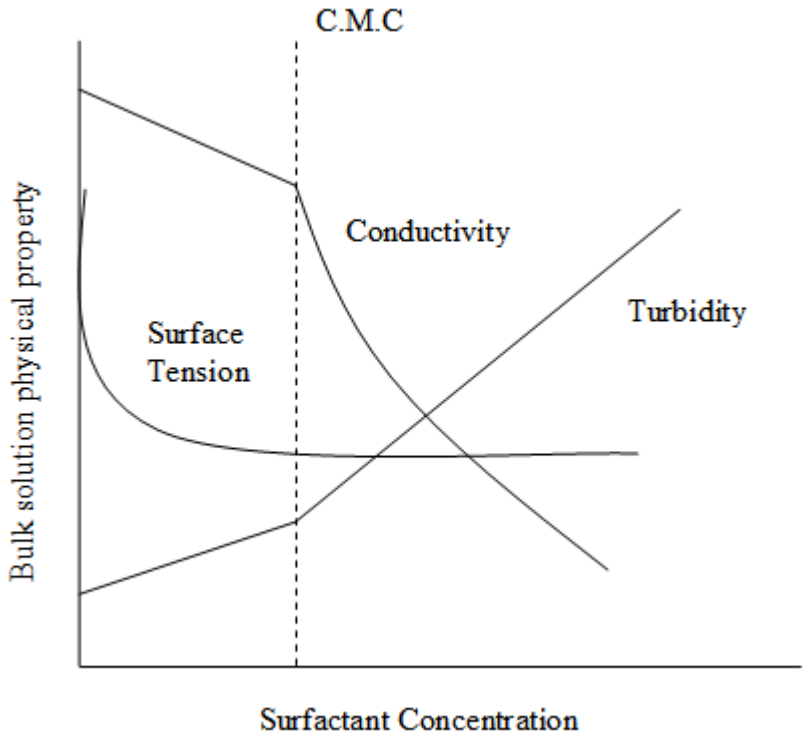

Figure 2-12 Change in the properties of solution as a function of surfactant concentration (Myers 1999)

These sudden changes in a property of solution can be interpreted as a significant change in the nature of the solute species in the solution. These observations serve as proof for the formation of aggregates or micelles in surfactant solutions. It is one of the characteristic properties of surfactant solutions to spontaneously form aggregates in aqueous phase. Micelles are classically seen as a spherical association of surfactant molecules with a dynamic structure (Sharma 1995; Myers 1999; Butt, Graf et al. 2006). The hydrocarbon chains meet inside the aggregate and the polar head groups form the outer surface of the micelle. There is a constant interchange of molecules between the aggregates and the bulk solution. The residence time of a given molecule

in a micelle is estimated to be between 10^{-5} and 10^{-3} s (Myers 1999). If one could get a picture of a micelle, freezing the motion of molecules, the picture will look like the one shown in **Figure 2-13**.

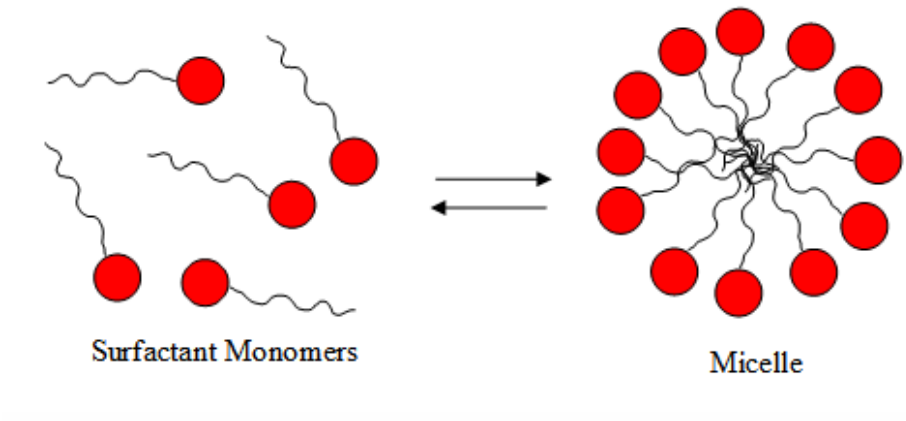

Figure 2-13 Structure of a micelle (2D section)

Above a critical surfactant concentration (Critical micelle concentration, CMC), micelles are formed in the surfactant solution. Micelle formation is due to different pushing and pulling effects that surfactant molecules undergo in aqueous solutions. These pushing and pulling effects could be the result of different interactions including: interactions between the hydrocarbon tail and the water, attractive interaction between hydrocarbon tails on separate molecules, and the interactions between solvated head groups (Butt, Graf et al. 2006). It is well know that most surfactants molecules in aqueous solutions undergo aggregate formation to form micelles. These micellar structures have an average of 30-200 monomers arranged in

such a way that the hydrophobic portions of the molecules are associated together. One of the ideas which is not accepted universally about micelles is the idea concerning the shape of these aggregates. Classically, micelles were recognized to have a spherical structure with 50-100 molecules associated with each one and having a radius equal to the length of the hydrocarbon chain of the surfactant molecule. However, other structures were found to exist and are shown in **Figure 2-14.**

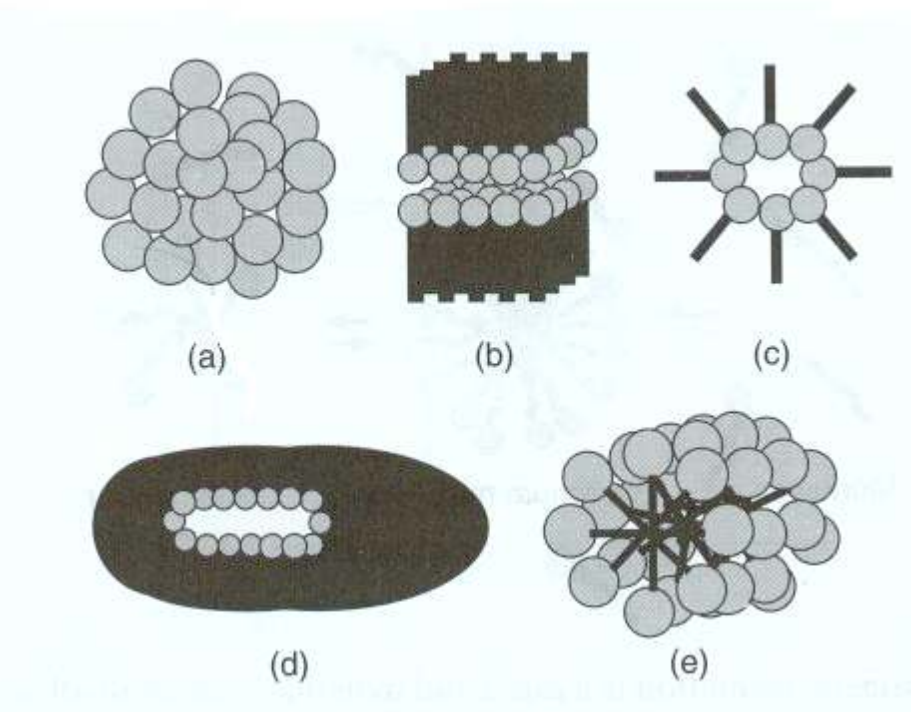

Figure 2-14 Most common micelle shapes: (a) normal spherical, (b) lamellar, (c) inverted spherical, (d) oblate ellipsoidal, and (e)cylindrical or rod-shaped (Butt, Graf et al. 2006)

2.4.4 Surface Tension Gradients and Related Effects (Marangoni Effect)

In many practical systems involving capillary flow, variation in the solid-liquid and/or liquid-vapor interfacial tensions causes complications to the analysis of

capillary flow (Dukhin, Kretzschmar et al. 1995; Myers 1999). Significant changes in interfacial tension from point to point in a system will lead to liquid flow unrelated to capillary phenomena. In liquid systems the existence of surface tension gradients will causes spontaneous flow from regions of low to those of high surface tension. This liquid flow, arising from surface tension gradients, is referred to as "Marangoni flow" (Myers 1999). Marangoni effects can be observed in both single and multi-component liquid systems. It is generally known that surface tension will decrease with increase in temperature. For a pure liquid, differences in temperature from one point to another can result in surface tension gradients. In such a situation, liquid flows away to cooler regions of the liquid as shown in **Figure 2-15**. This flow is completely related to the surface effect and is independent of the curvature, which controls capillary flow.

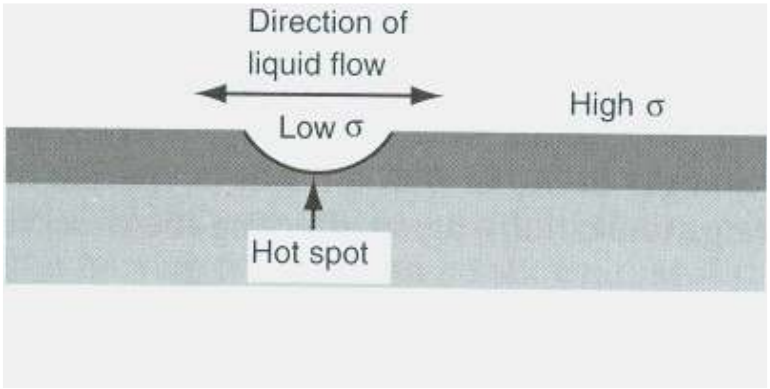

Figure 2-15 Marangoni Effect due to Temperature Difference (Myers 1999)

For multi-component liquid systems like surfactant solutions, the presence of surface tension gradients could be due to adsorption-related phenomena or, to different rates of evaporation from the system. If there are two liquids of different volatility, the

more volatile liquid will evaporate more quickly resulting in localized surface tension differences. If the surface-active component evaporates (or adsorbs), the local surface tension of the liquid will rise and flow will be toward the evaporation (adsorption) site as shown in **Figure 2-16**.

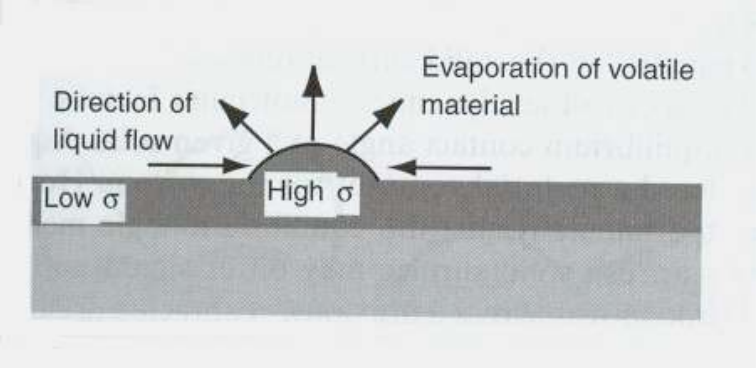

Figure 2-16 Marangoni Effect due to Evaporation (Myers 1999)

2.5 Adsorption

Adsorption is the preferential accumulation of one component of a system at an interface (Myers 1999; Butt, Graf et al. 2006). It is appropriate to start this section with some important definitions regarding adsorption. In an adsorption process, the material in the adsorbed state is called adsorbate. Adsorpt is the material to be adsorbed on the surface and the substance onto which adsorption takes place is called adsorbent (**Figure 2-17**).

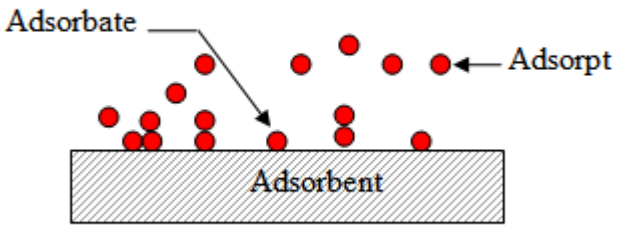

Figure 2-17 Definitions of adsorpt, adsobate and adsorbent (Butt, Graf et al. 2006)

The amount adsorbed (Γ) on the surface is a function of adsorpt concentration and a graph of Γ vs. concentration at constant temperature is called an adsorption isotherm. Studies related to the application of surfactants in EOR processes indicated that surfactant lost by adsorption is only one of the several mechanisms responsible for surfactant retention. Other mechanisms may include precipitation by divalent ions, partitioning and entrapment in a residual (immobile) oil phase. Surfactant loss by adsorption is one the important criteria that governs the economics of the dilute surfactant flooding methods (Tabatabai, Gonzalez et al. 1993).

The adsorption of molecules at a solid-liquid interface creates a transition region on the order of molecular dimensions in which the composition of the system changes from that of the bulk solid to that of the bulk liquid. For a solution, a higher concentration of the solute near the interface is an indication of positive adsorption of the solute molecules. From both theoretical and practical standpoints, it is of interest to know the characteristic of adsorption profile for a given system in order to understand the mechanism of the adsorption process, as well as its consequences.

There are several quantitative and qualitative factors that we would like to know such as (1) the amount of the material adsorbed per unit mass or area of solid, (2) the solute concentration at which surface saturation occurs, (3) the orientation of the adsorbed molecules relative to the surface and solution, and (4) the effect of adsorption on the properties of the solid relative to the rest of the system (Myers 1999; Butt, Graf et al. 2006). Based on the nature of the interfacial region, the total concentration of a given component in a system of fixed volume and interfacial area will be determined by the shape of the concentration profile at the interface. In a solid-liquid system the concentration profile is similar to that shown in **Figure 2-18**, assuming no dissolution of the solid in the liquid and no absorption of liquid.

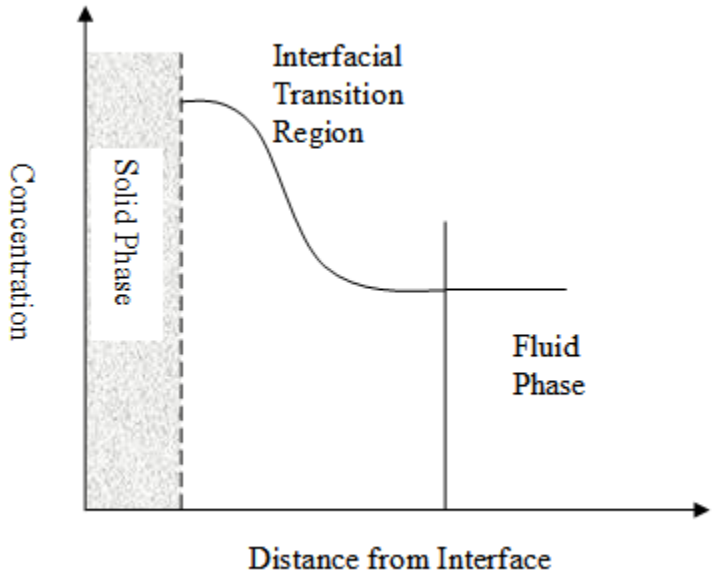

Figure 2-18 Concentration Profile (Myers 1999)

There is no direct procedure for quantitative measurement of the concentration profiles. Gibbs introduced a simple indirect approach to obtain the concentration profile for the components of a system in the interfacial region (Myers 1999). Let's look at a system composed of two phases α and β with substance *i* present in one or both phases (**Figure 2-19**). If the concentration of *i* in phase α is the uniform value of C_i^{α} and that for phase β is C_i^{β}, then for the given volumes of phase α, (V_α), and β, (V_β), the total amount of component *i*, n_i is:

$$n_i = (C_i^{\alpha} V_{\alpha} + C_i^{\beta} V_{\beta}) \qquad (2.6)$$

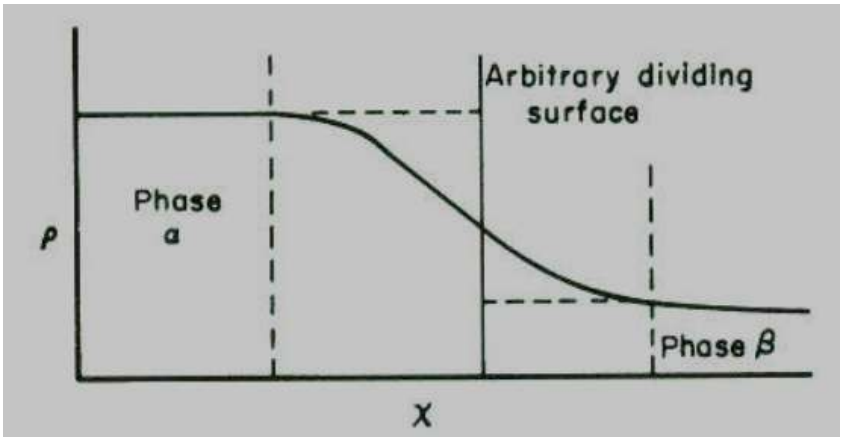

Figure 2-19 Surface excess illustration (Huang 1985)

Because of the presence of the interfacial region and since the local value of C_i changes going through the interface (existence of concentration profile), the actual amount of component *i* in the interfacial region is different than the values given by Equation (6). The difference which is defined as the surface excess amount of *i* (n_i^{σ}) is given by:

$$n_i^{\sigma} = n_i - (C_i^{\alpha} V_{\alpha} + C_i^{\beta} V_{\beta}) \qquad (2.7)$$

Surface excess is dependent on the shape of the concentration profile between the two phases α and β. Practically, the surface excess of component *i* can be regarded as the amount of that component adsorbed at the interface. One major issue with this approach is the definition (location) of the interface between the two phases α and β. Gibbs defined the interface (Gibbs Dividing Surface, GDS) as the region where the surface excess of one phase becomes zero. In a solution, the phase α can be seen as the solvent. **Figure 2-20** shows the definition of the dividing surface. GDS is defined as the plane (**Figure 2-20**(a)) in which the solvent surface excess is zero (the shaded areas on each side are equal). At $n_{\alpha}^{\sigma} = 0$, the component *i* will have a relative excess amount with respect to α as shown in **Figure 2-20**(b) which is the difference of concentration on either side of the GDS plane.

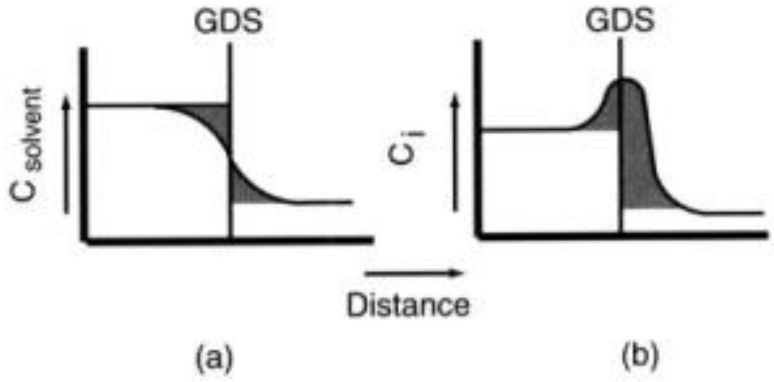

Figure 2-20 Gibbs Dividing Surface (Myers 1999)

The experimental evaluation of adsorption from solution at solid-liquid interface usually involves the measurement of changes in the concentration of solute in the solution before and after adsorption has occurred. The usual method for evaluating the adsorption mechanism is through the adsorption isotherm. The factors to be considered are (Sharma 1995; Myers 1999):

1. The nature of the interactions between the adsorbate and the adsorbent
2. The rate of adsorption
3. The shape of the adsorption isotherm and the significance of plateaus, points of inflection and so on
4. The extent of adsorption, i.e., monolayer or multilayer
5. The orientation of adsorbed molecules at the interface, and
6. The effect of environmental factors such as temperature, solvent composition, and pH on these effects

The interactions between the adsorbate and adsorbent may fall into two categories: the adsorption could be purely physical which is relatively weak and reversible, or stronger and sometimes irreversible adsorption or chemisorption (Butt, Graf et al. 2006). Since there are many possibilities of adsorption mechanisms, a variety of isotherm shapes have been determine experimentally.

An adscription isotherm shows the amount of surfactant adsorbed on the substrate vs. the equilibrium surfactant concentration, or in other words, it shows the dependence

of adsorption amount on the equilibrium surfactant concentration in the bulk phase. **Figure 2-21** shows the schematic plot of commonly observed adsorption isotherms.

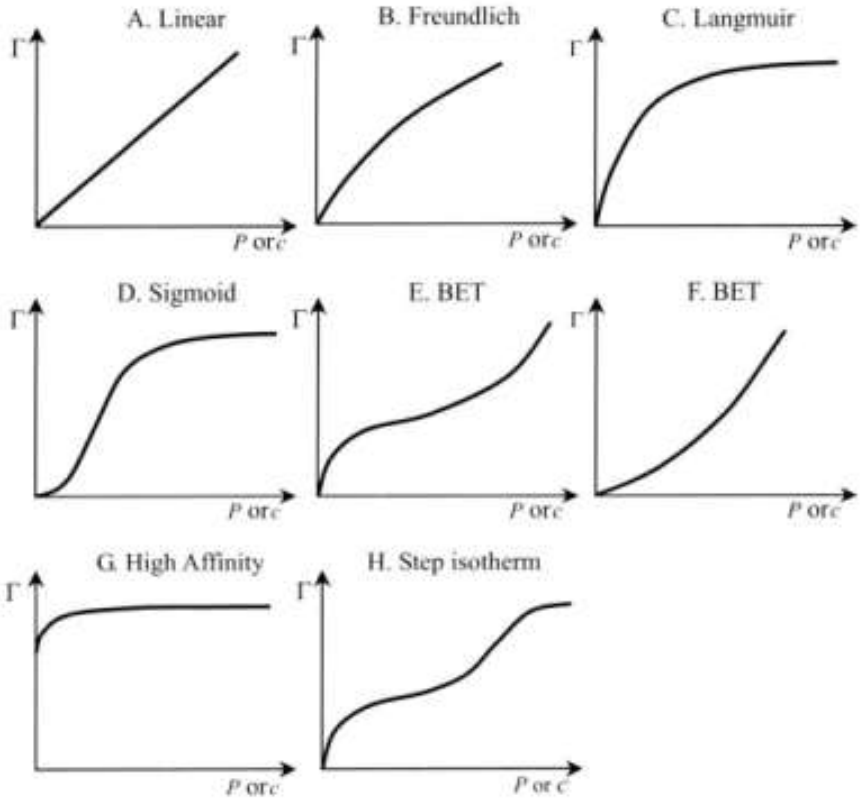

Figure 2-21 Different Adsorption Isotherms (Butt, Graf et al. 2006)

The simplest type of adsorption isotherm is the linear increase described by the Henry equation (Butt, Graf et al. 2006) and shown in **Figure 2-21**(A):

$$\Gamma = k_H C \qquad (2.8)$$

where Γ is the amount adsorbed, C is the concentration, and k_H is a constant in units of L/m^2.

Another common isotherm is described by Freundlich equation (Butt, Graf et al. 2006) and shown in **Figure 2-21**(B):

$$\Gamma = k_F C^n \qquad (2.9)$$

where k_F and n are constants. These isotherm best describes the adsorption on heterogeneous surfaces with the high affinity regions (sites) being occupied first, which accounts for the steep increase in low concentrations. The lateral repulsion between the adsorbed molecules could result in a decrease in adsorption value. Another type of isotherm is the Langmuir adsorption isotherm described by the following equation and shown in **Figure 2-21**(C):

$$\frac{\Gamma}{\Gamma_{\max}} = \frac{k_L C}{1 + k_L C} \qquad (2.10)$$

Where k_L is a constant called the Langmuir constant and $\Gamma_{\max}$ is the maximum amount adsorbed, which in the case of the Langmuir model is a monolayer adsorption. This isotherm is characterized by having a concave initial region with respect to the concentration axis and reaching a plateau (saturation) at higher concentrations.

The type shown in **Figure 2-21**(E) is called a Brunauer-Emmett-Teller (BET) isotherm (Myers 1999) and best describes the adsorption of gases. The initial concave region is related to the formation of a monolayer. However, higher pressure causes the adsorption of more layers on top of the first one and it is possible to have

condensation when reaching the saturation vapor pressure. BET isotherm can be described by the following equation:

$$\frac{p}{V(p_o - p)} = \frac{1}{V_m c} + \frac{(c-1)p}{V_m c p_o} \qquad (2.11)$$

where V is the volume of adsorbed vapor at standard temperature and pressure, V_m is the monolayer capacity at standard temperature and pressure, p is the partial pressure of the adsorbate, p_o is the saturation vapor pressure of the adsorbate, and

$$c \approx \exp\frac{(\Delta H_A - \Delta H_L)}{RT} \qquad (2.12)$$

The BET model modifies the Langmuir model by considering multilayer adsorption. The BET model assumes that the monolayer formation has a characteristic heat of adsorption ΔH_A, but subsequent layers are controlled by the heat of condensation of the vapor in system, ΔH_L (Myers 1999; Erbil 2006). This isotherm is found for the adsorption of inert gases (N_2, Ar, He,..) on polar surfaces. It can be used to measure the surface area of finely divided solids and generally produces good results at pressures, p between $0.05p_o$ and $0.35p_o$ (Rosen 1986; Sharma 1995; Erbil 2006)

The monolayer capacity V_m is the most important parameter because it can be used to calculate the surface area based on the area occupied by each adsorbed gas molecule (Sharma 1995; Myers 1999). Based on Equation (11), a plot of $\frac{p}{[V(p_o - p)]}$ versus $\frac{p}{p_o}$ produces a linear graph over the pressure region mentioned above. V_m can be

obtained from the slope of the line, $S = \frac{(c-1)}{V_m c}$ and the intercept, $I = \frac{1}{V_m c}$. The specific surface area, A_s, can be calculated in the following way;

$$V_m = \frac{1}{S+1} \qquad (2.13)$$

$$A_s = \frac{V_m k}{sampleweight} \qquad (2.14)$$

$$k = \frac{N_a A}{M_v} \qquad (2.15)$$

where

N_a = is Avogadro's number

A = the area per molecule of the adsorbed gas, and

M_v = the molar volume of gas, 22.4 L at standard temperature and pressure (STP)

The most common adsorbate used for BET surface area calculation is nitrogen with an effective area per molecule, A, of 0.162 nm^2. Other useful gases include argon (A = 0.138 nm^2) and krypton (A = 0.195 nm^2) (Myers 1999; Erbil 2006).

2.5.1 The effect of solid phase on surfactant adsorption

In the process of adsorption on solid surfaces, the mode and extent of surfactant adsorption depend greatly on the nature of the solid surface involved (Myers 1999). There are three principal groups for the nature of an adsorbent surface: (1) nonpolar and hydrophobic surfaces such as polyethylene; (2) polar surfaces that do not posses significant surface charges, such as polyesters and natural fibers; and (3) those that

have strongly charged surface sites (Butt, Graf et al. 2006; Erbil 2006). For nonpolar surfaces, adsorption occurs as a result of dispersion force interactions. The orientation of adsorbed molecules is in a way that the hydrophobic portion of the molecule will be toward the solid surface, while the hydrophilic group will be directed toward the aqueous phase. In the early stages of adsorption process (low concentration) the hydrophobe will be lying on the surface like trains or L's as shown in **Figure 2-22.** With the increase in concentration, the molecules will become oriented more perpendicular and finally a closely-packed assembly of molecules will result. Since the molecules are adsorbed by their tail with their hydrophilic group directed outward from the solid surface, there is no possibility for the formation of a second adsorbed layer and adsorption is limited to a single or monolayer formation.

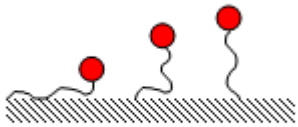

Figure 2-22 Adsorption on a nonpolar surface (Erbil 2006)

In the case of polar, uncharged surfaces the dipolar interactions as well as dispersion forces are the potential forces in determining the mode of adsorption. If dispersion forces dominate, adsorption will occur in a manner like that for the non-polar surfaces. If polar interactions dominate the reverse case will happen as shown in **Figure 2-23**, i.e., the surfactant molecules will be oriented with the hydrophilic head group toward the solid surface and the hydrophobic group toward the aqueous phase.

The final orientation in an aqueous system is also affected by the solvent-adsorbent and solvent-adsorbate interactions and small changes in the nature of the solvent like pH, electrolyte content, or presence of co-solvent can change the adsorption mode (Myers 1999).

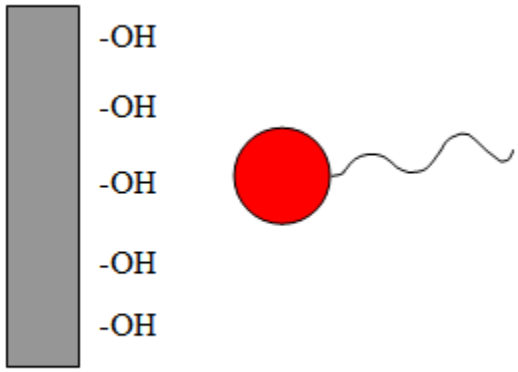

Figure 2-23 Adsorption on a polar, uncharged surface (Myers 1999)

Surfaces having electrical charges can undergo adsorption by all the mentioned mechanisms. As adsorption progresses, the dominant mechanism may change from ion exchange through ion bonding to dispersion or hydrophobic interactions as shown in **Figure 2-24**. A typical surfactant-adsorption isotherm can be divided into 4 identifiable regions (Tabatabai, Gonzalez et al. 1993; Sharma 1995).

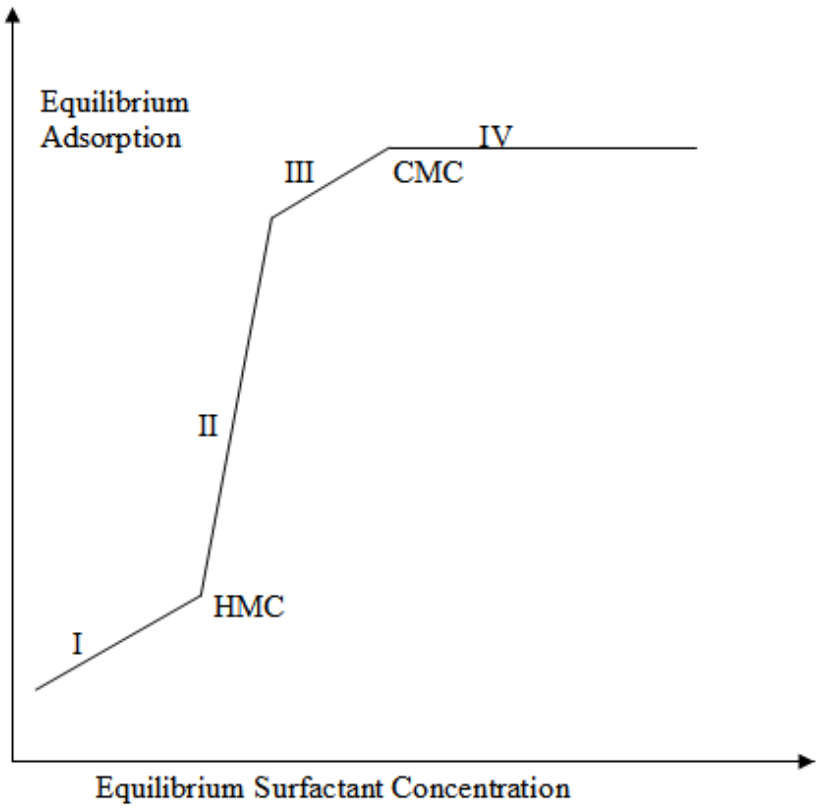

Figure 2-24 Schematic of a typical adsorption isotherm (Tabatabai, Gonzalez et al. 1993)

Region I corresponds to low surface coverage by adsorbed surfactant monomers. In Region I, also known as the Henry's law region (Butt, Graf et al. 2006), a linear relationship exists between the surfactant equilibrium concentration and adsorption density. The mechanism responsible for the surfactant adsorption is mainly the electrostatic attraction between the charged surface of the solid and the charged head group of the surfactant molecule. A characteristic feature of surfactant adsorption at concentrations below CMC is that adsorbed surfactants form local aggregates on the surface. These aggregates have been referred to as hemi-micelles, admicelles, and surface micelles, implying a micelle-like structure. Region II is characterized by a

sharp increase in the adsorption caused by the formation of local monolayer or bilayer aggregates on the surface. Hydrophobic bonding between the surfactant tail groups contributes significantly to the aggregation phenomenon in this region. In Region III, the forces influencing adsorption are the same as those in Region II; the Region II/Region III transition is identified by a decrease in slope of the adsorption isotherm and may be either distinct or gradual. The decrease in the slope of the isotherm is also related to the interfacial charge reversal caused by the adsorption of charged species. In this region, both the adsorbent and adsorbate are similarly charged. Region IV correspond to the maximum surface coverage and begins at the critical micelle concentration (CMC) of the surfactant; in Region IV, micelle formation competes with surfactant adsorption and results in a plateau region where surfactant adsorption becomes nearly constant despite increasing surfactant concentration.

2.5.2 Adsorption Models

Adsorption at solid/liquid interfaces is of importance in the processes of enhanced oil recovery (EOR) using surfactants since it affects both the efficiency and the cost of the process. Adsorption is one of the main mechanisms for surfactant loss in these processes. The surfactant must survive the environment where it will be used (Novosad 1981; Butt, Graf et al. 2006). Also, since the injected surfactant is a major portion of the overall cost of the project; its loss should be minimized to optimize process economics. Adsorption from surfactant solution at the solid/liquid interface is believed to take place from the monomer phase since experimental data indicated that the surfactant adsorption generally increases as the surfactant concentrations go

higher, but almost keeps constant at its plateau value if the monomer concentration has already become as high as the critical micelle concentration (CMC) (Song and Islam 1994).

2.5.2.1 Langmuir Model

Surfactant adsorption at the solid/liquid interface can be modeled with either Longmuir-type model or a surface excess model. The Langmuir model has been used for simulating the adsorption of a variety of chemical agents including surfactants and polymers used in EOR processes. In the Langmuir model, both instantaneous and time-dependent (or rate-controlled) adsorption models can be simulated (Novosad 1981; Hunag 1985).

The Langmuir model which is given by Equation (16) below has been used in simulating adsorption and desorption of chemical flooding in EOR applications:

$$C_r = \frac{aC}{1+bC} \qquad (2.16)$$

where

$C_r =$ amount adsorbed surfactant per gram of solid (mg/g)

$C =$ surfactant concentration (mg/ml)

$a = bC_r^*$ (ml/mg)

$b = \frac{K_1}{K_2}$ (ml/mg)

$C_r^* =$ maximum equilibrium adsorption of surfactant per gram of solid (mg/g)

$K_1 =$ kinetic constant for adsorption (ml/g.hr)

$K_2 =$ kinetic constant for desorption (ml/g.hr)

This model is able to describe many adsorption data both for the gas/solid and liquid/solid interfaces. Its two adjustable parameters *a*, and *b* give the model flexibility to be matched to many sets of data (Hunag 1985).

A mass transfer equation describing the characteristics of dispersion and adsorption of a chemical component in a solution flowing through porous medium can be derived as (Ramirez, Shuler et al. 1980; Huang 1985):

$$D\frac{\partial^2 C}{\partial x^2} - \frac{q}{A\phi}\frac{\partial C}{\partial x} = \frac{\partial C}{\partial t} + \frac{(1-\phi)}{\phi}\rho_r \frac{\partial C_r}{\partial t} \qquad (17)$$

This equation is an extension of the well-known dispersion equation. There are several assumptions in deriving the Equation (17):

1. the porous medium is homogenous with constant cross section
2. fluid and rock compressibility are negligible
3. fluid flows at a constant rate under isothermal condition
4. dispersion of the chemical occurs only in the longitudinal direction
5. molecular diffusion is negligible and the dispersion coefficient is independent of the chemical concentration
6. chemical reaction between the injected chemical solution and the in-place fluid or rock is negligible

By using the Langmuir model, the adsorption kinetics term can be expressed as:

$$\frac{\partial C_r}{\partial t} = \frac{\partial C_r}{\partial C}\frac{\partial C}{\partial t} = \frac{a}{(1+aC)^2}\frac{\partial C}{\partial t} \qquad (2.18)$$

$$D\frac{\partial^2 C}{\partial x^2} - (\frac{q}{A\phi})\frac{\partial C}{\partial x} = \left[1 + \frac{(1-\phi)\rho_r a}{\phi(1+bC)^2}\right]\frac{\partial C}{\partial t} \qquad (2.19)$$

or an alternative expression proposed by Trogus *et al* (1979) can be used:

$$\frac{\partial C_r}{\partial t} = k_1 C(C_{rm} - C_r) - k_2 C_r \qquad (2.20)$$

To obtain the adsorption isotherm, these equations are solved simultaneously. To get the adsorption value at each concentration, the simulation data are matched with experimental data. Adsorption isotherms are obtained by history matching the experimental data with the model that was used to describe the flow of the adsorbing chemical in porous media.

2.5.2.2 Surface Excess Model

A thermodynamically consistent approach to modeling adsorption of surfactants at the solid/liquid interface can be achieved by using a surface excess model (Song and Islam 1994). This model is also more flexible and generally applicable for modeling surfactant adsorptions. Mannhardt and Novosad (1988; 1990) made comparisons between the simulation results that they obtained from both the surface excess and the Langmuir model, and they found that the surface excess model is better in modeling the adsorption of surfactants as shown in **Figure 2-25**.

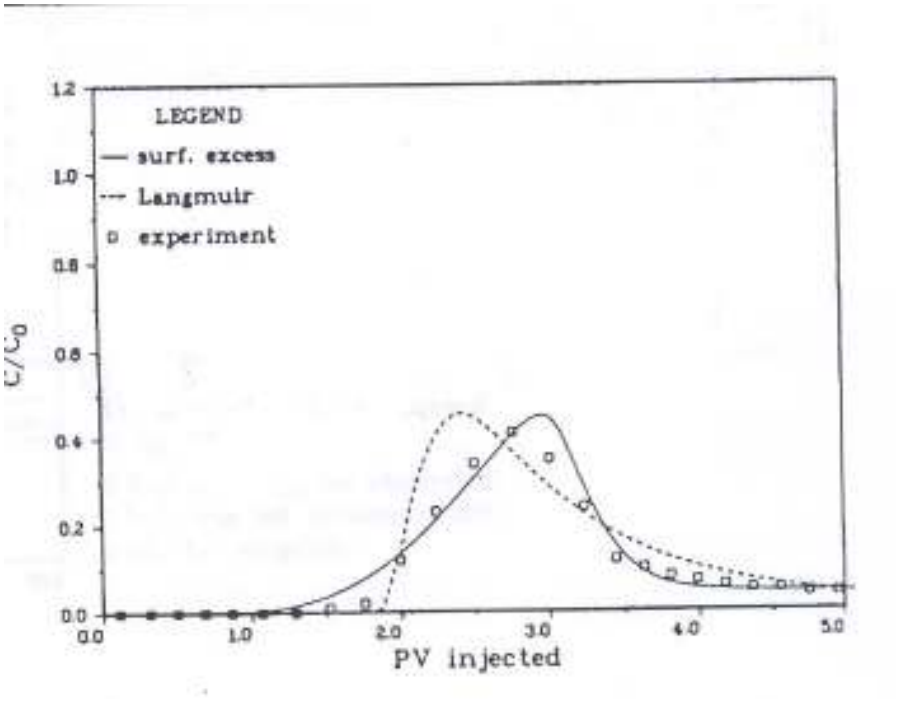

Figure 2-25 Comparison of simulation results obtained by surface excess and Langmuir models (Huang and Novosad 1986)

Figure 2-26 shows the adsorption phenomena from a binary solution of surfactant in an aqueous phase.

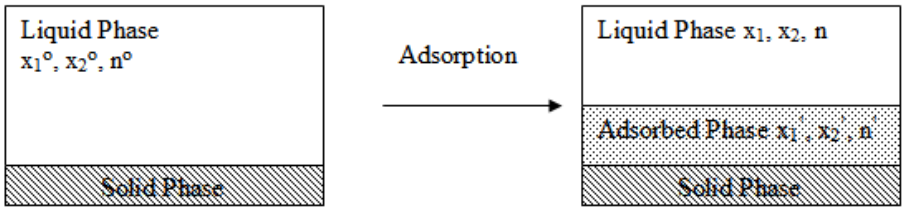

Figure 2-26 Adsorption process for surface excess model (Huang and Novosad 1986)

As can be seen from **Figure 2-26** after adsorption, there is an adsorbed phase close to the solid phase. This phase is the portion of the liquid phase where the liquid

molecules interact with the solid. The surface excess for component *i* is defined as (Huang 1985; Huang and Novosad 1986):

$$n^{e}{}_{i} = n^{o}(x_{i}^{\ o} - x_{i}) \qquad (2.21)$$

where *i* denotes surfactant (*i*=1) and solvent (*i*=2).

By material balance:

$$n^{o} = n + n^{'} \qquad (2.22)$$

$$n_{i}^{\ o} = n_{i} + n_{i}^{'} \qquad (2.23)$$

Combining Equations (21), (22), and (23) gives:

$$n^{e}{}_{i} = n'(x^{'}{}_{i} - x_{i}) \qquad (2.24)$$

Which can be rearranged to obtain:

$$n_{i}^{'} = n_{i}^{\ e} + n^{'}x_{i} \qquad (2.25)$$

This equation shows that surface excess is a measure of adsorption and for very dilute solutions the amount adsorbed can be approximated by the surface excess. **Figure 2-27** shows a schematic of both adsorption and surface excess.

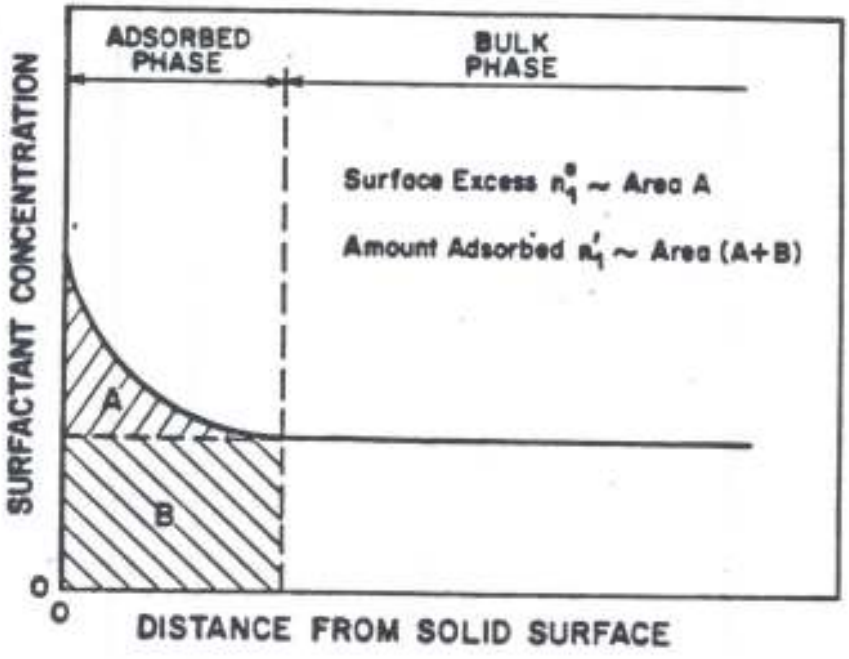

Figure 2-27 Presentation of surface excess and adsorption (Huang 1985)

The surface excess can be evaluated by measuring n^o, x_i^o, and x_i on the right hand side of the Equation (21) above and no measurement is required in the adsorbed phase and there is no need to define the position of the dividing line between the adsorbed and bulk phases. The surface excess is a relative measure of adsorption. The quantity of practical interest is usually the amount adsorbed rather than the surface excess. To define the amount adsorbed at the solid/liquid interface, the monolayer model can be used (Mannhardt, Schramm et al. 1990):

$$\frac{1}{n'} = \frac{x_1'}{m_1} + \frac{x_2'}{m_2} \qquad (2.26)$$

To have a measure of relative compositions in the bulk and adsorbed phases, the selectivity term, S, defined below, has been used (Mannhardt and Novodas 1988):

$$S = \frac{x_1^{'} / x_2^{'}}{x_1 / x_2} \qquad (2.27)$$

With the definition of selectivity, the surface excess for surfactant can be written as:

$$n_1^{e} = \frac{m_1 x_1 x_2 (S-1)}{S x_1 + (m_1 / m_2) x_2} \qquad (2.28)$$

The amount of surfactant adsorbed $(n_1' = n' x_1^{'})$ is then:

$$n_1^{'} = \frac{m_1 x_1 S}{S x_1 + (m_1 / m_2) x_2} \qquad (2.29)$$

A typical adsorption isotherm for two completely miscible components in terms of surface excess and amount adsorbed is shown in **Figure 2-28**. We can see from this figure that the surface excess equals zero at $x_i = 0$ and $x_i = 1$. Surface excess goes through a maximum, making it a difficult variable to extrapolate.

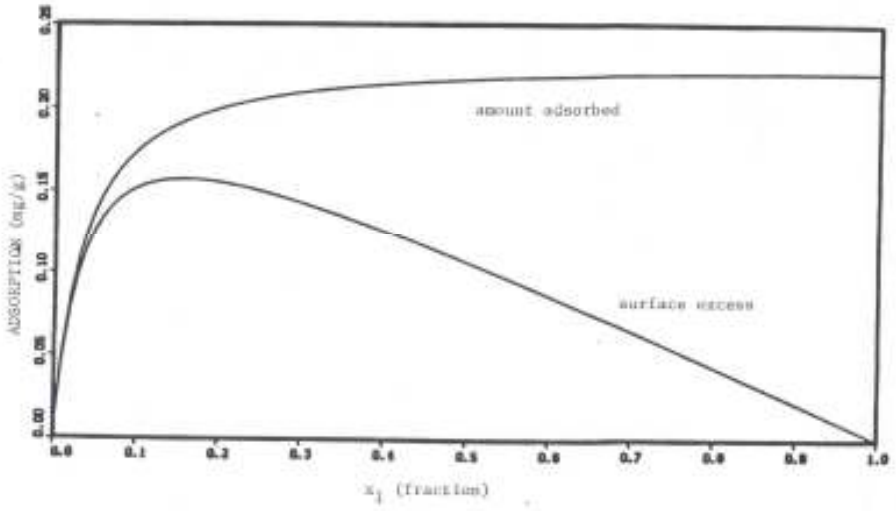

Figure 2-28 Surface excess and amount adsorbed as a function of composition (Mannhardt and Novodas 1988; Mannhardt, Schramm et al. 1990)

Mannhardt and Novosad (1988; 1990) performed flow experiments for evaluating surfactant adsorption and used Equations (24) and (25) to calculate the adsorption isotherm for the surfactant under study. **Figure 2-29** shows the adsorption isotherm based on both surface excess and amount adsorbed. It can be seen that the difference between the surface excess and the amount adsorbed is very negligible for low concentrations of surfactant.

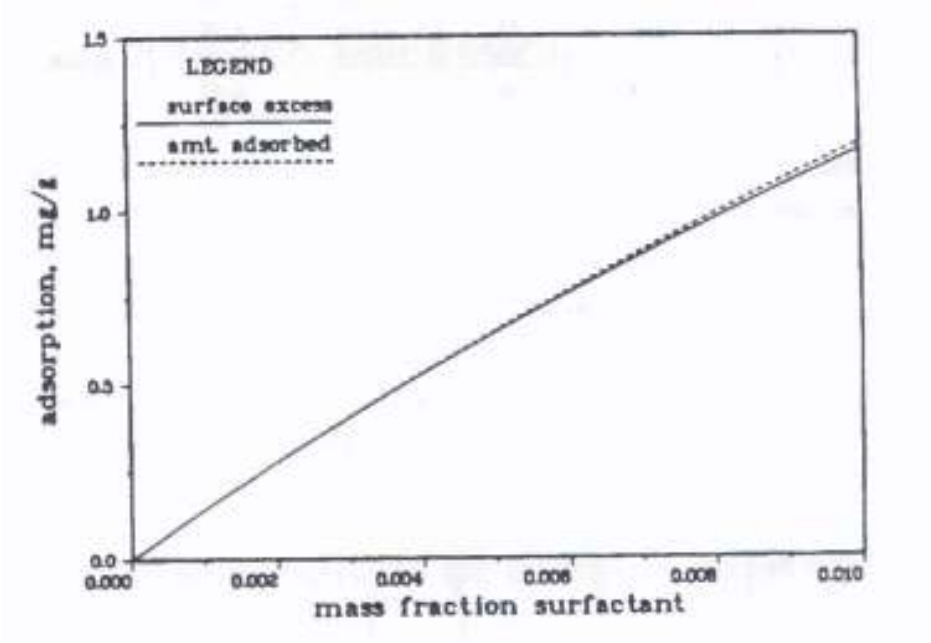

Figure 2-29 Adsorption isotherms showing surface excess vs. amount adsorbed (Mannhardt and Novodas 1988)

The mass transfer equation for the flow of an adsorbing chemical through a porous medium can be derived as (Huang 1985):

$$\lambda \frac{q\rho_l}{A\phi}\frac{\partial^2 x_1}{\partial x^2} - \frac{q\rho_l}{A\phi}\frac{\partial x_1}{\partial x} = \frac{1-\phi}{\phi}\rho_r n^o \frac{\partial x_1}{\partial t} + \frac{1-\phi}{\phi}\rho_r \frac{\partial n^{ea}{}_1}{\partial t} \qquad (2.30)$$

This equation, with appropriate initial and boundary conditions, along with the kinetic term defined as below is solved to get the adsorption isotherm (Huang 1985):

$$\frac{\partial n_1^{ea}}{\partial t} = k_i (n_1^{e} - n_1^{ea}) \qquad (2.31)$$

where n_1^{e} is the equilibrium surface excess given by previous equations and n_1^{ea} is the actual surface excess. When $n_1^{e} > n_1^{ea}$, adsorption takes place, and $k_i = k_1$. When $n_1^{e} < n_1^{ea}$, desorption takes place, and $k_i = k_2$. The calculated concentrations from solutions of Equation (30) are matched to experimental data using the six adjustable parameters: the dispersion coefficient λ, monolayer coverages m_1 and m_2, selectivity S, and kinetic constants k_1 and k_2. Some researchers suggested that values of m_1 and m_2 can be estimated independently from the molecular area of components 1 and 2 and the specific surface area of the rock, reducing the number of parameters to four (Huang and Novosad 1986).

2.5.3 Environmental Effects on Adsorption

Charged surfaces in aqueous solvents are very sensitive to environmental conditions such as electrolyte content and pH of the system (Sharma 1995; Myers 1999). In the case of high electrolyte concentration, ion exchange is the only mechanism of adsorption available other than dispersion or hydrophobic interactions because the

solid surface has a high degree of bound counterions. Also, high electrolyte concentration causes the attraction between unlike charge groups on the solid surface and the surfactant, and the repulsion between the like charges of the surfactant molecules to be suppressed. The adsorption isotherm in this case is usually almost linear. An increase in electrolyte content causes a decrease in adsorption of surfactants onto surfaces of opposite charge and an increase in adsorption of like charged molecules. As an example, the presence of polyvalent cations such as Ca^{2+} or Al^{3+} in the solution increases the adsorption of anionic surfactants onto like-charged surfaces. These ions can have two effects: (1) they can neutralize charge repulsion by binding tightly to a negatively charged surface, or (2) they can serve as a bridging ion by association with both the negative surface and the anionic surfactant head group as shown in **Figure 2-30.**

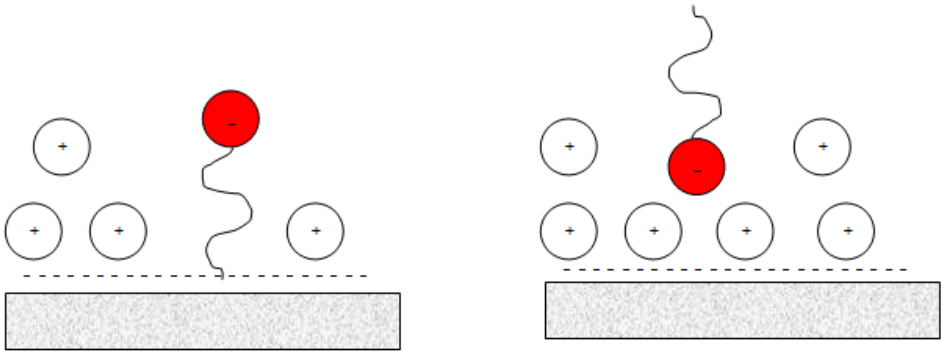

Figure 2-30 Effect of electrolyte content on adsorption (Sharma 1995)

For solid surfaces having weak acid or basic groups such as proteins, and cellulosics, adsorption of surfactants onto solids is very sensitive to changes in solution pH. For surfaces having weak acid groups such as carboxylic acids, as the pH of the solution

is reduced, the ionization of the weak acid group will be suppressed resulting in a surface more favorable for the adsorption of surfactants of like charge and less favorable for adsorption of opposite charges as shown in **Figure 2-31**. For surfaces containing weak basic groups, the opposite is true, i.e., lowering the pH will lead to ionization of surface basic groups increased adsorption of oppositely charged (negative) molecules and decreased adsorption of materials with the same charge (Myers 1999).

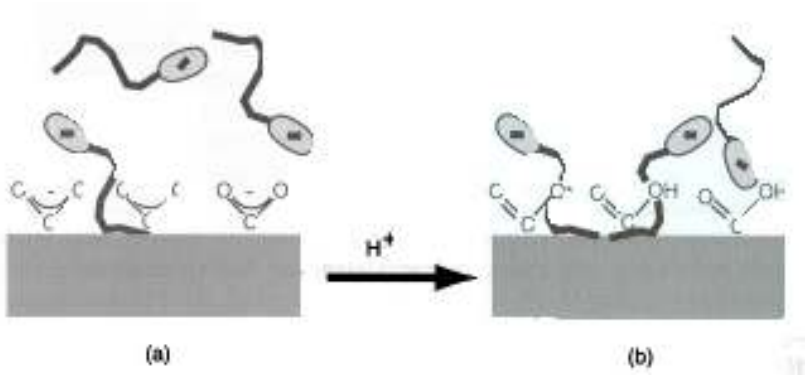

Figure 2-31 Effect of pH on adsorption (Myers 1999)

For ionic surfactants, an increase in temperature results in a decrease in the adsorption of these surfactants. The change caused by temperature is usually small when compared to those due to pH and electrolyte changes. For nonionic surfactants the opposite is true, i.e., the adsorption will increase as the temperature increases. The reason is that they are solubilized by hydrogen bonding and have an inverse temperature-solubility relationship (Ziegler and Handy 1981; Myers 1999).

2.5.4 Effect of Adsorption on the Nature of the Solid Surface

The dominant mechanism of adsorption is responsible for the changes in the nature of the solid surface. For highly charged surfaces, adsorption by ion exchange will not alter the electrical nature of the solid surface. However, when adsorption by ion pairing becomes the dominant mechanism, complete neutralization of the surface may happen. In addition, surfactant adsorption by ion exchange or ion pairing results in the orientation of the surfactant molecules with their hydrophobic groups toward the aqueous phase and their hydrophilic groups toward solid surface. This causes the surface to become more hydrophobic and adsorption can continue by dispersion force interactions as shown in **Figure 2-32**. When this happened, the charge on the surface will be reversed, since the hydrophilic groups will now be oriented toward the aqueous phase (Myers 1999).

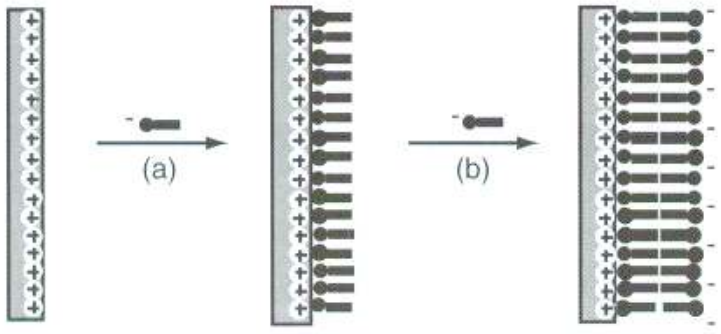

Figure 2-32 Effect of adsorption on solid surface nature (Myers 1999)

2.6 Wettability Alteration Using Surfactant

Enhanced oil recovery by wettability alteration of the reservoir rock is the main subject in this work. The subject has been tested in laboratory by performing imbibition tests on sandstone and carbonate cores. Several mechanisms are proposed in the literature for wettability alteration using surfactants, but none have been verified experimentally. In 1998 Austad *et al*. and Milter (1996; 1998) observed improved imbibition rates with the cationic surfactant dodecyltrimethylammonium bromide (C12TAB) present in the aqueous phase for initially oil-wet chalk cores and related that to the ability of the surfactant to make the chalk surface more water-wet. They tried to explain the mechanism behind wettability alteration by proposing that the selected surfactant partitioned between the aqueous and oil phase and formed reverse micelles in the oil phase. The water dissolved in these micelles may act as a powerful nucleophile toward the chalk surface and results in water adsorption onto the chalk surface. This makes the surface more water-wet and improves the imbibition process. This mechanism is shown in **Figure 2-33**.

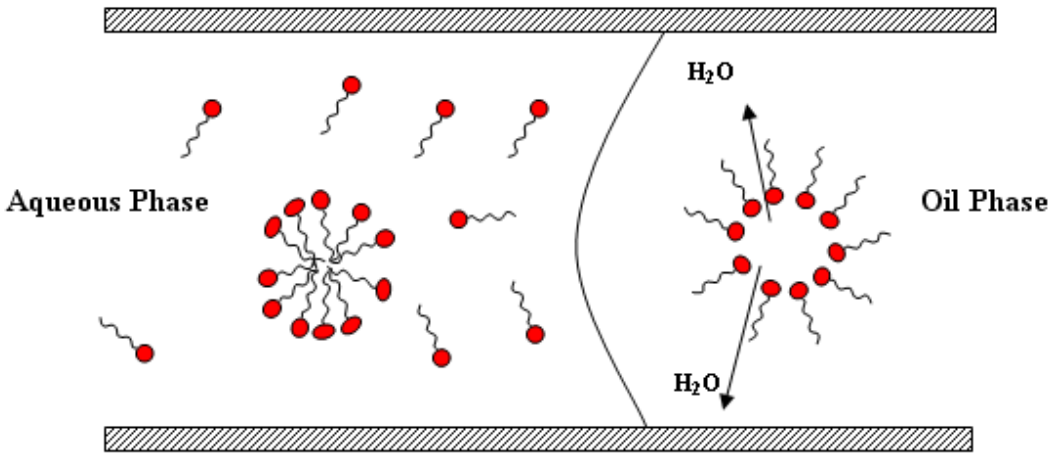

Figure 2-33 Proposed model for wettability alteration using cationic surfactant C12TAB (Austad, Matre et al. 1998)

In 2000 Standnes and Austad (2000) proposed another set of wettability alteration mechanisms describing both cationic and anionic surfactants on oil-wet chalk cores. Based on experimental results, in the case of cationic surfactant C12TAB, they proposed that ion-pair formation between the positive head groups of the surfactant monomers and the negatively charged adsorbed material, mostly carboxylic groups from crude oil on the surface of the chalk, is the mechanism responsible for making the core more water-wet. This ion-pair formation driven by electrostatic interaction was also stabilized by hydrophobic interactions. The process is shown schematically in **Figure 2-34**. The imbibition mechanism is proposed as (1) the formation of ion-pairs by the interaction between surfactant monomers and adsorbed organic carboxylates from the crude oil, (2) water-wettability of the solid surface due to dissolution of the ion-pair in the oil phase and micelles, (3) counter-current imbibition

of brine due to capillary pressure. They also observed an increase in imbibition rate with temperature and a decrease with initial water saturation. They found that most of the anionic surfactants tested were not able to desorb adsorbed organic carboxylates. Anionic surfactants on the other hand may change the wettability of the oil-wet surface by forming a surfactant double layer. The surfactant adsorbs with the hydrophobic part onto the hydrophobic surface of the chalk as shown in **Figure 2-35**, leaving the water soluble head-group toward the solution. This will result in forming a small water zone and creating weak capillary forces during the imbibition process. Due to the weak hydrophobic interactions, this process could be reversible. Knowledge of the mechanisms behind wettability alteration could help to improve the performance of the process and also aid in identification of alternative surfactants for use in field applications. In this study, the proposed mechanisms were tested experimentally through observations of surfactant adsorption isotherms and Amott-Harvey wettability indices in oil-wet synthetic and crude oil-aged sandstone core plugs.

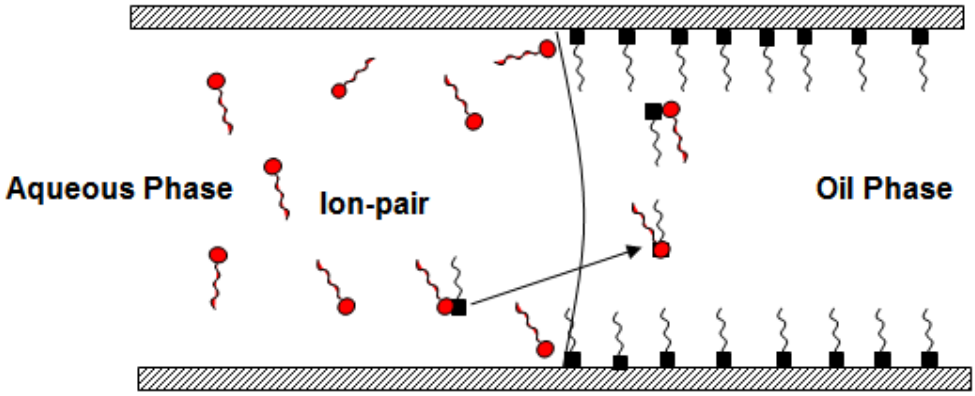

Figure 2-34 Schematic model of suggested wettability alteration mechanism by cationic surfactant C12TAB. Circles are cationic surfactant monomers and squares are anionic organic materials from crude oil (Standnes and Austad 2000)

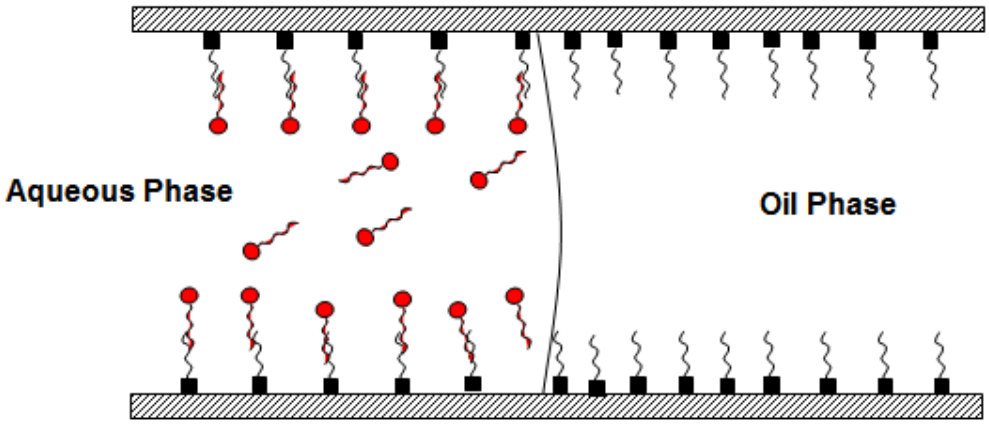

Figure 2-35 Schematic model of suggested wettability alteration mechanism by anionic surfactant and bi-layer formation. Circles are anionic surfactant monomers and squares are anionic organic materials from crude oil (Standnes and Austad 2000)

3 Materials and Experimental Procedures

This chapter describes the materials and experimental procedures used in this research. The first section goes through the materials used. Experimental procedure and equipments used during core cleaning, core flooding, tracer tests, IFT measurements, imbibition tests, adsorption test, and titration tests are described in the second part.

3.1 Materials

3.1.1 Aqueous phases

A sample of the Lansing Kansas City C zone brine analysis was provided by Dr. Allan Byrnes from Kansas Geological Survey (KGS). Early studies showed that biosurfactants (surfactin) will precipitate using this brine as the aqueous phase, so deionized water was used in most tests. The distilled water used was a reverse-osmosis (RO) water (18 MΩ) produced in our lab. For tests involved sandstone cores, a 10 g/l solution of NaCl was used to avoid clay swelling. A few tests were performed using brine described by Standnes and Austad termed Brine 1. Table 3.1 lists the components and their corresponding composition of the all brines used. Table 3.2 summarizes the density and viscosity of all the phases at room temperature (25°C) and at reservoir temperature (45°C).

Table 3.1 Composition of brines

	Composition (g/l)	
Component	LKC brine	Brine 1
Ca^{2+}	6.15	3.43
Mg^{2+}	2.17	0.93
Na^{+}	30.31	12.14
K^{+}	0.14	0.25
$HCO3^{-}$	0.05	0.09
SO_4^{2-}	0.05	1.56
Cl^{-}	63.77	26.54
Total	102.64	44.94

Table 3.2 Physical properties of aqueous phases at room and reservoir temperature

Fluid ~~Temperature~~	Room (25°C)		Reservoir (45°C)	
Property	ρ (g/cm^3)	μ (cp)	ρ (g/cm^3)	μ (cp)
RO-water	0.996	0.92	0.981	0.61
10 g/l Brine	1.021	0.92	0.997	0.61
Brine 1	1.015	0.96	0.979	0.63

3.1.2 Surfactants

Synthetic commercial anionic and cationic surfactants, a biosurfactant (surfactin), and a Gemini surfactant were used in this study.

3.1.2.1 Synthetic commercial surfactants

Three anionic chemical surfactants were obtained from Stepan Chemical Company. **Figure 3-1** shows the chemical structure of these surfactants. Table 3.3 summarizes the properties of these surfactants based on the Certificate of Analysis provided by Stepan Chemical Company. These surfactants were dissolved in deionized water to the desired concentration. The cationic surfactant dodecyltrimethylammonium

bromide (C12TAB, MW = 308.4) was obtained from Sigma as a 99 % pure powder and dissolved in deionized water or brine as required. The molecular structure is shown in **Figure 3-2**.

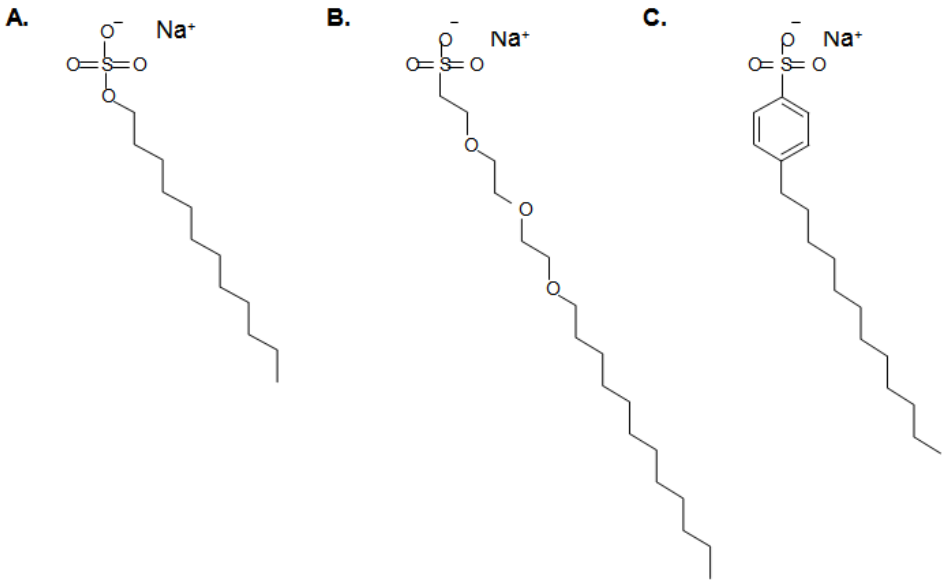

Figure 3-1 Anionic chemical surfactants: A. Sodium dodecyl sulfate (SDS), B. Sodium laureth sulfate (SLS), C. Sodium dodecylbenzene sulfonate

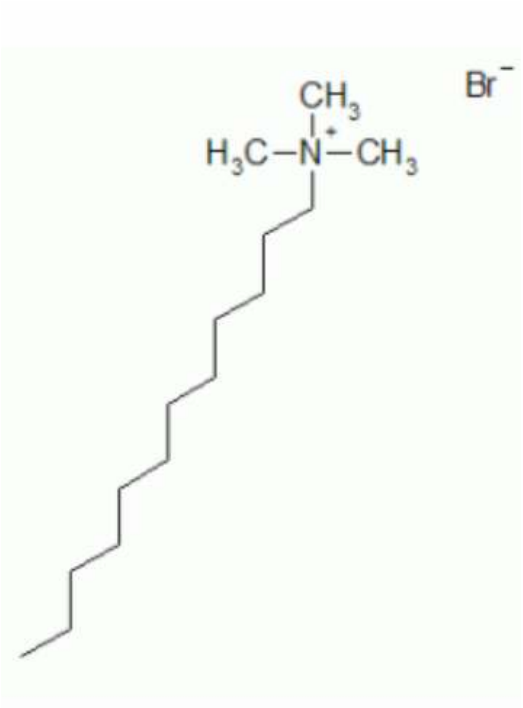

Figure 3-2 Cationic surfactant chemical structure

Table 3.3 Properties of anionic chemical surfactants

Surfactant	**STEPANOL WA-EXTRA**	**STEOL CS-330**	**BIO-SOFT D-40**
Lot No.	7106243	7071688	710385
Synonyms	Sodium lauryl sulfate, Sodium dodecyl sulfate, SDS	Sodium laureth sulfate, SLS	Sodium dodecylbenzene sulfonate
Appearance @ 25°C	Clear liquid	Clear liquid	39.71% solids
Appearance @ 30°C			Clear liquid
pH (10% in H_2O)	7.71	8.36	7.59
Active component	28.55 %	29.14 %	38.93 %
Unsulfated alcohol	0.38 %	0.1 %	0.59 %
Color transmittance (420 nm)	91 %	92.5 %	41 %
Viscosity	90 cp	73 cp	
Cloud point	10°C	5°C	
Formaldehyde	400 ppm	484 ppm	
CMC	8.18×10^{-3} mol/L (@ 25 °C)	1.00×10^{-4} mol/L (@ 25 °C)	1.19×10^{-3} mol/L (@ 75 °C)

Source: Certificate of Analysis by Stepan Chemical Co.

3.1.2.2 Gemini surfactant

Gemini surfactants are a new class of surfactants where two surfactant monomers are attached through a spacer such as -$(CH_2)_2$-, as shown in **Figure 3-3**.

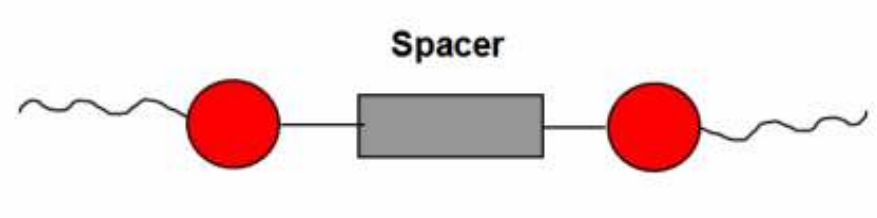

Figure 3-3 Molecular structure of Gemini surfactants

A sample of a Gemini surfactant was obtained from Oil-Chem Company. The sample received was a xylene di C14/16 sulfonate surfactant. It was received in a 100 % active acid form and was dissolved in distilled water and neutralized with NaOH to form a water soluble salt. The Chemical Abstracts Service (CAS) name is di-tetradecane sulfonic acid (dimethylphenyl) and di-hexanedecane sulfonic acid (dimethylphenyl) with an average molecular weight of 746. The molecular formula is shown in **Figure 3-4**.

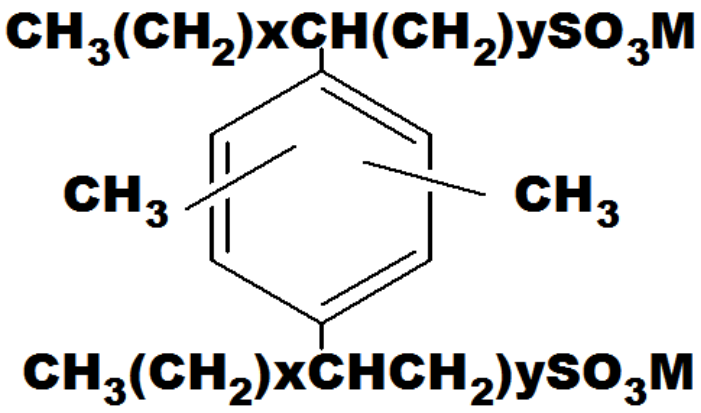

Figure 3-4 Chemical molecular of sulfonate Gemini surfactant

3.1.2.3 Biosurfactant

The biosurfactant (surfactin) used in this research was prepared and characterized by Mr. Greg Bala and Ms. Sandra Fox at Idaho National Lab (INL). This crude surfactin extract was received at KU and diluted in deionized water to desired concentration for testing. It was determined by surfactant concentration testing that the active surfactin concentration of the crude surfactin produced at INL was approximately 40-60% by weight for different batches received. Chemical structure of this surfactant is shown in **Figure 3-5**.

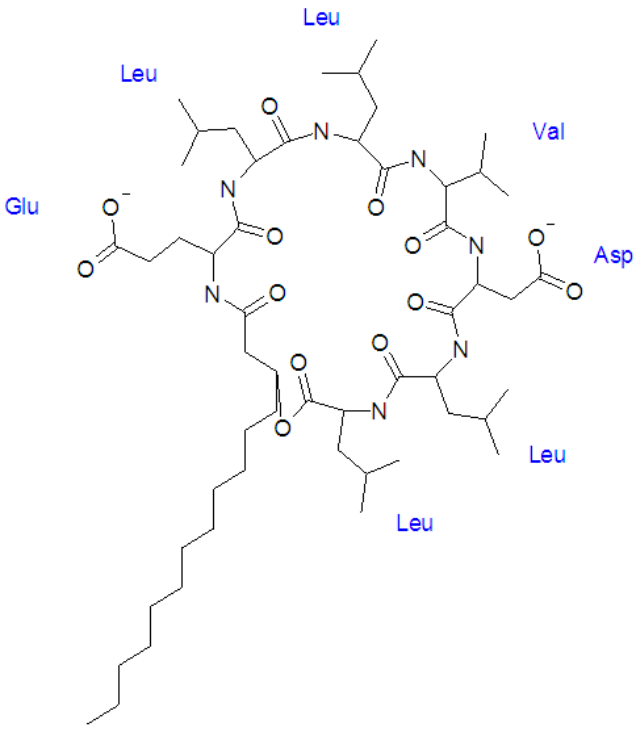

Figure 3-5 Surfactin molecular structure
(Drawn by Stephen Johnson, used by permission)

Surfactin was prepared and characterized by INL and was sent to KU for further studies. Surfactin was produced by growing *Bacillus subtilis* strain 21332 on high-starch industrial and agricultural waste effluents (Cooper, MacDonald et al. 1981; Gallet, Deleu et al. 1999; Morikawa, Hirata et al. 2000; Grangemard, Wallach et al. 2001; Heerklotz and Seelig 2001). This crude surfactin preparation was diluted in RO-water as required for subsequent testing. Surfactin was checked for stability in brine and found to be sensitive to salt concentration, especially that of divalent cations. In order to avoid precipitation of surfactants, all aqueous tests were performed using deionized water. Surfactin is an anionic, amphiphilic, lipopeptide

compound with a molecular weight (MW) of approximately 1047 g/mol. These properties are the reason for its ability to lower surface tension so effectively (Dworkin 1991; Gallet, Deleu et al. 1999). Its cation-complexing property, due to two negative charges on the aspartyl and glutamyl residues, is probably fully utilized in systems containing ubiquitous amounts of Ca^{++} and Na^{+} ions. Critical micelle concentrations (CMC) at 25 °C reported in the literature are 7.5 μmol/l (Heerklotz and Seelig 2001), 9.4 μmol/L (Ishigami, Osman et al. 1995), and 0.025 g/l (24.1 μmol/l). Surfactin CMCs measured at INL are in the range 140-450 ppm depending on the medium, with a value of 0.23 g/L (221 μmol/L) in the mineral salts medium and 0.16 g/L (154 μmol/L) in a portion of crude surfactant from a simulated potato medium purified with methylene chloride.

3.1.3 Oils

Laboratory grade dodecane was first used for saturating the cores and core flooding tests. The density and viscosity of the oil at 25°C are 0.745 g/cm^3 and 1.35 cp respectively. Its viscosity at 45°C is 1.0 cp. Later Soltrol 130 (Chevron Philips Chemical Company), a commercial mixture of C10-C13 isoalkanes, was used as oil phase in all IFT measurements, imbibition and flow tests. Soltrol 130 density and viscosity at 25°C are 0.754 g/cm^3 and 1.42 cp respectively.

A crude oil sample was obtained from the Lansing - Kansas City field C Zone at ~880 m (~2900 ft). The oil was used to restore the wettability of the field cores to their original wetting state, and modify the wettability of the outcrop cores by aging the core plugs in the stabilized crude oil at elevated temperatures. Crude oil from the same field had

previously been characterized by TORP staff and the components are given in Table 3.4.

Table 3.4 LKC crude oil composition

Component	SCN	Mole %	Weight %	Density (g/cm^3)	MW	Volume %
≤ iso-Butane	3	0.45	0.1	0.507	44.1	0.17
n-Butane	4	3.95	1.16	0.584	58.1	1.64
iso-Pentane	5	1.45	0.53	0.624	72.2	0.7
n-Pentane	5	5.13	1.87	0.631	72.2	2.45
Hexanes	6	7.14	3.03	0.685	84	3.65
Heptanes	7	10.81	5.24	0.722	96	6
Octanes	8	11.99	6.48	0.745	107	7.19
Nonanes	9	8.53	5.21	0.764	121	5.63
Decanes	10	6.87	4.65	0.778	134	4.94
Undecanes	11	5.87	4.36	0.789	147	4.57
Dodecanes	12	4.44	3.61	0.8	161	3.73
Tridecanes	13	4.57	4.04	0.811	175	4.11
Tetradecanes	14	3.7	3.55	0.822	190	3.57
Pentadecanes	15	3.29	3.42	0.832	206	3.4
Hexadecanes	16	2.68	3	0.839	222	2.96
Heptadecanes	17	2.43	2.91	0.847	237	2.84
Octadecanes	18	2.23	2.83	0.852	251	2.74
Nonadecanes	19	1.93	2.57	0.857	263	2.48
Eicosanes	20	1.58	2.2	0.862	275	2.11
Heneicosanes	21	1.18	1.73	0.867	291	1.65
Docosanes	22	1.29	1.98	0.872	305	1.88
Tricosanes	23	1.06	1.7	0.877	318	1.6
Tetracosanes	24	0.9	1.5	0.881	331	1.4
Pentacosanes	25	0.76	1.32	0.885	345	1.23
Hexacosanes	26	0.76	1.38	0.889	359	1.28
Heptacosanes	27	0.71	1.35	0.893	374	1.25
Octacosanes	28	0.66	1.3	0.896	388	1.2
Nonacosanes	29	0.51	1.03	0.899	402	0.95
≥ Triacontanes	30	3.13	25.95	0.945	1641.6	22.69
TOTAL		100	100			100

This crude oil has a density of 0.82 g/cm^3 and a viscosity of 4.58 cp at 45°C. It was centrifuged and then filtered through a 2.7 μm cellulose filter before use. The crude oil has a base (2007) and acid number (2007) of 0.12 and 2.38 mg KOH/g oil respectively. Mineral oil was used for filling the syringe and the hydraulic pump. It has a density and viscosity of 0.852 g/cm^3 and 1.2 cp at 25°C.

3.1.4 Core Materials

Core materials were obtained from several sources (Table 3.5). These include high permeability oolitic limestone outcrop from Florida and the Bahamas as well as low-to-medium permeability oomoldic outcrop and reservoir samples from Missouri and Kansas. Cores were provided by Alan Byrnes, Kansas Geological Survey (KGS). Porosity and permeability of the cores were measured as part of the characterization work.

The core materials exhibit a variety of pore architectures (oolitic vs. oomoldic) and porosity, and as a result, they represent a wide range of permeability. The different pore architectures will have a great influence on the residual oil saturation. Large pores, combined with small pore throats resulting in high aspect ratio as seen in oomoldic material favors trapping of oil.

Table 3.5 Characterization of different core materials

	Miami Outcrop	Bethany Falls Outcrop	Heartland Quarry LKC Outcrop	Joulters Cay Outcrop	Luerman #7 LKC Reservoir	Luerman #7 LKC Reservoir (1-inch)
Abbreviation	M	BF	HQ	JC	L7	L7B
Structure	Oolitic	Oomoldic	Oomoldic	Oolitic	Oomoldic	Oomoldic
Porosity	0.31 (M01) 0.42 (M02)	0.21 (BF01) 0.21 (BF02) 0.22 (BF03)	0.31 (HQ01) 0.22 (HQ02)	0.43 (JC01)	0.26 (L701) 0.25 (L702) 0.24 (L703)	0.22 (L7B1) 0.23 (L7B2) 0.22 (L7B3)
Permeability (md)	5 (M01) 320 (M02) 100 (M03)	0.7 (BF01) 2.1 (BF02) 16 (BF03)	43 (HQ01) 2 (HQ02)	1100 (JC01)	43 (L701) 16 (L702) 13 (L703)	23 (L7B1) 20 (L7B2) 13 (L7B3)
Bulk density (g/cm^3)	1.43	2.09	1.84 – 2.02	2.05	2.05 - 2.09	2.05 - 2.09
Grain density (g/cm^3)	2.09	2.67	2.68	2.67	2.67	2.67

For the part of the thesis dealing with the mechanistic studies of wettability alteration by surfactants, Berea sandstone cores along with synthetic polyethylene cores were used. Berea cores were cut from larger plugs available in lab and synthetic cores were obtained from Pore Technology Company, Inc. Table 3.6 summarizes the properties of these cores.

Table 3.6 Characterization of sandstone and synthetic core materials

	Berea Sandstone	Polyethylene Synthetic cores
Abbreviation	B	S
Porosity	0.21 (B02) 0.21 (B03) 0.21 (B04) 0.21 (B05) 0.21 (B06) 0.21 (B07)	0.33 (S02) 0.31 (S03) 0.32 (S04)
Permeability, md	490 (B02) 510 (B03) 590 (B04) 560 (B05) 512 (B06) 480 (B07)	560 (S02) 550 (S03) 580 (S04)
Bulk density, g/cm^3	2.08	0.55
Grain density, g/cm^3	2.63	0.87

3.2 Procedures and Equipments

3.2.1 Core cleaning

In order to compare the effectiveness of different treatments on the same core and being able to "restore" (Hirasaki, Rohan et al. 1990) the core state, it is important that the core can be cleaned to a repeatable initial state. Restored state analysis requires that the core be cleaned to the water-wet state that existed before oil accumulated in the formation. The core is then saturated with crude oil to a capillary pressure typical of the formation and the system allowed to equilibrate or "age" under formation conditions. The traditional method for cleaning core samples is Dean-Stark extraction, which usually involves boiling toluene followed by a mixture of chloroform and methanol. In a study performed by Hirasaki *et al*. (1990) it was found

that Dean-Stark extraction alone was insufficient in making North Sea reservoir cores water-wet; Soltrol 130 oil used to evaluate wettability after a first cleaning was visibly discolored. Hirasaki recommended employing a sequence of solvents to clean the cores further. During cleaning, effluent was analyzed by UV-visible spectrophotometry and gas chromatography. Concentrations of solutes in the effluent were found to be much greater if the system had been shut-in overnight than in that of "flowing" concentrations; greater contact time led to better adsorption of solutes. Testing of effluent indicated that the solvents were extracting a significant amount of crude oil and prior solvents even when the effluent looked colorless. The sequence found to be most effective for cleaning cores is to first flush with tetrahydrofuran (THF), chloroform, and then methanol, and finally water (Hirasaki, Rohan et al. 1990). Core cleaning was performed in a fume hood and **Figure 3-6** shows the setup for one of the cores. Initially a gear pump was used to inject he solvents into the cores, but due to the low permeability values, the pump was not able to overcome the pressure gradient across the core. So, a glass transfer cylinders and a Consta Metric pump were used in the cleaning set-up as shown in **Figure 3-6**. The cleaning procedure was modified as follows:

1. flood the core with THF for 4 days
2. flood the core with chloroform for several days
3. inject methanol into the core for 4 h
4. flood the core with water and let it to dry to constant weight in oven at 90°C

Glass transfer cylinders were filled with solvent to be used for cleaning above the piston and RO-water below. The glass transfer cylinders were placed in a fume hood with a stand; 1/16 inch plastic tubing was connected from a pump to the glass column base and PEEK tubing was connected from the column top to the core. The pump forces oil into the top of the transfer cylinder, which in turn pushes water into the bottom of the glass column, this moves the Teflon piston, which pushes the solvent from the top of the column through a length of PEEK tubing and into the core. For each core approximately 2 pore volumes of tetrahydrofuran (THF) was injected daily until the effluent was no longer colored. THF was displaced by injecting at least 2 PV chloroform ($CHCl_3$) daily for several days. Finally, the chloroform was displaced with several PV of methanol (CH_3OH) and the methanol was displaced with several PV of RO water. The core was then oven dried. The crushed rock used in static adsorption tests and in qualitative wettability tests were also cleaned by the same series of solvents.

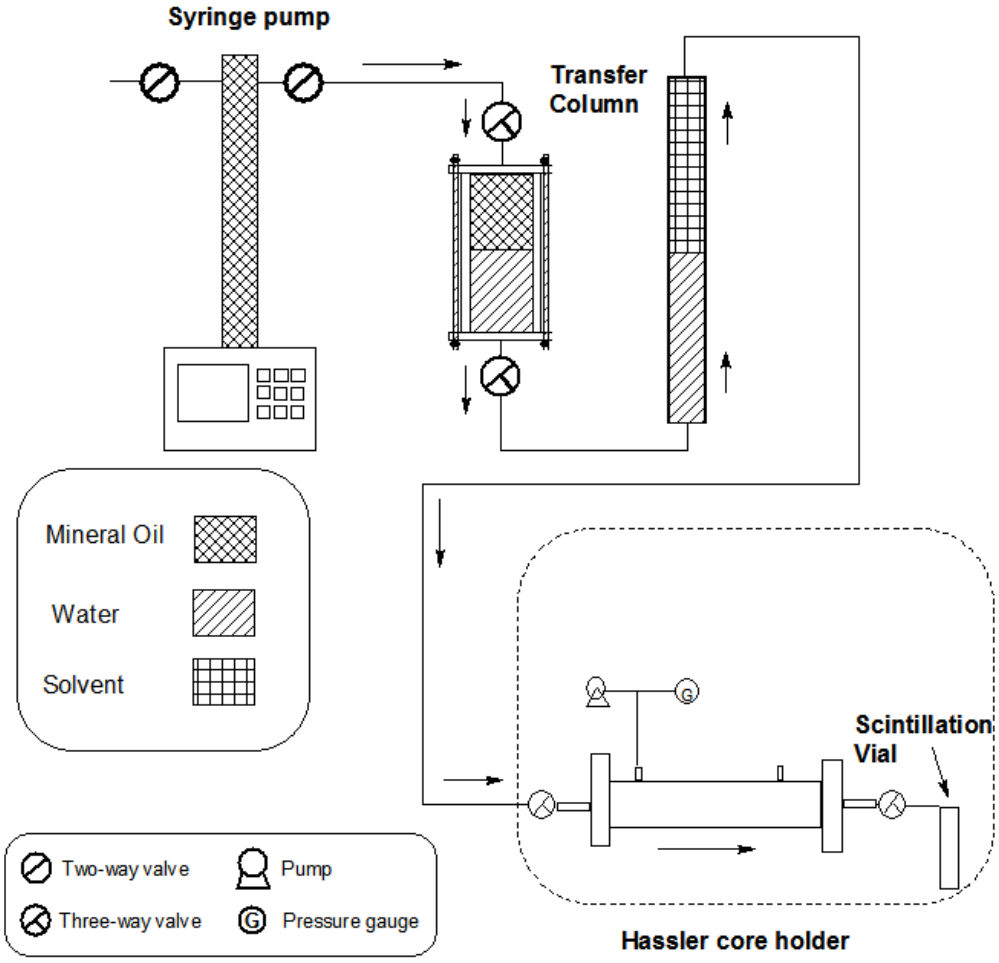

Figure 3-6 Core cleaning set up (modified after Stephen Johnson, used by permission)

The Viton sleeve used in the core holder was found to be sensitive to THF and chloroform, and was damaged by both solvents. The cores, along with the distribution plugs, were shrink-wrapped using FEP Teflon heat-shrinkable tubing (Zeus Industrial Products Inc, Orangeburg, SC) as shown in **Figure 3-7** and placed in an oven at 190°C before cleaning to isolate the cores from the core sleeves. This protects the sleeve from the solvents being used.

Figure 3-7 Core and distribution plugs covered with Teflon heat shrink material

3.2.2 Core characterization

Core characterization includes saturation, flooding and tracer tests in order to determine the pore volume, porosity, permeability, and the degree of homogeneity for each core. Two identical temperature controlled cabinets were used for core flow testing and tracing. Cabinet "A" was used primarily for water/brine flooding and water tracer test, and cabinet "B" was used primarily for oil flooding and oil tracer test. Temperature was maintained at 45 °C in both cabinets.

3.2.2.1 Core dimensions measurements

Five measurements of the diameter and length were obtained for each core and the average values used to calculate the area and the bulk volume of the cores. The dry weight was obtained using an analytical balance.

3.2.2.2 Core saturating

Before saturating, the cores were dried to constant weight. Dried cores were placed in a Hassler-Type core holder and overburden pressure in the range of 400-800 psi was applied using oil from a manual pump (Enerpac Model P392) to form a tight seal between core and core sleeve as shown in **Figure 3-8.** Vacuum was applied to the core for 30 minutes. The saturating fluid (RO-water, Brine, or Soltrol 130) was degassed in a container by sparging with helium gas for at least 30 minutes. Valves on both ends of the core holder were closed to isolate the core, and an inlet line was filled with the saturation fluid and connected to one end of the core holder. The other end of the inlet line was placed in a container of the saturation fluid; by opening the inlet valve saturation fluid was allowed to spontaneously enter the core for at least 30 minutes. An estimate of the pore volume could be obtained from the volume of fluid imbibed into the core.

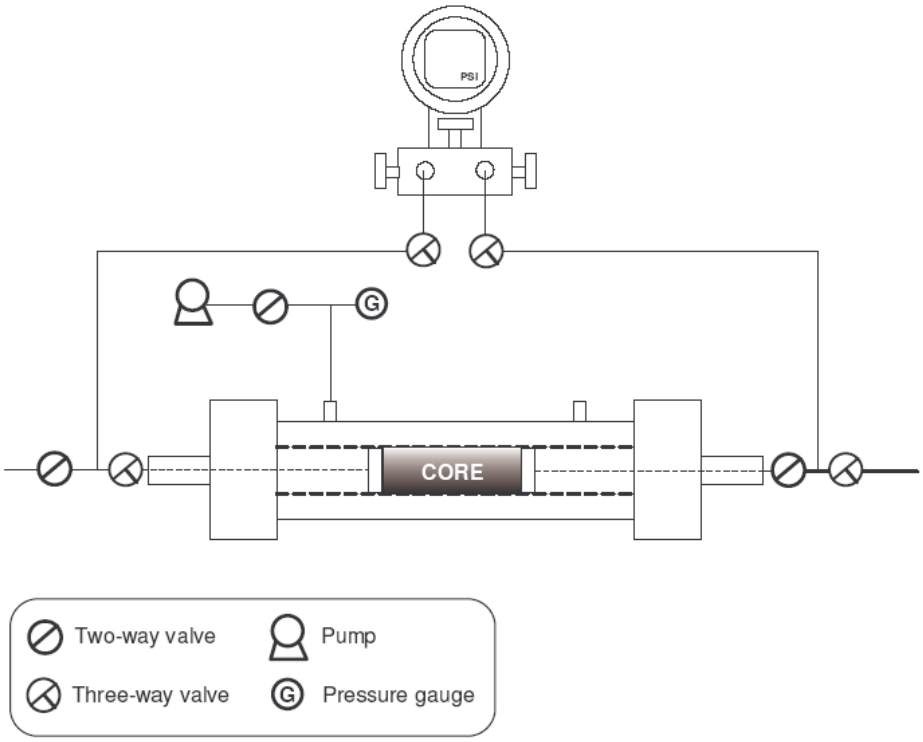

Figure 3-8 Hassler-Type core holder (Drawn by Stephen Johnson, used by permission)

Finally, the core was transferred to one of the flow cabinets (A or B) and flooded with several pore volumes of the same fluid used during core saturation with a 40 psi backpressure regulator (BPR) attached to the fluid outlet in order to pressurize any gas in the core back into solution. In the case of synthetic polyethylene cores, these cores were preferentially more air-wet than water-wet and lost water by gravity drainage as soon as the cores were taken out of the Hassler-Type core holder (**Figure 3-9**). To ameliorate this problem, all the imbibition tests on these cores were performed while the cores were contained in a specially designed core holder (**Figure 3-10**).

Figure 3-9 Synthetic cores losing water in contact with air

Figure 3-10 Core holder used for synthetic cores to reduce draining during exposure to air

3.2.2.3 Core flooding

During core flooding, a saturated core (inside a Hassler-Type core holder) was placed in an appropriate cabinet for RO-water/brine or Soltrol 130 flooding. **Figure 3-11** shows the flow set up used during core flooding. Pumps and fluid transfer cylinders were checked and filled as necessary before starting a flood. Tubing lines (1/8" ID Stainless Steel) leading to and from the transducer were injected with Soltrol 130 oil using a syringe to ensure that no air could get into the transducer. Overburden pressure in the range of 400-800 psi was applied to the cores using an overburden pump to ensure good contact between the core and core sleeve. Flow rates were adjusted to give a desired pressure drop. Mineral oil from the syringe pump (ISCO 500D) entered the first transfer cylinder and then depending on the fluid to be injected into the core, the values were manipulated to control the fluid flow.

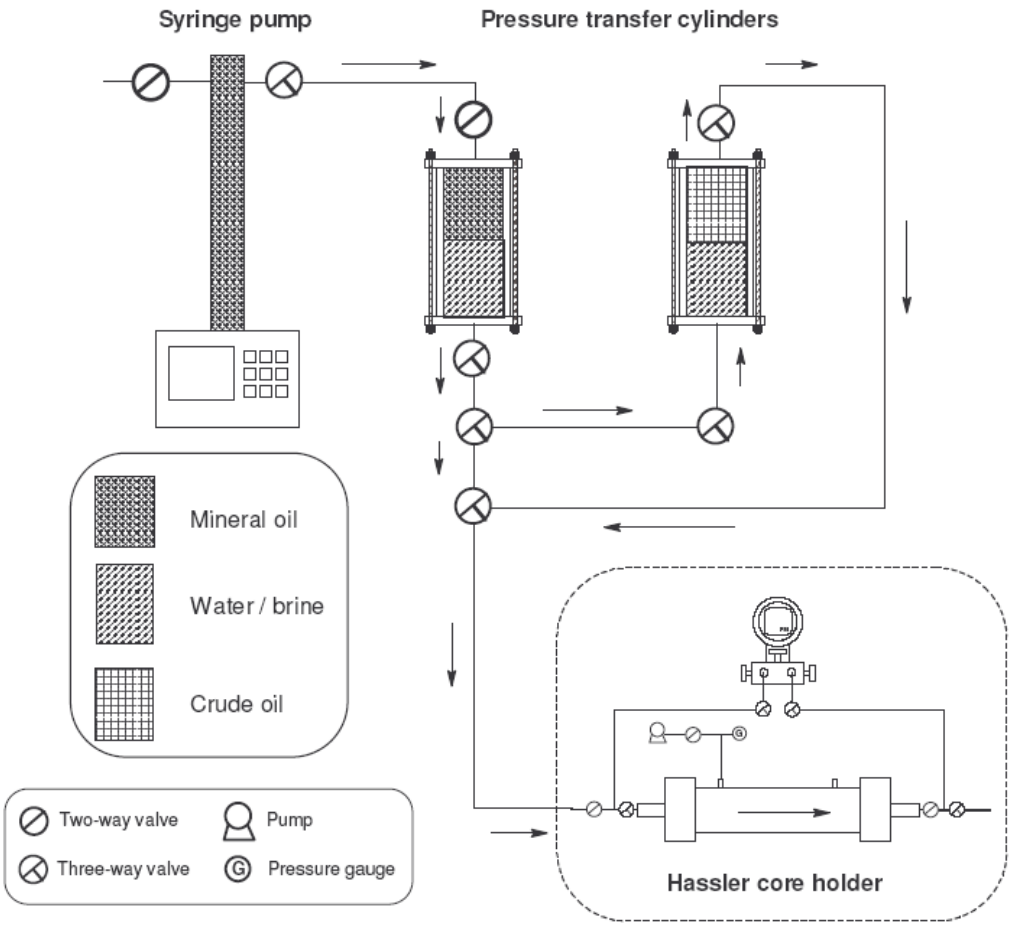

Figure 3-11 Schematic of flow set up (drawn by Stephen Johnson, used by permission)

LabView (National Instruments Corporation) software was used during core flow experiments to record real-time variables of pressure drop, flow rate, permeability, and tracer concentration. A picture of the LabView software screen is shown in **Figure 3-12**.

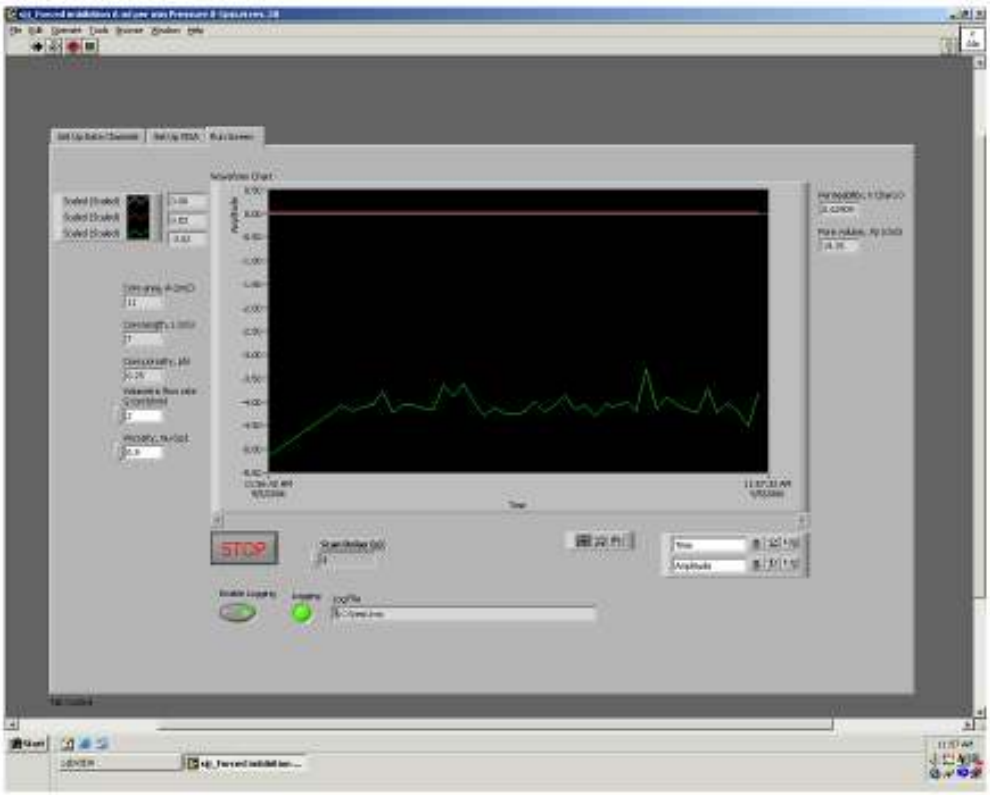

Figure 3-12 Data Acquisition software (LabView)

After inputting the required parameters into the software, a log file was created for each specific core and test with the date specified (example: 2008_08_25 B01 Brine flood in cabinet A) and flow test started after that. During the flow tests, the injection flow rate was changed several times to make sure that the same permeability values were obtained and check for any leakage in the set up. Permeability of each core was calculated from Darcy's Law and recorded by Labview as:

$$k = q\left(\frac{\mu}{A}\right)\left(\frac{L}{\Delta P}\right) \qquad (3.1)$$

where

q = flow rate (cm^3/s)

k = permeability (Darcies)

A = area (cm^2)

μ = viscosity (cp)

ΔP = pressure drop (atm)

L = length (cm)

After the flow test was over, the core holder confining pressure was released and the core was taken out and the saturated weight was recorded for pore volume and porosity calculation. Each core's pore volume, and hence porosity, was determined from up to 4 independent measurements: weight of core at 100% RO water saturation, potassium nitrate (KNO_3) water tracer calculation, weight of core at 100% Soltrol 130 saturation, and *trans*-stilbene oil tracer calculation. Core pore volumes (volume taken up by fluid at 100% saturation) were calculated gravimetrically according to the equation:

$$PV = \left(\frac{W_s - W_d}{\rho} \right) \qquad (3.2)$$

where

PV = pore volume, cm^3

W_s = saturated core weight

W_d = dry core weight

ρ = density of fluid saturating the core, g/cm^3

Core porosities were calculated:

$$\phi = \left(\frac{PV}{BV} \right) \qquad (3.3)$$

where

ϕ = porosity, fractional

PV = pore volume, cm^3

BV = bulk volume, cm^3

3.2.2.4 Tracer tests

In order to verify the homogeneity of a sample core, tracer tests were performed. Tracer tests may also be performed to calculate the pore volume (PV) of fluid in a core, either from 100% saturation or from a residual saturation. A tracer is an injected substance that is both measurable (e.g. through UV-visible detection) and conserved (i.e. not retained, destroyed or created by the core). If tracer concentration at the outlet of the core being tested is recorded against time, an S-shaped tracer curve will form. This S-shape is caused by dispersion (mixing and diffusing of the two fluids); if there were no dispersion there would be an instantaneous change to tracer concentration when breakthrough occurred at 1 PV. The symmetry of the curve is an indicator of homogeneity; a perfectly homogeneous core will have a perfect S-shape. Several primary assumptions are made in tracer testing (Green and Willhite 1998):

- Fluid B is displacing Fluid A, and the two fluids are miscible
- There is no viscous fingering of one fluid into another, only dispersion
- Flow is single phase

- Fluids are incompressible
- Fluids are of equal density
- Flow is in only one direction
- Fluid velocity is constant
- Flow is through a porous medium of constant porosity and cross-sectional area

These are all reasonable assumptions for the experiments performed in this research with oil and water tracers displacing pure oil and water, respectively in core samples. Theoretically, for a homogeneous core PV is indicated at the time when effluent tracer concentration reaches 50% of injected concentration, that is, at a normalized tracer concentration of 0.5. Tracer data is typically normalized to scale the tracer concentration values from zero to one.

Normalized concentration is calculated as:

$$C_B = \frac{(C_B^* - C_{BO})}{(C_{Bi} - C_{BO})} \qquad (3.4)$$

where

C_B = normalized tracer concentration

C_B^* = measured tracer concentration

C_{Bi} = injected or maximum tracer concentration

C_{B0} = initial concentration of fluid B in the system

Core PV can then be calculated as:

$$PV = \left(\left(t_{50} - t_o\right) \times q\right) - d_v \qquad (3.5)$$

where

t_{50} = time normalized concentration equals 0.5

t_o = time tracer begun

q = tracer flow rate

d_v = dead volume

Note that any dead volume (tubing etc. filled by tracer solution before or after the core) must be subtracted from the calculated pore volume. However, cores are rarely perfectly homogeneous and so a tracer "tail" typically forms due to core in-homogeneity and/or pore space that is not readily accessible to the main flow paths in the core (Green and Willhite 1998). From the effluent concentration curve the core PV may be calculated by means of an equal area method (**Figure 3-13**). The time that areas on both sides of the normalized concentration curve versus time becomes constant, is used to obtain the core PV as:

$$PV = \left(\left(t_{eq} - t_o\right) \times q\right) - d_v \qquad (3.6)$$

where

t_{eq} = time equal area reached

t_o = time tracer begun

q = tracer flow rate

d_v = dead volume

Again, note that any dead volume in the setup must also be subtracted from the calculated pore volume. A typical normalized tracer curve with a long "tail" is shown

in **Figure 3-13** below. For a perfectly homogeneous core the pore volume calculated by equations 5 and 6 would be identical; the equal area point would lie exactly at a normalized concentration of 0.5

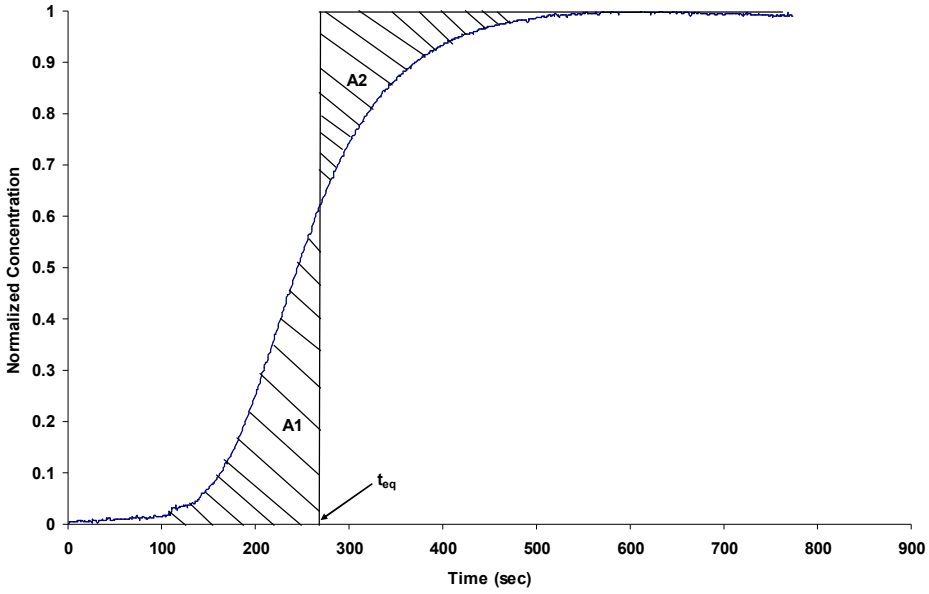

Figure 3-13 Equal area technique in calculating the PV of a core from tracer test

For water-based tracer tests, potassium nitrate can be used as a tracer based on the assumption that there is no retention of potassium nitrate in the cores. Laboratory grade KNO_3 and NaCl can be dissolved in deionized water to form a 0.1 M/L KNO_3, 1% NaCl tracer solution. Two pore volumes of 0.1 M KNO_3 solution in 1% NaCl were injected into a core saturated with 1% NaCl brine solution and displaced by the same pore volumes of 1% NaCl brine solution. The concentration of KNO_3 in the effluent can be detected by an in-line UV spectrophotometer at the wavelength of 302

nm, where the NaCl absorbance is zero, and then it can be plotted as a function of pore volumes injected.

Before performing a tracer test the UV-visible detector was turned on and set to read at a desired wavelength of 302 nm for aqueous tracer and 323 nm for oil tracer. The flow cell of the UV-visible was cleaned before each use by injecting 20 mL of acetone followed by 20 mL of RO-water with a syringe. The UV-visible detector was zeroed after injecting pure RO water or Soltrol 130 as appropriate before beginning a tracer test. The flow diagrams for water and oil based tracer test are shown in **Figure 3-14** and **Figure 3-15** .

Constant flow rates were used when performing tracer tests. When tracer testing at a residual saturation, care was taken that the tracer test pressure drop did not exceed that of the previous flood to establish residual saturation. This is necessary in order to keep the capillary number lower or equal to the previous flood so that no additional residual fluid would be displaced during the tracer test. Before starting flow it was checked that the fluid A and fluid B (tracer) transfer cylinders were both full and connected to the same system pressure. In this setup it was possible to switch the flow between tracer and non-tracer fluid by changing the direction of only one valve. After flow had begun, the flow was allowed to reach steady state with absorbance in the UV-visible detector reading a steady initial value C_{B0}. The valve was switched to tracer injection and concentration values were recorded. The switchover time was recorded in LabView by setting the recorded flow rate to 0.0 ml/min at the exact time

the valve was turned. The flow rate was then changed back again several seconds later. Once the tracer tail was complete, flow was returned to fluid A and the backside of the tracer was recorded to displace the tracer solution from the core. The switchover time was recorded in Lab View exactly as was done before. Once a tracer test was complete the data was exported to an Excel file; graphs were generated showing pore volumes of fluid injected versus normalized tracer values. Areas on each side of the tracer curve were calculated using trapezoidal rule, and the areas were summed until the areas were as closely equal as possible. Pore volume was then calculated by using Equation 3.6. Dead volumes were calculated for each cabinet setup both by separate tracer test calculation and by measurement of fluid injected with a syringe through the tubing lines making up the dead volume.

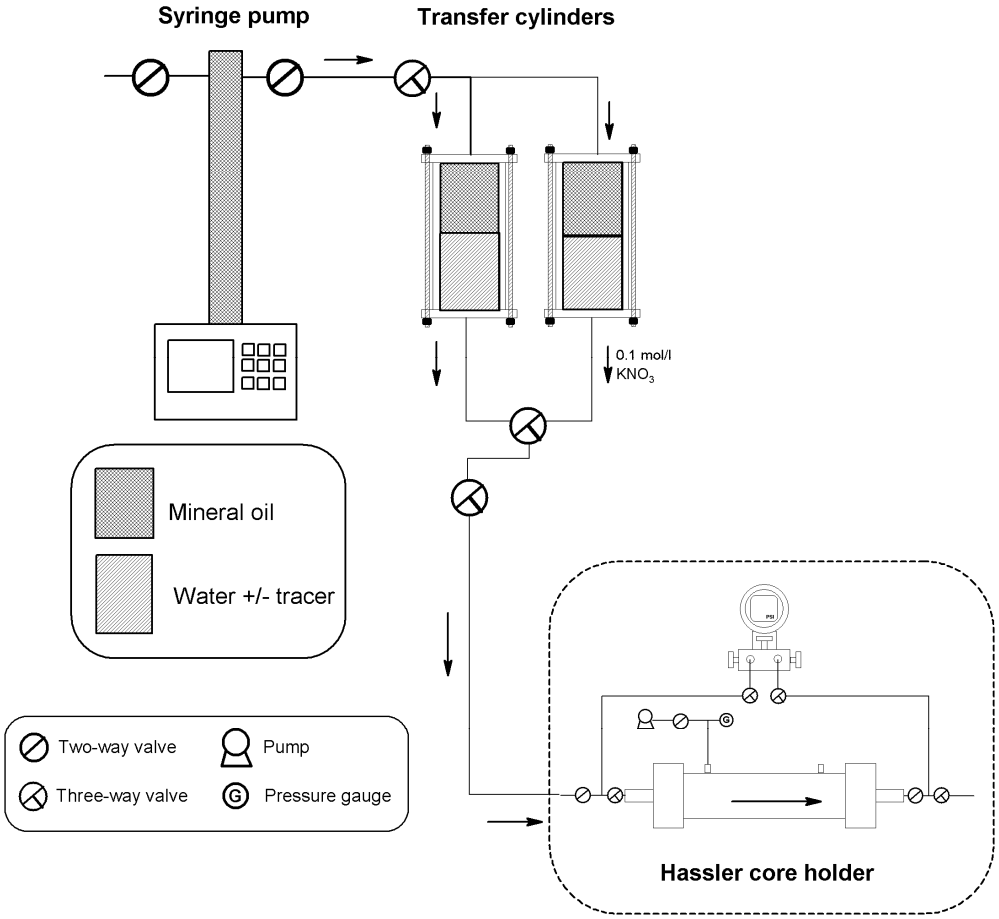

Figure 3-14 Schematic of flow set up during water (0.1 M KNO_3) tracer test

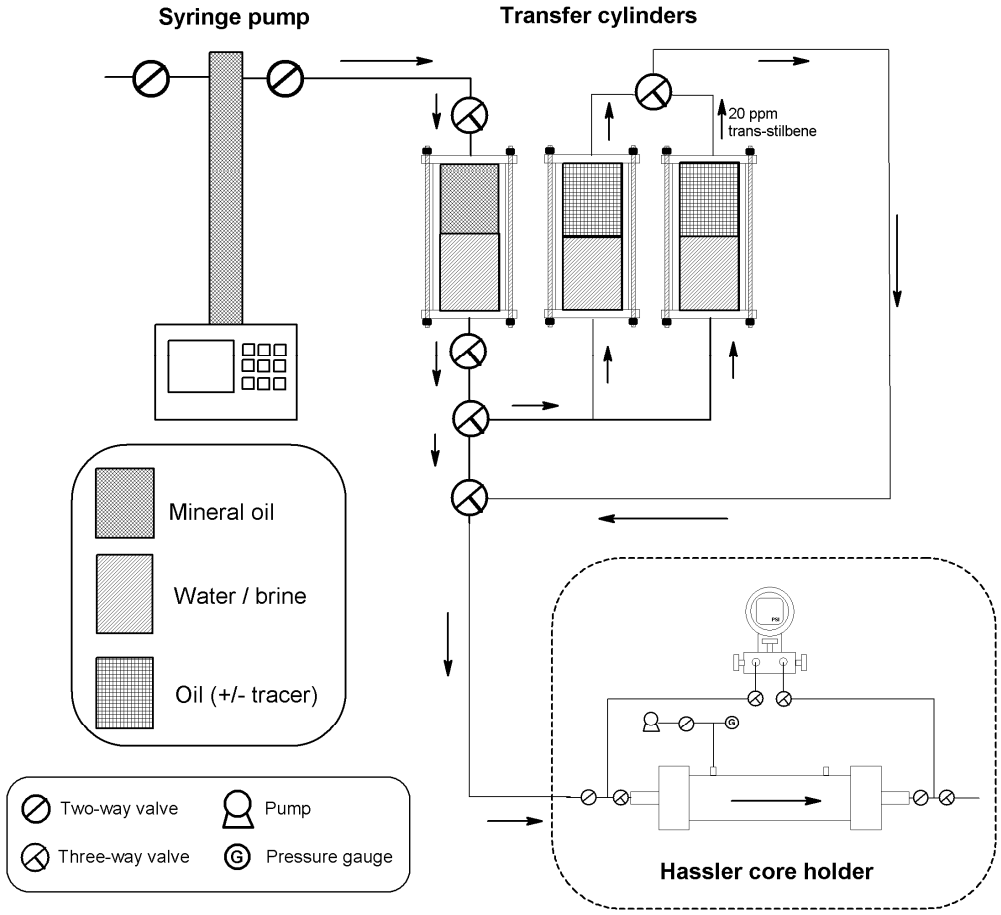

Figure 3-15 Schematic of flow set up during oil (20 ppm trans-stilbene) tracer test (drawn by Stephen Johnson, used by permission)

3.2.3 Crude oil filtering and core aging

LKC crude oil was used to render cores and crushed rock samples into an oil-wet state. The objective of the aging process is to re-establish adsorption equilibrium between the rock and the crude oil that had been established over geological times in reservoirs. Approximately 500 ml of crude oil was poured into two centrifuge bottles and centrifuged for 30 minutes at 3000 rpm to precipitate any emulsified water or solid materials such as sand and high melting-point waxes. The top four fifths of the

centrifuged oil was poured into another container and pumped through a 2.7 μm filter followed by a 1.6 μm filter. Filters were replaced each 1,000 ml of crude oil. Filtered crude oil was pumped into a transfer cylinder to be used for injection.

In order to turn a core into an oil-wet state, a Soltrol 130 saturated core at initial water saturation, (which could also be zero), was placed in a Hassler-Type core holder and flooded with at least 2 PV of crude oil in a fume hood using a Consta Metric pump at a pressure drop lower than that used to establish the initial water saturation. After that the core was transferred to a glass container and immersed in the same sample of fresh crude oil. The container lid was closed and placed in the oven at a temperature of 90°C. After aging for two to four weeks, the core was taken out of the container, placed in a core holder with confining pressure and flooded with Soltrol 130 to displace the crude oil. The core was then ready for further testing. The core weight before and after aging was used to ensure that the initial water saturation remained constant.

3.2.4 Imbibition

The imbibition cell is schematically shown in **Figure 3-16**. Imbibition cells were constructed by the KU glass blower (Custom Lab Glass Services) and consisted of a tubular glass base into which the core was placed. The top was mated to the base via a ground glass joint lubricated with inert grease (Fluorolube). The top incorporated a burette to allow the produced oil to be quantified. A magnetic stirrer bar under the core, and a bent wire inserted through the burette allowed for oil drops adhering to

the core surface to be dislodged periodically. The fluid to be used for spontaneous imbibition testing was degassed in a 1-gallon collapsible container by sparging with helium gas for 30 minutes. The degassed fluid was sealed in a container and put in one of the cabinets (air baths) to reach 45°C for tests that were conducted at that temperature; otherwise it was kept at room temperature. To prepare the imbibition cell for testing, Fluorolube grease was smeared in the ground glass joint. The two cell pieces were twisted together several times to form a tight seal and eliminate vertical flow paths in the grease. Additionally rubber bands were employed on each side of the imbibition cell to hold the pieces together. The cell was initially filled with Deionized water by siphoning through a tube inserted in the top of the pipette and let sit for 30 minutes to make sure that it would hold water before starting the actual imbibition test. It was then taken apart and reassembled with the core stand, stir bar, and bent wire. A paper towel was wetted with Soltrol 130 oil and used to remove the core to be spontaneous imbibition tested from its core holder. The core to be tested was weighed, placed on the core stand inside the imbibition cell, and the imbibition cell was reassembled. The imbibition cell was refilled with degassed deionized water or surfactant solution through the burette up to a desired height. The imbibition cell was set on a magnetic stirrer in one of the cabinets at 45ºC or at room temperature during imbibition. Spontaneously produced oil was monitored and recorded versus time on a daily basis or as often as appropriate. The wire was used to knock any formed oil drops from the core surface (the wire volume was accounted for in produced oil measurements). In the case of imbibition in oil, a modified cell shown in

Figure 3-17(b) was used. In this case, after filling the cell with the oil phase (Soltrol 130), the cell was turned upside down and water production versus time was monitored. For synthetic cores, the imbibition tests performed in a large beaker filled with the imbibing solution while the core was contained in a specially designed core holder.

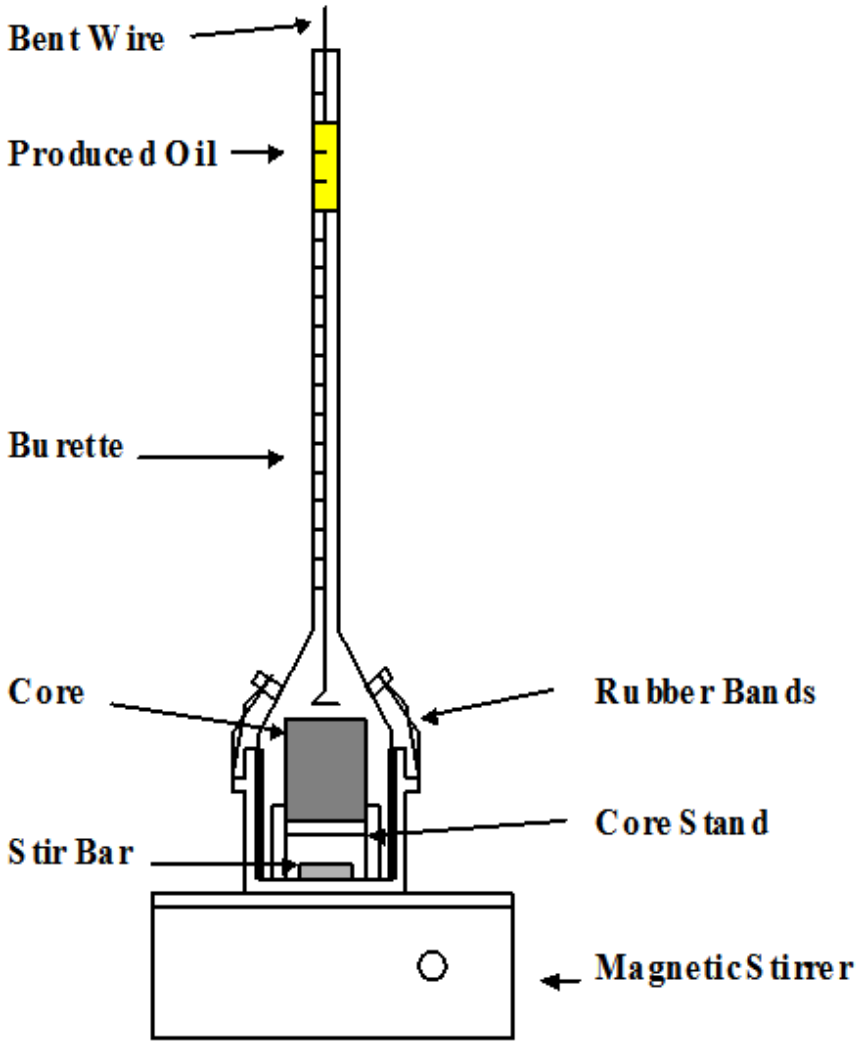

Figure 3-16 Schematic of imbibition cell and its parts (Eisert 2006)

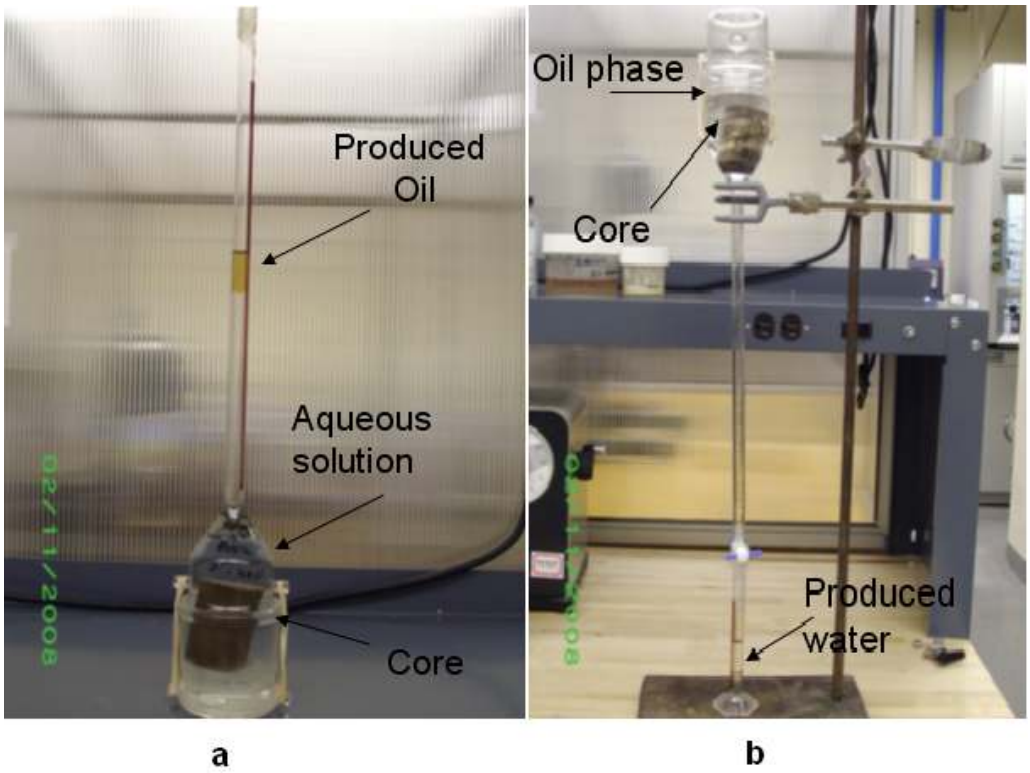

Figure 3-17 Imbibition cells for (a) aqueous phase imbibition and (b) oil-phase imbibition

3.2.5 Interfacial Tension Measurements (IFT)

A Fisher Model 20 Surface Tensiometer was used to determine the interfacial tension of surfactant solutions in contact with Soltrol 130 oil at room temperature. The tensiometer works by lowering a small metal ring into the interface of a sample of two fluids and measuring the force required to pull the ring out of the interface.

Briefly, tensiometer calibration is performed by first selecting a known weight of approximately 500 mg and then calculating a value of S according to the formula (Instrument Division; Fisher Scientific Undated):

$$S = \frac{M \times g}{2 \times L} \qquad (3.7)$$

where

S = apparent IFT (dynes/cm)

M = mass of weight used (g)

g = acceleration due to gravity (980 cm/s^2)

L = circumference of the ring (cm)

The tensiometer is zeroed by first releasing the lever arm arrest mechanism and lining up the pointer on the torsion arm with the index line on the mirror using the knob on the right side of the tensiometer case. A knob beneath the main dial is then set to read zero dynes/cm. The known weight of approximately 500 mg is then placed upon the ring and the arm is again lined up with a marked horizontal line. The reading from the main dial is then compared with the calculated value for S. If the reading is greater than the calculated value then the arm length must be shortened by means of a turn screw; if the reading is lower than the calculated value then the arm length must be increased. Calibration is repeated until the final reading agrees with the calculated value. To perform surface tension measurements, the ring is first cleaned by dipping it in benzene, rinsing it with acetone, and then burning it in the flame of a Bunsen burner. The ring is then hung from the tensiometer hook with the arrest mechanism in place. A beaker containing the liquids to be tested is placed on the sample table and raised to immerse the ring to 1/8 inch below the surface level. The arm arrest mechanism is released and the knob on the right side of the tensiometer case is used

to line up the pointer on the torsion arm with the index line on the mirror. While keeping the ring immersed in the liquid, the knob beneath the main dial is turned to read zero dynes/cm. Finally, the sample table and the knob on the right side of the case are simultaneously lowered while keeping the pointer on the torsion arm lined up with the index line on the mirror. The surface tension will increase as the ring pulls through the interface, and the apparent surface tension is read from the main dial at the break point. The true surface tension of the liquids is then calculated by multiplying the apparent surface tension by a correction factor, F, calculated as:

$$F = 0.725 + \sqrt{\left(\frac{0.01452 \times P}{C^2 \times (D\text{-}d)}\right) + .04534 - \left(\frac{1.679 \times r}{R}\right)} \qquad (3.8)$$

where

P = dial reading for apparent surface tension

C = ring circumference (cm)

r = radius of the wire (cm)

R = radius of the ring (cm)

D = density of the lower phase (g/cm^3)

d = density of the upper phase (g/cm^3)

3.2.6 Absorbance measurements

A UV-visible spectrometer (Lambda 20) was used for determining absorbance of effluents samples from cores and for determination of absorbance peak for surfactant

solutions. During tracer test, an in-line UV-visible detector was used to measure the absorbance of the tracer fluid. Wavelengths used were 302 nm for aqueous tracer (KNO_3) and 323 nm for oil tracer (trans-stilbene).

3.2.7 Qualitative wettability tests

Qualitative wettability tests were performed on crushed rock material in order to check the effectiveness of our core cleaning and aging procedures as well as the effectiveness of the surfactants in changing the wettability of the crude-oil aged crushed rocks. Rock material was crushed using an analytical mill (A-10 Analytical Mill, Tekmar Company, Germany) and sorted with standard testing sieves (270 and 48 mesh standard testing sieves, Fisher Scientific Company) to a size range of 53-300 μm. Rock material was cleaned by contact with the same sequence of solvents used to clean the cores as in Section 3.2.2. Cleaning was performed in a fume hood by immersing the crushed rock in solvent in a glass jar. Solvent was changed periodically until there was no further discoloration of solvent with additional contact time before changing to the next solvent stage. After cleaning with the solvents, the crushed rock was dried in an oven. Any rock material that had clumped together was manually broken up before testing. Some the crushed rock materials were also aged under crude oil at 90°C and after aging for several weeks were washed with Soltrol 130. Using these clean and fresh rocks and aged materials two qualitative test were performed to determine the wettability state of these materials.

3.2.7.1 Flotation Test

In flotation test, 0.2 g of crushed rock sample was added to a scintillation vial almost filled with RO-water. If the rock material floated on top of the water, the rock was classified as oil-wet as shown in **Figure 3-18(a)**. If the crushed material sank to the bottom of the vial, they were water-wet as shown in **Figure 3-18(b)**.

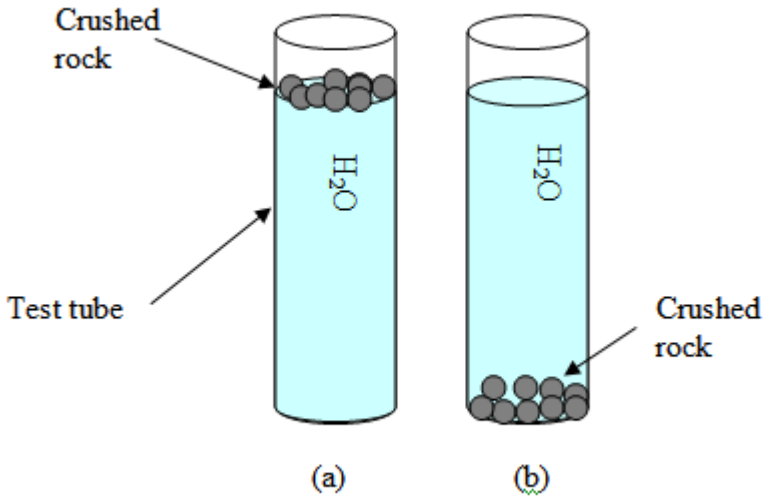

Figure 3-18 Flotation test (a) oil-wet rock and (b) water-wet rock

3.2.7.2 Two-phase separation

To perform the qualitative wettability tests, 0.2 g of prepared crushed rock material was weighed out in a 40 ml scintillation vial. Next, 20 ml of RO water were added to the crushed material followed by 20 ml of Soltrol 130 oil. The vial was gently shaken and then allowed to settle. The amount of core material remaining in each phase gives a qualitative indication of wettability, i.e. if all crushed material remains in the oil

phase then the material is strongly oil wet (Salehi 2006) (**Figure 3-19(a)**), if it sinks into the aqueous phase, where carrying with it a "shell" of oil, it is water-wet (**Figure 3-19(b)**).

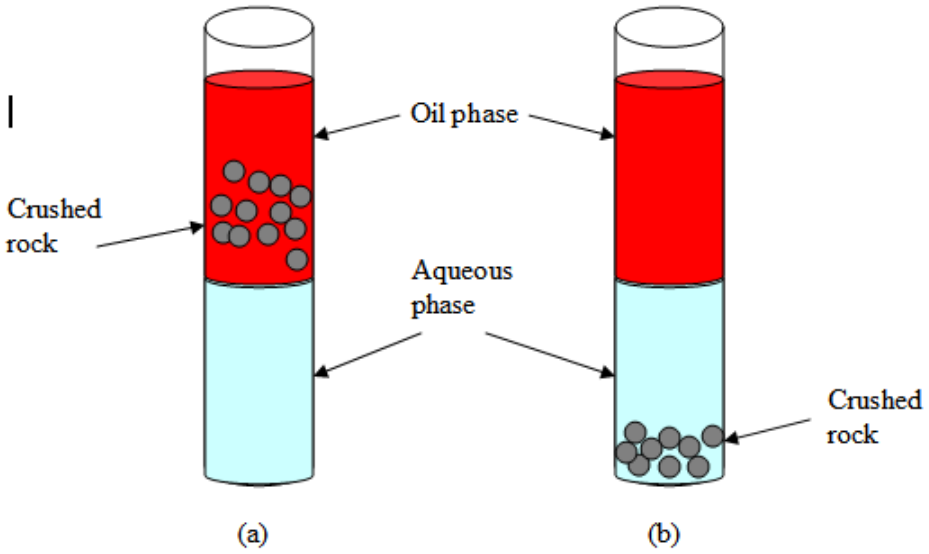

Figure 3-19 Two-phase separation test (a) oil-wet and (b) water-wet rock

3.2.8 Adsorption

Adsorption experiments for different concentrations of surfactant solutions both in benchmark static tests on crushed rock samples and dynamically on core plugs were performed to obtain the adsorption isotherms.

3.2.8.1 Static Adsorption

Static adsorption isotherms were obtained by measuring surfactant concentrations

before and after equilibrating with crushed rock. Thirty ml of the surfactant solution with a known initial concentration was added to a 50 ml centrifuge tube containing a known mass of crushed rock (2 g) as shown in **Figure 3-20**. The tubes were capped and shaken horizontally at 50 min^{-1} for 24 h in an orbital shaker to establish adsorption equilibrium. The samples were then centrifuged for 30 min at 3000 min^{-1}. Supernatants were separated and analyzed for residual surfactant concentrations. The difference in concentration between the stock solutions and the samples was used to evaluate the adsorption. All static adsorption experiments were carried out at room temperature. Adsorption values were obtained by the material balance as:

$$\Gamma = \frac{M_s (C_i - C_f)}{M_R} \qquad (3.9)$$

where

Γ = amount adsorbed (mg/g)

M_s = mass of surfactant solution (mg)

M_R= mass of crushed rock (g)

C_i = initial surfactant concentration (mg/l)

C_f= final (residual) surfactant concentration (mg/l)

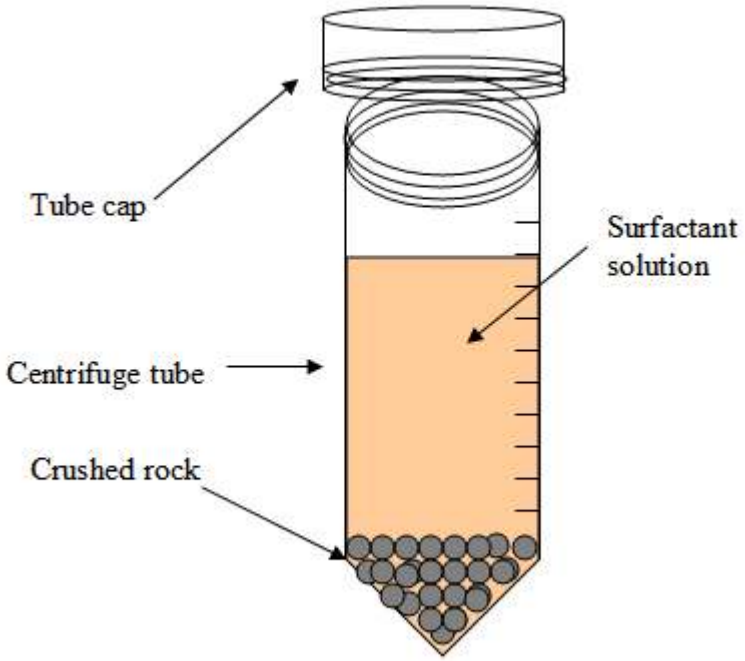

Figure 3-20 Static adsorption test apparatus

Adsorption isotherms were generated by varying the initial concentration and plotting amounts adsorbed vs. the equilibrium concentrations.

3.2.8.2 Dynamic Adsorption

Dynamic adsorption was measured on a one-inch diameter L7 core plug saturated with Deionized water in a Hassler type core holder. A circulation method developed by Grigg (2003) was used. A known mass and concentration of surfactant solution was circulated through the core for 24 h at 2 ml/min using a Consta Metric pump as shown in **Figure 3-21**. The solution was stirred during the experiment to keep the solution well mixed. Final equilibrium concentration of the solution was

determined by potentiometric titration for replicate samples. This was repeated for several concentrations and the relation between adsorption and equilibrium concentration was plotted. The pump and tubing were drained between concentrations and the core holder and pore volume were considered in calculating the dilution factor of the next solution. The adsorption amount was determined by mass balance. In the case of synthetic cores, the set up shown in **Figure 3-22** was used.

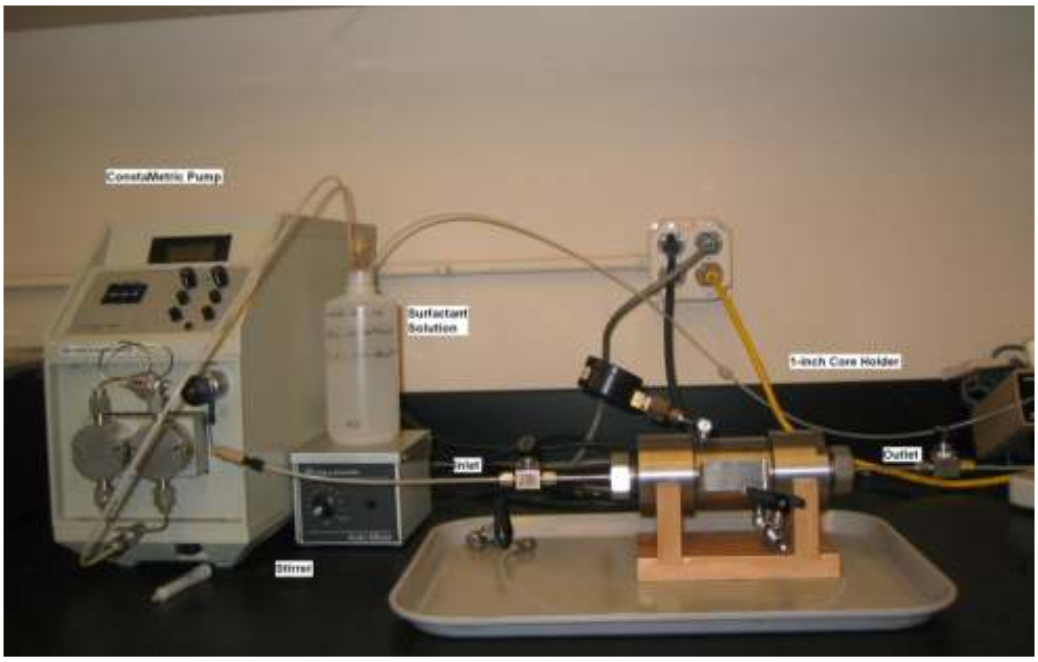

Figure 3-21 Dynamic adsorption set up for reservoir 1-inch core plug

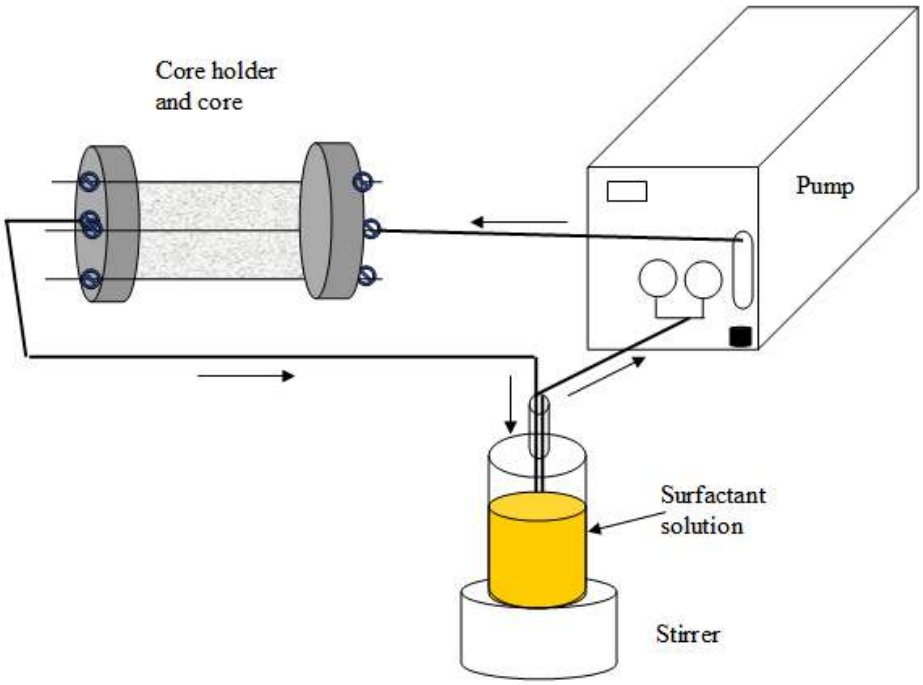

Figure 3-22 Schematic of the dynamic adsorption apparatus for synthetic cores

3.2.9 Titration

A surfactant-ion selective electrode (SUR1502 from phoenix Electrode Company, Houston, TX) was used to identify the potentiometric endpoint in titration of the surfactants with Hyamine 1622 (Benzethonium chloride), a cationic surfactant. The chemical structure of Hyamine 1622 is shown in **Figure 3-23**.

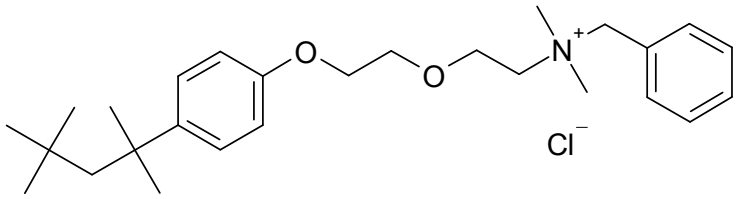

Figure 3-23 Hyamine 1622 (Benzethonium chloride)

This method has been used successfully by Hirasaki & Zhang (2004). The end point is indicated by the inflection point in the curve of E (mV) vs. Volume (ml) of titrant added, most easily identified by looking for a maximum in the first derivative or by the second derivative passing through zero (**Figure 3-24**). **Figure 3-25** shows the phenomena happening during a titration process.

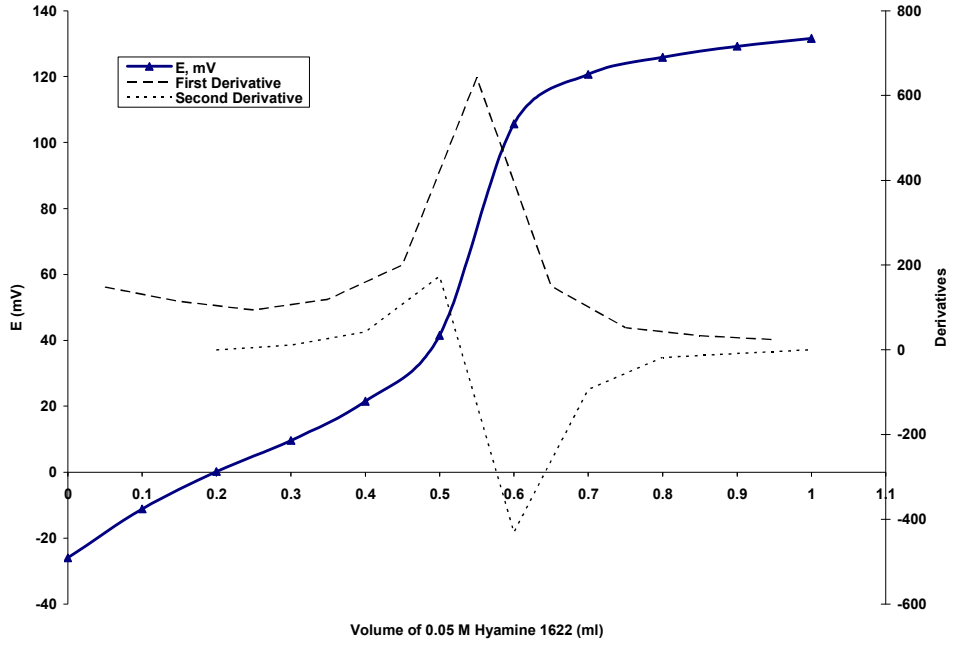

Figure 3-24 Example titration of anionic surfactant STEOL CS-330 with 0.05 mol/l Hyamine 1622 showing the inflection point

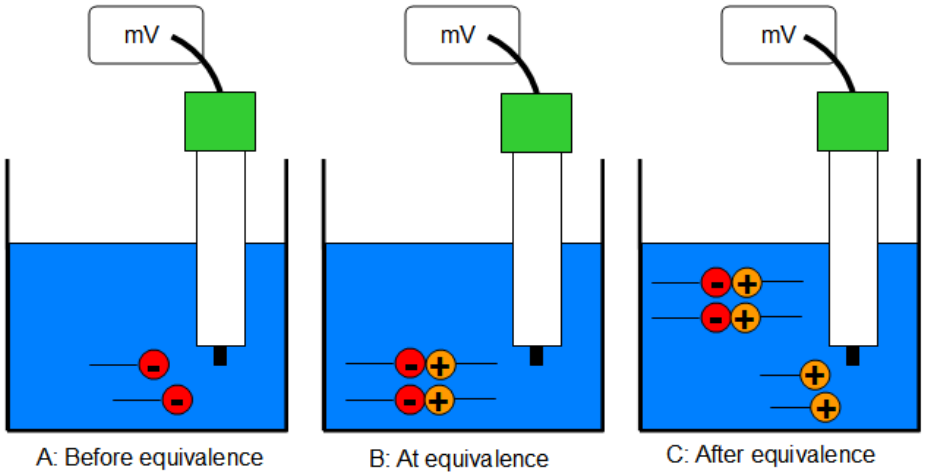

Figure 3-25 Schematic of the titration process

The procedure to determine concentration consists of adding 1.5 mL of 0.01 molar HCl to 25 mL of surfactant solution to be analyzed in order to adjust the pH into the range of 2-4. The electrode is first filled with a saturated solution of 4 M KCl and connected to a volt meter and inserted into the center of the tested solution at an angle as shown in **Figure 3-26**. A stirbar is employed to keep the solution well mixed. Voltage is recorded while incrementally adding a known concentration of Hyamine 1622 cationic surfactant. On a plot of mL titrant (Hyamine) added versus voltage the inflection point represents the equivalence point at which the cationic Hyamine added has reacted with all the anionic surfactant. The inflection point can be accurately determined from first and second derivatives of the curve (where first derivative reaches a maximum and second derivative passes through zero). A sample inflection point graph from a concentration determination performed on STEOL CS-330 is shown in **Figure 3-24**. Concentration is calculated using the following equation (pHOENIX ELECTRODE COMPANY April 17, 2006).

$$C_s = \frac{V_h \times C_h}{V_s} \qquad (3.10)$$

where

C_s = concentration of surfactant (mmol/l)

V_s = volume of surfactant (ml)

C_h = concentration of hyamine (mmol/l)

V_h = volume of hyamine 1622 (ml) at the inflection point

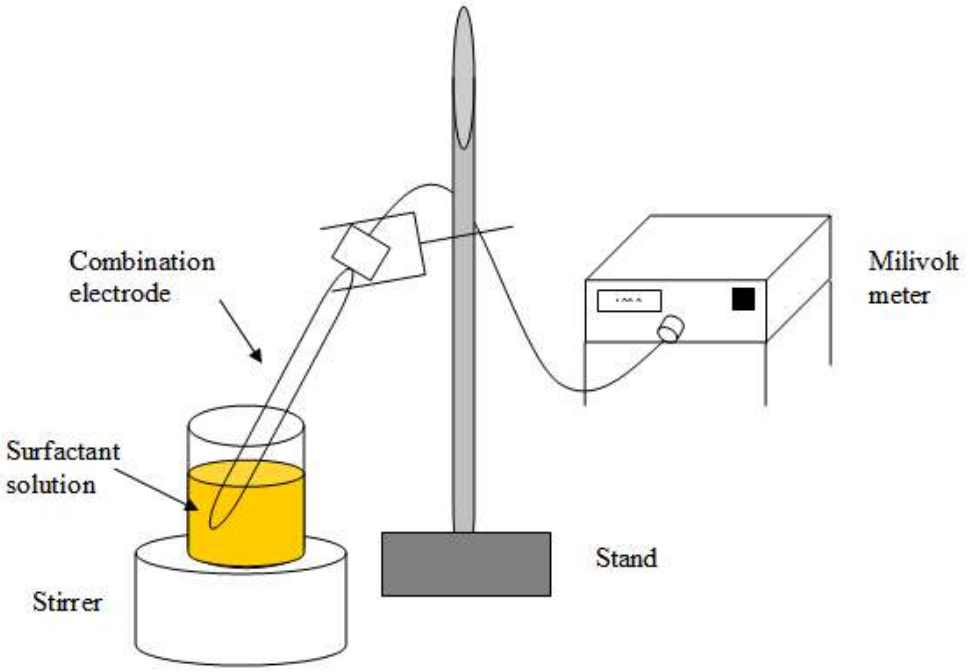

Figure 3-26 Titration set up

4 Results and discussions

This chapter covers the experimental work that has been done during the study and the related discussions. Section 4.1 describes the core cleaning and core characterization data. In Section 4.2 the results of biosurfactant comparison with a bench-mark chemical surfactant are presented. Section 4.3 shows the results of a mechanistic study of wettability alteration by surfactants.

4.1 Core Cleaning and Characterization

Several different carbonate core types were provided for testing by Mr. Alan Byrnes at the Kansas Geological Survey (KGS). These core types include Miami outcrop (oolitic from Miami Florida), Heartland Quarry (oomoldic from Kansas), Bethany Falls (oomoldic from Missouri), and Joulters Cay (oolitic from Caribbean) and Lansing Kansas City field cores (oomoldic Luerman #7 LKC reservoir). In addition to these cores, Berea sandstone cores were cut from larger core plugs available in-house. Also, several synthetic cores made of polyethylene were purchased from Pore Technology Inc. Each core was characterized first by measuring the dimensions to get the length, diameter and bulk volume. Then it was saturated with either aqueous or oil phase according to the procedure given in Chapter 3.

4.1.1 Core Cleaning

In order to compare the effectiveness of different treatments on the same core and to be able to restore the core state, it is important that the core can be cleaned to a

repeatable initial state. Restored state analysis requires that the core be cleaned to the water-wet state that existed before oil accumulated in the formation. The core is then saturated with crude oil to a capillary pressure typical of the formation and the system allowed to equilibrate or "age" under formation conditions (Hirasaki, Rohan et al. 1990). The traditional method for cleaning core samples is Dean-Stark extraction, which usually involves boiling toluene followed by a mixture of chloroform and methanol. Early oil flooding investigations exposed a problem with the cleaning of the core materials. Cores had been cleaned by Soxhlet extraction using a toluene/methanol azeotrope and dried to constant weight before sent to us for further experiments. On flooding with oil, all cores produced effluent that was yellowish in color and supported relatively stable foam on shaking (**Figure 4-1**). The effluent oil also absorbed strongly in the ultraviolet and showed a different UV absorbance spectrum compared with the fluid injected into the core. It seemed that previous solvents used to clean the cores (especially toluene) were dissolved in the effluent samples from the core, causing a different UV spectrometry curve for the injected fluid compared with that of the pure fluid. The initial oil that was used for core characterization was dodecane. UV absorbance spectra of the collected effluent samples from core HQ01 are shown in **Figure 4-2** along with the one for pure dodecane. It can be seen that dodecane effluents from the core contained some material that caused a different UV spectrometry vs. the pure oil. The effluent samples were filtered through an alumina (Al_2O_3) column but the UV-absorbing component was only retained very weakly, suggesting that it represents non-polar

organic compounds that had been trapped in the core. It was very important for our study to be able to clean the cores to the same initial state before performing any test. In addition, the presence of UV-absorbing, oil-soluble material is problematic because it (a) is likely to be active in determining the wettability state of the carbonate surface (b) leads to inaccuracies in porosity measurements and (c) interferes with the detection of our oil tracer (trans-stilbene). To make sure the cores used in the study were clean and to eliminate these problems different cleaning procedure and set ups were used and an aggressive cleaning procedure was adapted as follows based on the results of a study published by Hirasaki et al (1990):

1. flood the core with tetrahydrofuran (THF) for 4 days
2. flood the core with chloroform for another 4 days
3. inject methanol into the core for 4 h to displace the chloroform
4. flood the core with water and dry in oven to constant weight

Cleaning was carried out in a fume hood using the set up and procedure given in Chapter 3. The procedure was to flood the core with tetrahydrofuran (THF) and allow it to soak overnight. This was repeated for up to four days until the effluent was colorless. The THF was displaced with chloroform, followed by methanol and finally water. **Figure 4-3** shows the THF effluents from the previously Dean-Stark cleaned reservoir core L701. The first effluent samples were very dark in color, indicating the dissolution of organic materials from the pore surfaces of the core. The UV spectra for the samples taken in one day are shown in **Figure 4-4**. When the core was soaked overnight, the first sample in the following day showed a higher UV absorbance as

shown in **Figure 4-5**. This indicated the importance of time needed for the THF to diffuse into the smaller pore spaces of the cores during overnight aging.

Figure 4-1 Effluents from core BF02 dodecane flood. Time increases from left to right. The lower image shows the same samples ~ 5 s after shaking to show the persistent foam associated with greater discoloration. The samples also exhibited appreciable UV absorbance

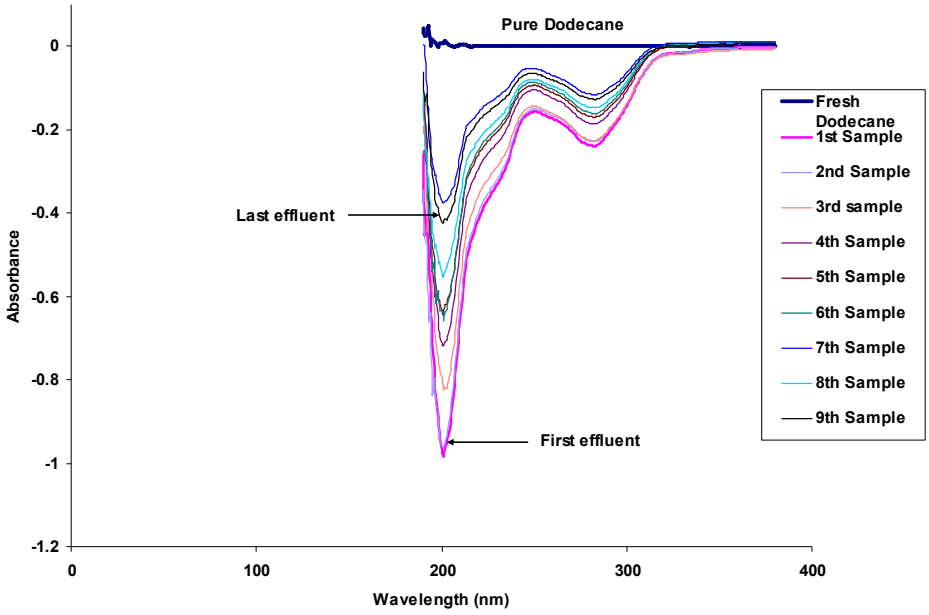

Figure 4-2 UV spectra of effluent dodecane samples from HQ01 core

Figure 4-3 Effluents from cleaning L701. Solvents are tetrahydrofuran (THF), chloroform, methanol and water.

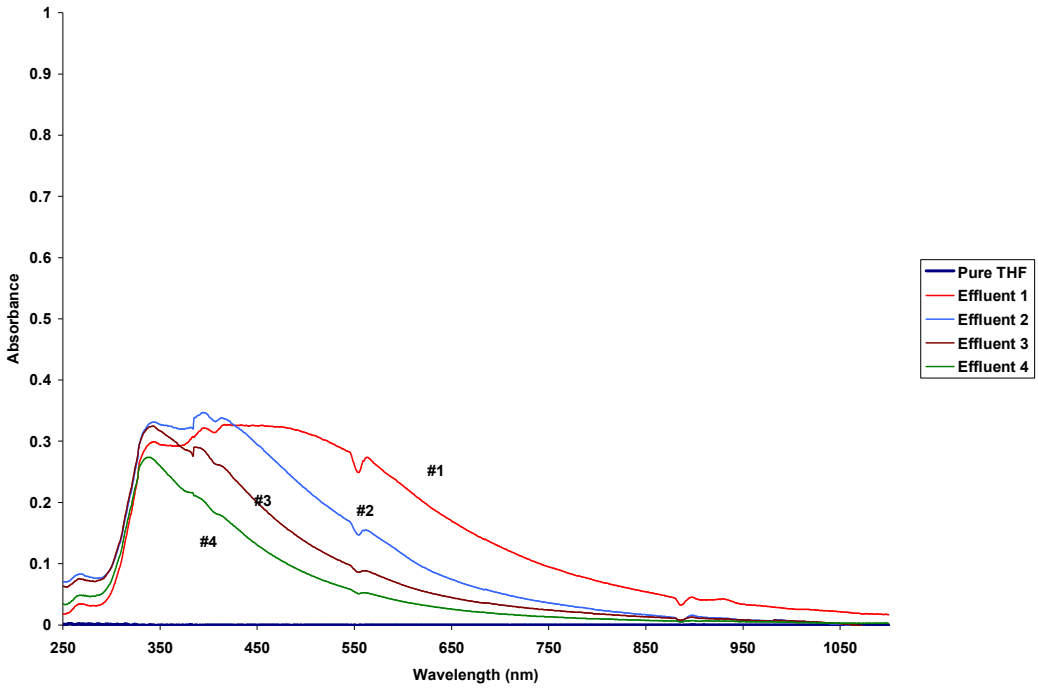

Figure 4-4 UV spectra of different THF samples during one day of cleaning L701 core

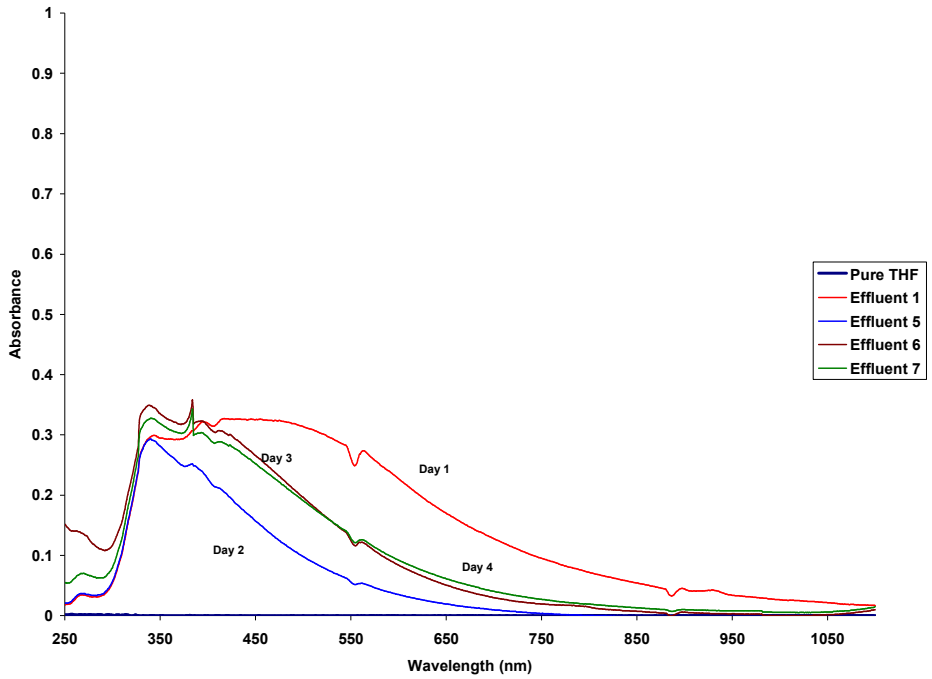

Figure 4-5 UV spectra of effluent THF at different days showing the effect of soaking overnight

4.1.2 Characterization of Core Materials

During the early stages of this project several different carbonate core types (besides the LKC field cores) were provided for testing by Mr. Alan Byrnes at the Kansas Geological Survey (KGS). These core types include Miami outcrop (oolitic from Miami Florida), Heartland Quarry (oomoldic from Kansas), Bethany Falls (oomoldic from Missouri), and Joulters Cay (oolitic from Caribbean). The core types were labeled M, HQ, BF, and JC, respectively. Initial flow tests were performed upon each core type with dodecane oil to determine permeability and porosity. It was determined that the oomoldic HQ and BF cores had extremely low permeability (both in the single md range) and were therefore unsuitable for imbibition testing because

spontaneous imbibition in such low permeability material would take too long for the present work. The M and JC core types were found to have very high permeabilities (M up to hundreds of md and JC as high as 2 Darcies) but were extremely fragile. They were easily deformed by overburden pressure in the core holders, and they dissolved with repeated contact with fluids (especially the Joulters Cay material). Miami M02 disintegrated after characterization with water and oil; these high-permeability oolitic core types are too fragile for repeated testing. It was decided not to continue using M or JC core material for this research and instead focus on intermediate permeability LKC field cores. In addition to LKC cores, 3-inch long Berea sandstone cores were cut from available large core plugs. I also acquired several synthetic core materials made of polyethylene from Pore Technology Inc.

After cleaning and drying to constant weight (field cores), cores were characterized with both water and Soltrol 130 to determine their pore volume, porosity, and permeability. Initially, water was used to saturate the core according to the procedure described in Chapter 3. Pore volume and porosity for each core was obtained from the difference in dry and water saturated weights of the core along with its dimensions. Aqueous tracer tests were carried out using 0.1 mol/l KNO_3 (302 nm) to confirm the porosity and pore volume data from material balance methods and check the homogeneity of the core. The tracer was displaced with water and the core was removed and dried to constant weight. The core was then characterized with Soltrol 130, and a tracer test was performed using 20-ppm *trans*-stilbene in Soltrol 130 (323 nm). The concentrations were chosen because they obey the Beer-Lambert law

(Equation 11), giving a linear relationship between concentration and absorbance (**Figure 4-6**).

$$A = a_{\lambda} \times b \times c \qquad (4.1)$$

where A is the measured absorbance, a λ is a wavelength-dependent absorptivity coefficient, b is the path length, and c is the analyte concentration. The solvent present in the core interfered with oil tracer data (*trans*-stilbene). The peak absorbance wavelength for *trans*-stilbene is 228 nm. However, there was a large peak at this wavelength for the effluent samples (**Figure 4-7**), so it was decided to use a different wavelength for oil tracer (323 nm) where the interference from effluent samples and stilbene were minimized.

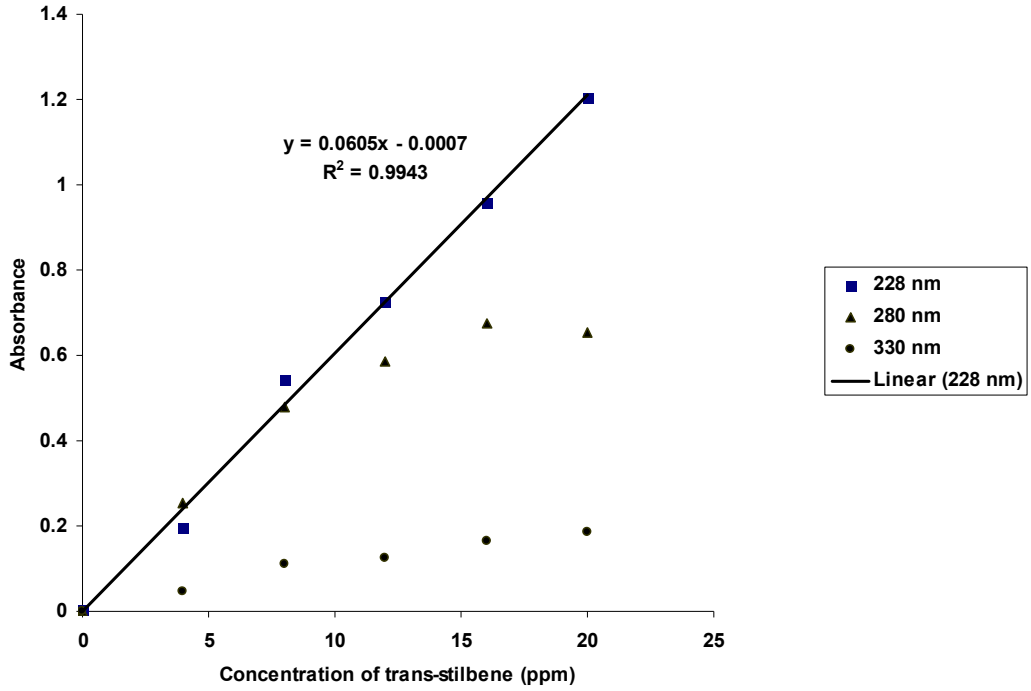

Figure 4-6 Linear relationship between absorbance and concentration at 228 nm for *trans*-stilbene

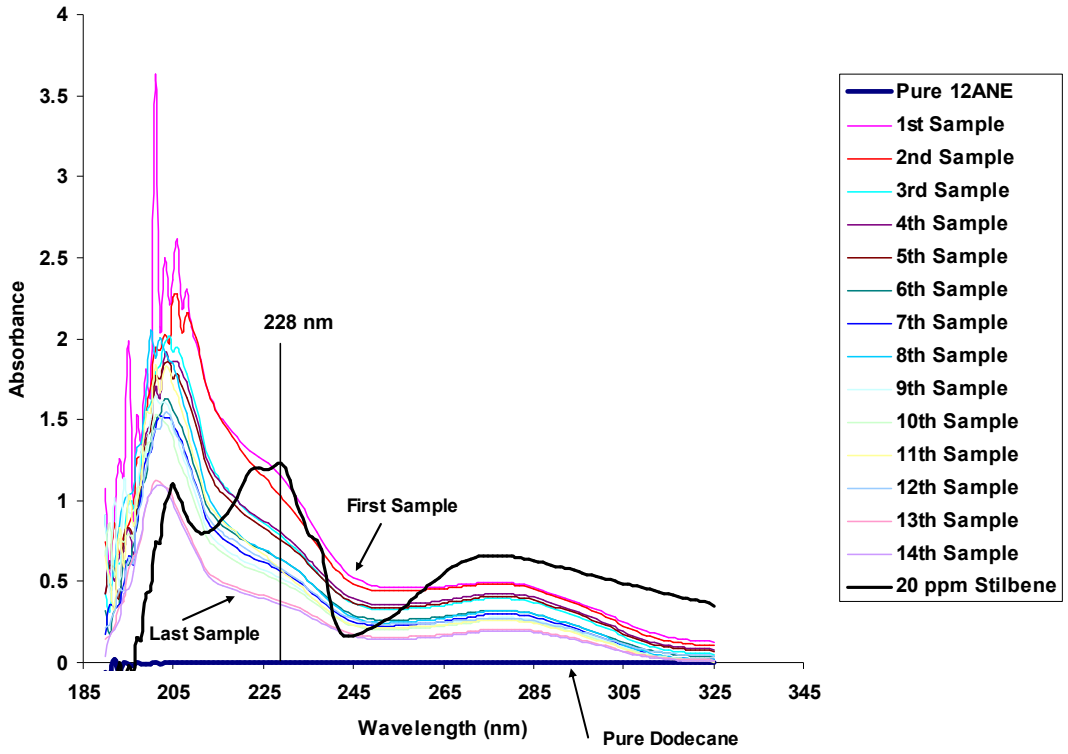

Figure 4-7 Interference of dodecane effluent samples with the oil tracer at 228 nm

Reservoir field cores were characterized according to the procedures given above using both water and Soltrol 130. The following tables summarize the properties of all field cores used in this study.

Table 4.1 Properties of L7 class 1.5-inch diameter field cores

Core	L701	L702	L703
Length (cm)	6.68	4.29	6.66
Diameter (cm)	3.81	3.80	3.81
Area (cm^2)	11.34	11.38	11.35
Bulk Volume (cm^3)	75.73	48.79	75.64
PV (mL) ($S_w = 1$), calculated by weight	20.00	12.08	17.67
PV (mL) ($S_w = 1$), calculated by tracer	19.04	13.23	19.20
PV (mL) ($S_o = 1$), calculated by weight	20.32	12.46	18.22
PV (mL) ($S_o = 1$), calculated by tracer	20.80	12.16	18.49
Mean PV (mL)	20.04	12.48	18.40
Porosity	0.26	0.26	0.24
Absolute Permeability, k (md) $S_w = 1$	40.00	16.00	11.00
Absolute Permeability, k (md) $S_o = 1$	45.50	15.50	13.30
Mean Absolute Permeability, k (md)	42.75	15.75	12.15

Table 4.2 Properties of L7B class 1-inch diameter field cores

Core	L7B1	L7B2	L7B3
Length (cm)	6.32	6.31	6.45
Diameter (cm)	2.55	2.53	2.54
Area (cm^2)	5.11	5.03	5.06
Bulk Volume (cm^3)	32.30	31.74	32.64
PV (mL) ($S_w = 1$), calculated by weight	7.30	7.28	7.21
PV (mL) ($S_w = 1$), calculated by tracer	7.20	7.23	7.13
PV (mL) ($S_o = 1$), calculated by weight	7.30	7.27	7.22
PV (mL) ($S_o = 1$), calculated by tracer	7.23	7.25	7.16
Mean PV (mL)	7.25	7.27	7.21
Porosity	0.22	0.23	0.22
Absolute Permeability, k (md) $S_w = 1$	23.00	20.00	13.00
Absolute Permeability, k (md) $S_o = 1$	23.00	20.50	13.45
Mean Absolute Permeability, k (md)	23.00	20.25	13.23

Figure 4-8 shows porosity and permeability values for all the cores characterized, overlaid on similar data from Watney (2006). Watney characterized Bethany Falls and Mound Valley oolites and found a wide range of porosity and permeability. Dubois et al. (2004) noted that the LKC was very similar to modern Caribbean oolites and our experimental data for moldic LKC outcrop and reservoir cores, as well as Miami and Joulters Cay oolite agree well with the published values for similar material. This confirms that the core-flooding protocol is effective, and that the material is representative of the range of porosity, permeability and pore architecture seen across the LKC.

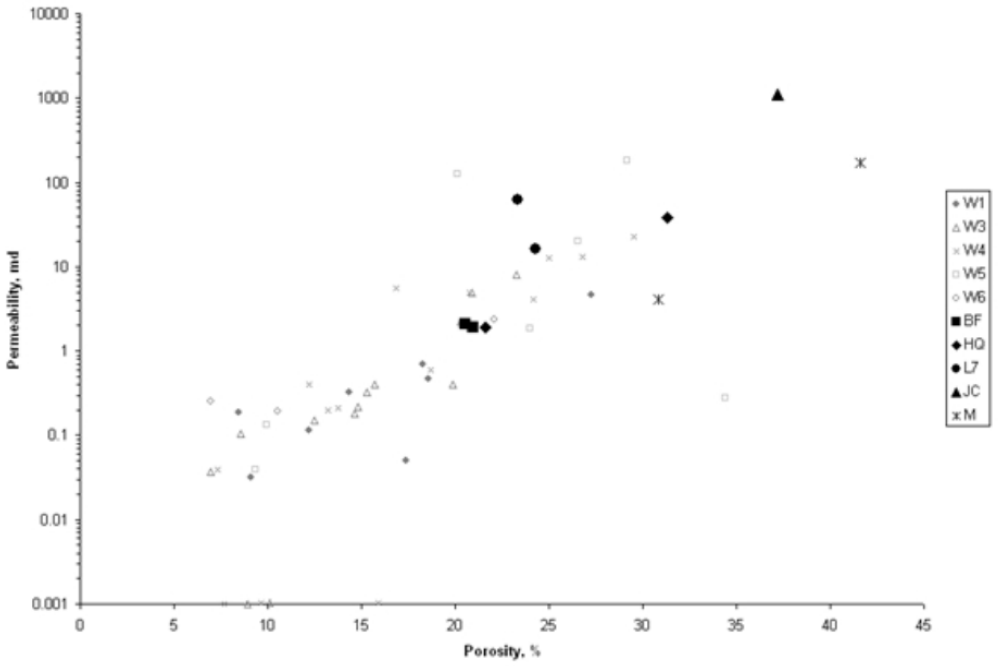

Figure 4-8 Porosity and permeability of Bethany Falls (BF), Heartland Quarry (HQ) and Luerman #7 (L7), Joulters Cay (JC) and Miami (M) cores. Points marked in gray (W1-6) represent Bethany Falls and Mound Valley oolites (after Watney 2006)

4.1.3 Magnetic Resonance Imaging of Pore Architectures

To visualize and confirm the pore architectures of our carbonate cores, samples of core materials were saturated with water and sent to ConocoPhillips, Bartlesville, OK for magnetic resonance imaging (MRI). The image data has been analyzed to obtain pore-body and pore-throat size distributions of the different carbonate cores. This information will be useful in future explanations of the distribution of residual fluid saturations after imbibition tests.

Magnetic resonance imagery of core materials are shown in **Figure 4-9**-**Figure 4-12**. Cores were fully saturated with water, which was visualized by MRI to show the pore volume. Color bar is a qualitative indicator of relative water saturation. The resulting images demonstrate the varying degrees of heterogeneity in the cores. The outcrop cores Miami and Bethany Falls were heterogeneous, LKC sample was relatively homogeneous and Joulter's Cay core was homogeneous. Color scale is an arbitrary scale of water content.

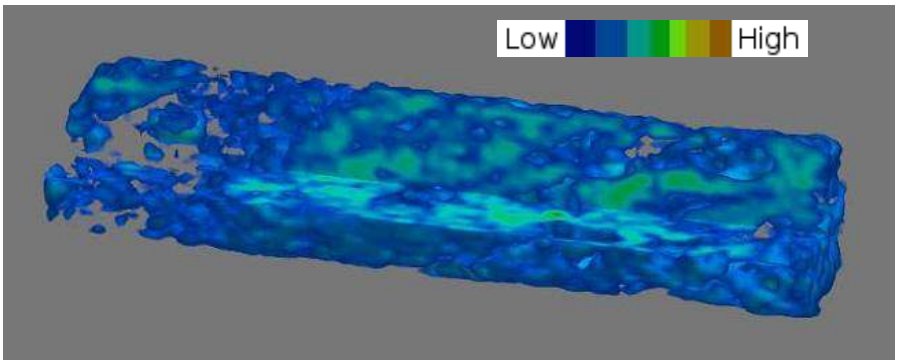

Figure 4-9 Heterogeneous Bethany Falls oomoldic outcrop core , ϕ = 0.21, k = 0.7 md

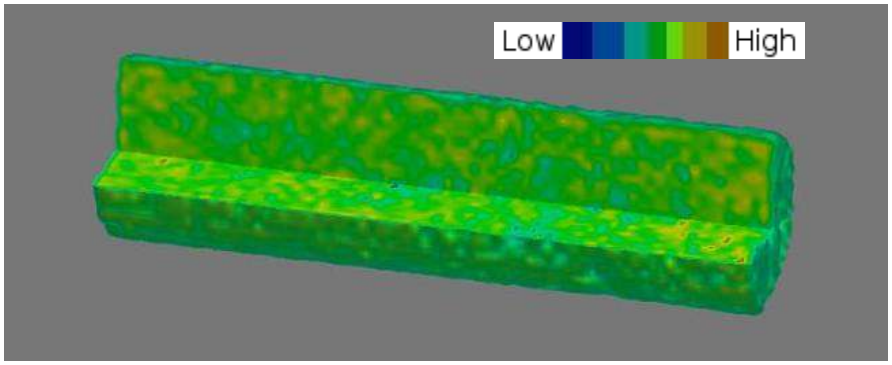

Figure 4-10 Relatively homogeneous Luerman #7 oomoldic reservoir core, ϕ = 0.24, k = 16 md

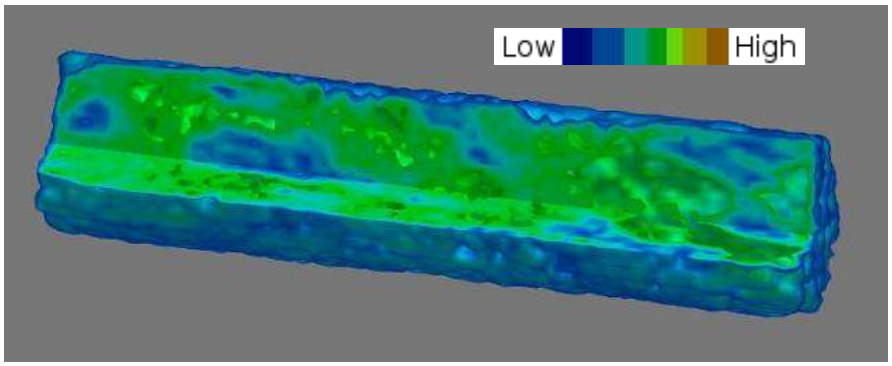

Figure 4-11 Heterogeneous Miami oolitic outcrop core, ϕ = 0.42, k = 170 md

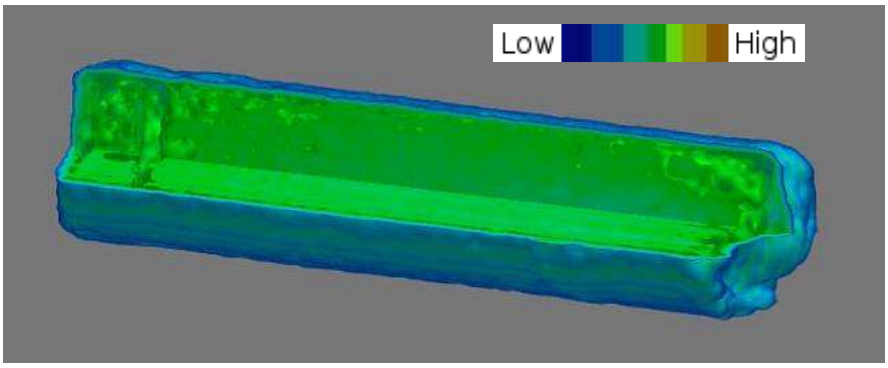

Figure 4-12 Homogeneous Joulter's Cay oolitic outcrop core, ϕ = 0.43, k = 1100 md

4.2 Comparison of Biosurfactant with Benchmark Chemical Surfactant

4.2.1 Screening and Selection of Benchmark Chemical Surfactants

A wide variety of surfactants has been assessed in the literature, both for their ability to reduce interfacial tension between brine and oil to ultra-low levels, and to mediate wettability changes in reservoir rocks. Bearing in mind that the dominant charged species in the adsorbed hydrocarbon layer on the carbonate rock surface is negative ($COOH^-$) and that of the carbonate rock (calcite) at basic pH is positive (Ca^{++}), three approaches have been tried to alter wettability using surfactants:

1) Cationic surfactants

Standnes (2000) found that cationic surfactants changed the wettability of an oil-wet carbonate rock toward a more water-wet state by irreversibly removing adsorbed anionic carboxylates from the rock surface, i.e. the interaction is between the organic carboxylates adsorbed on the rock surface and surfactants not surfactants and the rock surface. This has a positive implication on surfactant loss

because of the electrostatic repulsion between the like-charged surfactant molecules and the rock surface after the wettability change. They also used anionic surfactants mostly ethoxylated alkyl sulfates - and found that the anionic surfactants were less effective than cationic, probably because the interaction between surfactant-rock was reversible.

2) Anionic surfactants plus an alkali

Hirasaki et al. (2004) at Rice University evaluated the use of a range of ethoxylated and propoxylayed alkyl sulfates (anionic surfactants) with sodium carbonate to enhance oil recovery from fractured oil-wet carbonate rocks. The charge on calcite is positive below pH 9 and negative above pH 9. The effect of the sodium carbonate is to make the charge negative at lower pH. They found that altering the surface charge causes an electrostatic repulsion between the rock surface (calcite) and the adsorbed layer of anionic carboxylates. Incidentally, the alkali also causes some saponification of naphthenic acids, thus adding to the amount of surfactant in the system.

3) Anionic surfactants alone in a typical injection brine

Perhaps the most pertinent approach is that of a group at Phillips Petroleum (Spinler, Zornes et al. 2000B). They dealt with cores from Kansas and described an exemplar anionic surfactant, "Surfactant A" as an ammonium salt of ethoxylated and sulfated alcohols (C8-C10 alkyl ethers), injected in North Sea water.

Based on the above, some basic decisions can be made regarding the properties of suitable candidates for the role of benchmark surfactant:

1. Surfactin is an anionic surfactant; it carries two negative charges on the hydrophilic oligipeptide. None of the surfactants in the literature studied to date has a comparable charge density; however, the CMC of surfactin is much lower than synthetic surfactants so the total charge added to the system is not going to be comparable anyway. So as long as the charge has the same sign, this should not be an issue.
2. Tail lengths of most of the anionic surfactants studied are comparable to surfactin, though longer tails seem to be more effective.
3. Most anions studied have been ethoxylated alkyl sulfates.
4. All studies have been with synthetic brine or seawater.

Likely candidates include sodium dodecyl sulfate (SDS, STEPANOL WA-EXTRA, MW = 265) as the simplest possible benchmark, or one of the ethoxylated alkyl sulfates such as sodium laureth sulfate (SLS, STEOL CS-330, MW = 381). Another possibility is sodium dodecylbenzene sulfonate (BIO-SOFT D-40, MW = 325). Samples of these candidate benchmark synthetic surfactants were obtained from Stepan Chemical Company, Northfield, IL. All these surfactants are anionic with a hydrophobic tail of carbon number ~12, though they have only a single charge and a much smaller hydrophilic head than surfactin. They are readily available and are well studied. These surfactants were diluted using water and a ring tensiometer (Fisher Model 20) was used to measure interfacial tension between various concentrations of surfactants and Soltrol 130. Interfacial tension values for these chemical surfactants and surfactin at varying concentration against Soltrol 130 are shown in **Figure 4-13**. At low

concentrations, the IFT of sodium laureth sulfate (STEOL CS-330) was closest to that of surfactin and this surfactant was chosen for comparison in this work.

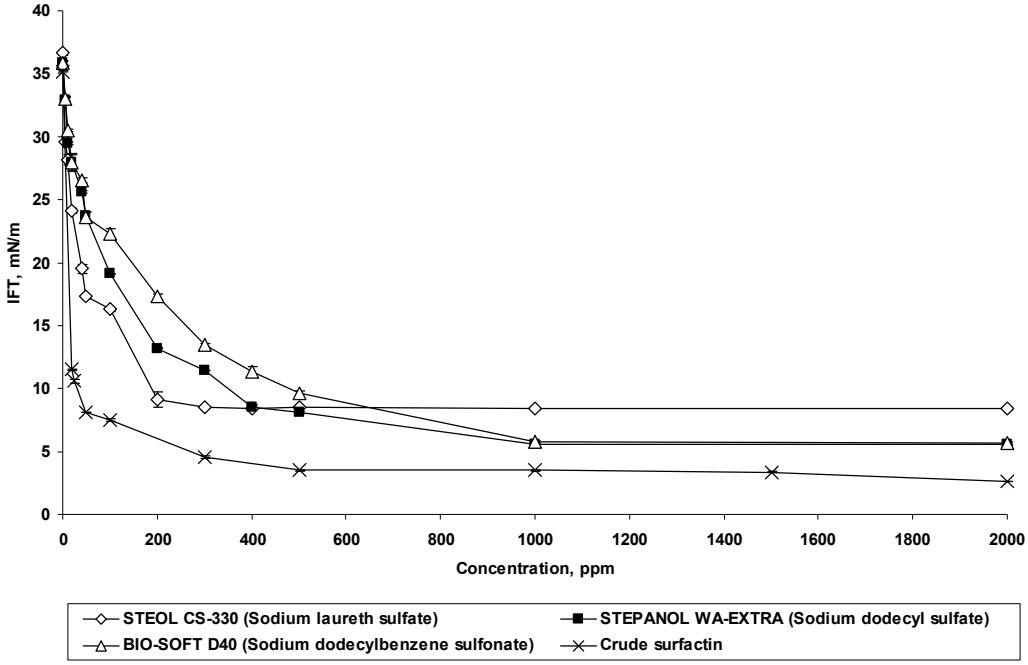

Figure 4-13 Interfacial tensions between surfactants and Soltrol 130 at room temperature obtained by a ring tensiometer

4.2.2 Adsorption

One of the key parameters controling the economics of any chemical EOR process is the amount of surfactant loss due to adsorption. One of the objectives of this work was to determine the surfactants' adsorption isotherms both through bench-top (static) and coreflood (dynamic) experiments on crushed rock samples and on reservoir cores from KLC formation respectively.

4.2.2.1 Static adsorption

4.2.2.1.1 Preparation of crushed carbonate rock

Crushed reservoir material was used for static wettability and adsorption testing. In order to produce a reproducible particle size distribution, small samples of material (~10 cm^3) were crushed in a ball mill (Spex Certiprep Model 8000M, provided by Kansas Geological Survey). Samples were pooled and blended before being sieved to check the size distribution (**Figure 4-14**) and to remove particles > 300 mm and < 53 mm.

The surface area per unit mass was measured using a Gemini II Surface Area Analyzer (Model Number 2370, Micromeritics Instrument Corporation, Norcross, GA). Miami crushed rock sample had a surface area of 0.67 m^2/g and that for Bethany Fall sample was 2.76 m^2/g. Crushed rock samples were cleaned using the same sequence of solvents used for cores before being used in adsorption tests. The procedure was to expose the crushed rock to the series of cleaning solvents (THF, chloroform, and methanol) and finally washed them with water and let them to dry.

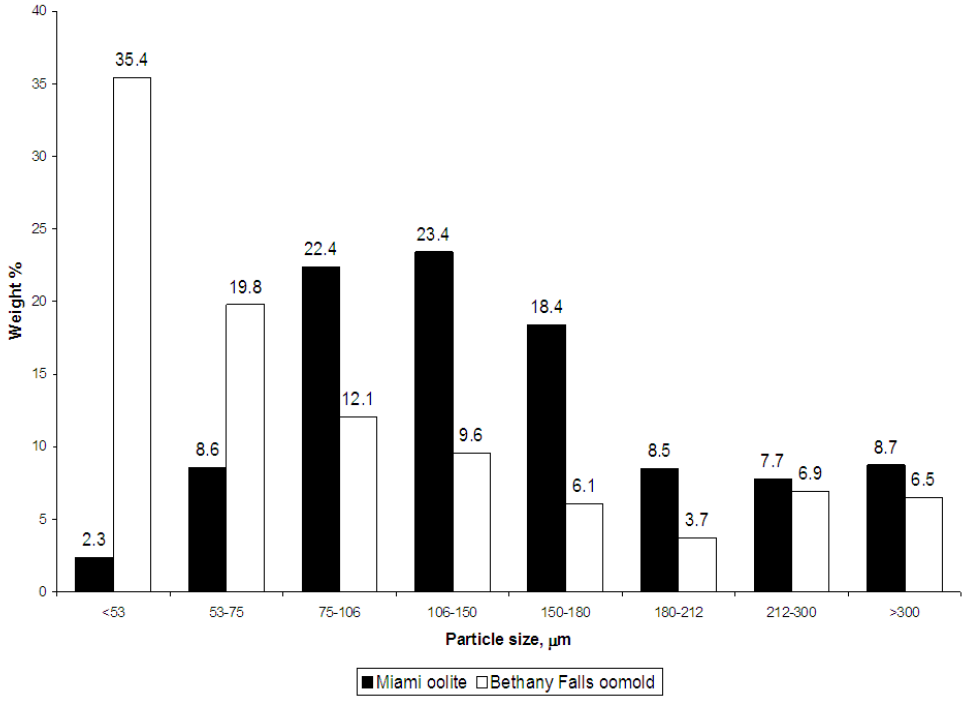

Figure 4-14 Particle size distribution of crushed carbonate rock. Only particles in the range 53-300 μm are used in the investigation.

4.2.2.1.2 Effects of rock/surfactant solution weight ratio

Static adsorption experiments were performed with different surfactant solution mass/rock mass ratios to identify whether this affects the degree of adsorption observed. Different masses of cleaned crushed rock were placed in 30 ml of surfactant solution of known concentration. **Figure 4-15** shows the adsorption values for a 1.44 mmol/l solution of STEOL CS-330 on both Miami and Bethany Fall rocks. Specific adsorption declines with increasing rock mass. It was noticed that despite constant agitation, there was a degree of settling of crushed rock in the test tubes. It appeared that this reduced the access of surfactant to a portion of the material. The same trend was observed for a 0.37 mmol/l solution of surfactin on BF rock (**Figure**

4-15) but adsorption of surfactin was higher than that of STEOL CS-330. The greater adsorption on Miami compared to Bethany Falls is consistent with Miami's crushed rock higher specific surface area.

Figure 4-16 shows STEOL CS-330 adsorption isotherms obtained using different masses of rock. The results are consistent with the earlier observations that higher masses of adsorbent exhibit lower specific adsorption. Good linear correlations were obtained between the residual concentrations and rock masses for the selected initial concentrations (**Figure 4-17**). Multiple tests confirmed that this effect was repeatable, and that for a given mass of rock, consistent results were obtained. Repeating the tests with a higher rate of shaking to ensure the rock material remained in suspension resulted in a further reduction in adsorption.

Since specific adsorption was seen to decline with increasing rock mass, all subsequent experiments were done using a fixed mass of rock (2.0 g) and surfactant solution (30 ml) to ensure that results were comparable.

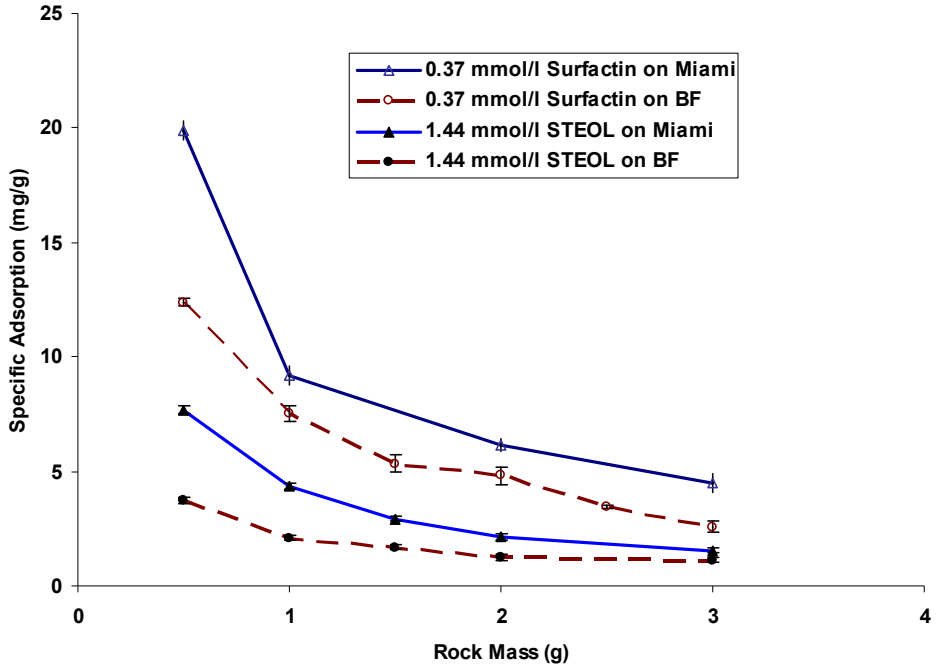

Figure 4-15 STEOL CS-330 and surfactin on different masses of BF and Miami crushed rocks

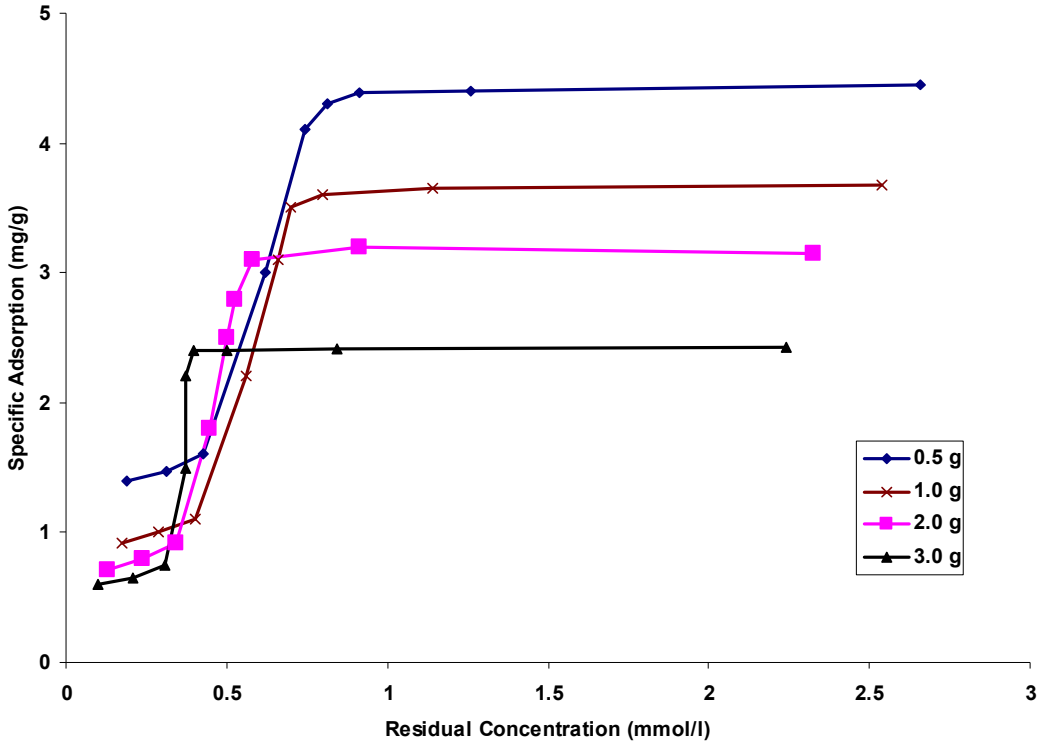

Figure 4-16 STEOL CS-330 adsorption isotherms on different masses of BF rock

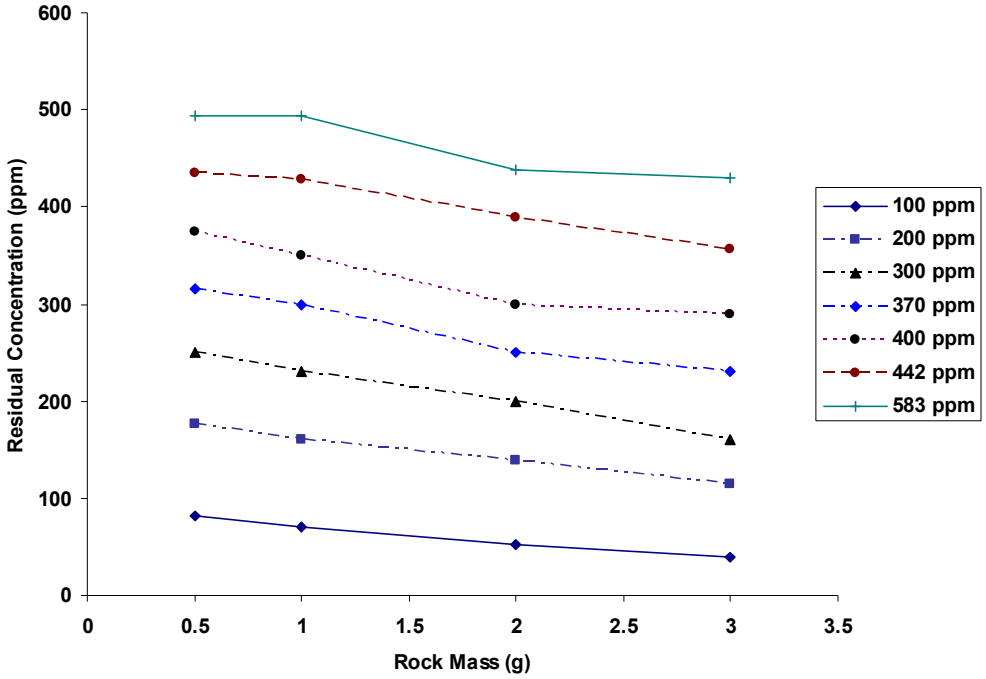

Figure 4-17 STEOL CS-300 residual concentrations for different masses of BF rock

4.2.2.1.3 Static Adsorption isotherms

To compare the adsorption levels of surfactin with STEOL CS-330, adsorption isotherms for both were obtained using crushed Bethany Falls and reservoir (L7) crushed rocks (**Figure 4-18**). In both cases, surfactin had a higher specific adsorption, and the maximum adsorption density was reached at a lower concentration. This reflects the lower critical micelle concentration (CMC) of surfactin at 25°C, variously reported as 7.5 μmol/l (Heerklotz and Seelig 2001), 9.4 μmol/l (Ishigami, Osman et al. 1995) and 24.1 μmol/l (Cooper, MacDonald et al. 1981), compared to 100 μmol/l for sodium laureth sulfate (Mukerjee and Mysels 1971).

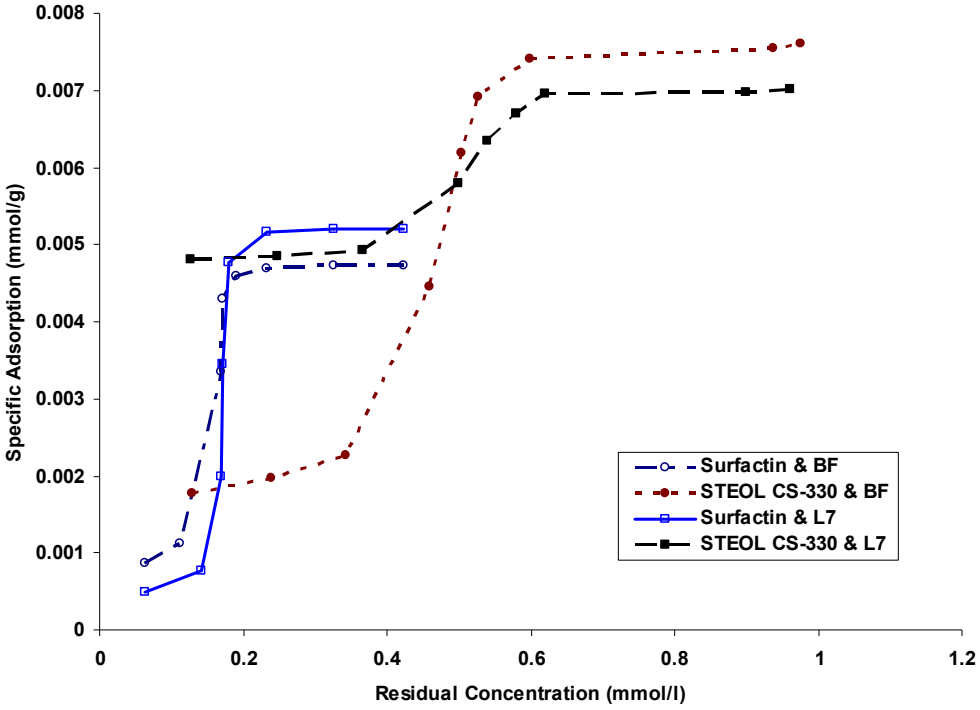

Figure 4-18 STEOL CS-330 and surfactin static adsorption isotherms on 2.0 g BF and L7 2.0 crushed rock samples

The adsorption isotherms for surfactin and STEOL CS-330 on both L7 and BF rocks exhibit the four regions seen in a typical adsorption isotherm (**Figure 4-19**). Region I, which is also known as the Henry's law region, corresponds to adsorption of surfactant monomers and there is a linear relationship between the concentration and adsorption density. The main mechanism of adsorption is electrostatic attraction between the charged head group of the surfactant molecule and surface of the rock. Region II is characterized by a sharp increase in the adsorption, corresponding to the formation of bilayers and aggregates on the solid surface. Surfactant tail groups can form aggregates by hydrophobic bonding in this region. In Region III the same forces

are responsible for adsorption. However, there is a decrease in the slope of the adsorption isotherm. In this region aggregate-aggregate interactions and formation of hemimicelles (monolayer aggregates) and admicelles (bilayer aggregates) become more important. Region IV shows the attainment of the critical micelle concentration (CMC) and adsorption density reaches a plateau as micelle formation competes with surfactant adsorption. Physical bases for these adsorption regimes are shown schematically in **Figure 4-20**.

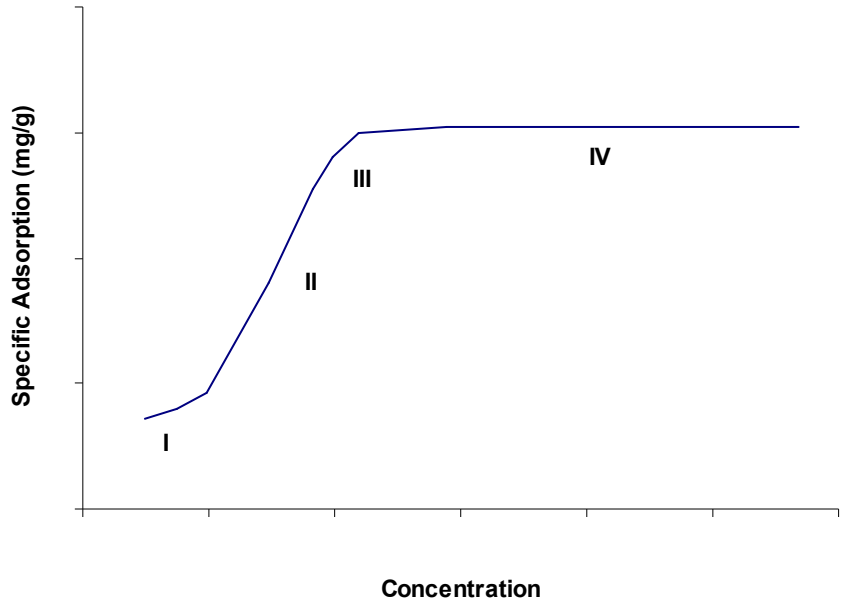

Figure 4-19 Typical adsorption isotherm of surfactant on rock indicating the four regions (after Tabatabai *et al.* 1993)

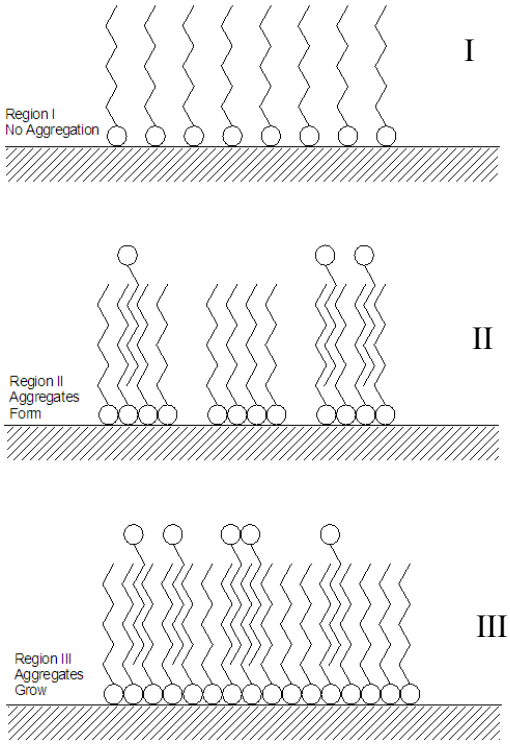

Figure 4-20 Suggested physical basis for the first three regions seen in a typical adsorption isotherm (after Sharma 1995)

4.2.2.2 Dynamic Adsorption Tests

Dynamic adsorption was measured in a one-inch diameter L7 core plug (L7B2) saturated with water in a Hassler-type core holder. To obtain the dynamic adsorption isotherms for the benchmark chemical surfactant and the biosurfactant (surfactin), the circulation method described in Chapter 3 was adapted. A known mass and concentration of surfactant solution was circulated through the core for 24 h at 2 ml/min at room temperature. Equilibrium concentration of the solution was determined by potentiometric titration for replicate samples to calculate the adsorption value through material balance. This was repeated for several

concentrations and the relation between adsorption and equilibrium concentration was plotted. The pump and tubing were drained between concentrations and the core holder and pore volume were considered in calculating the dilution factor of the next solution. Adsorption isotherms for both surfactants at room (25 °C) are shown in **Figure 4-21**.

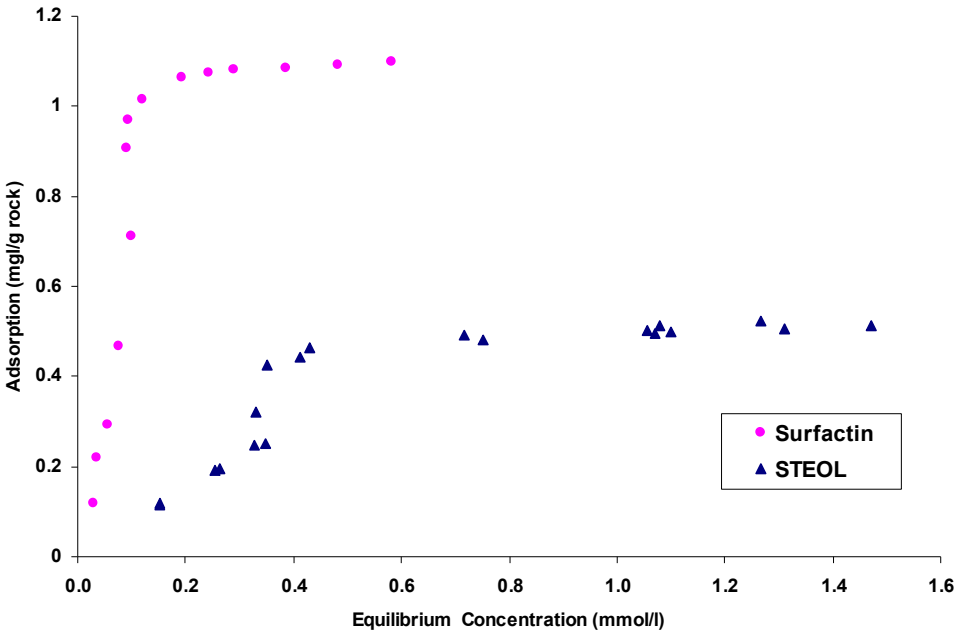

Figure 4-21 Dynamic adsorption isotherms for STEOL CS-330 and surfactin on reservoir core L7B2

Figure 4-21 shows that at low concentrations, surfactin is more strongly adsorbed onto LKC rock than is SLS. While the affinity for the rock surface at low concentrations indicates potential for wettability change, the large difference in ultimate adsorption was a concern until the data was plotted on a molar basis (**Figure**

4-22). It is clear that the apparent high adsorption of surfactin is an artifact of its high molecular mass compared to SLS.

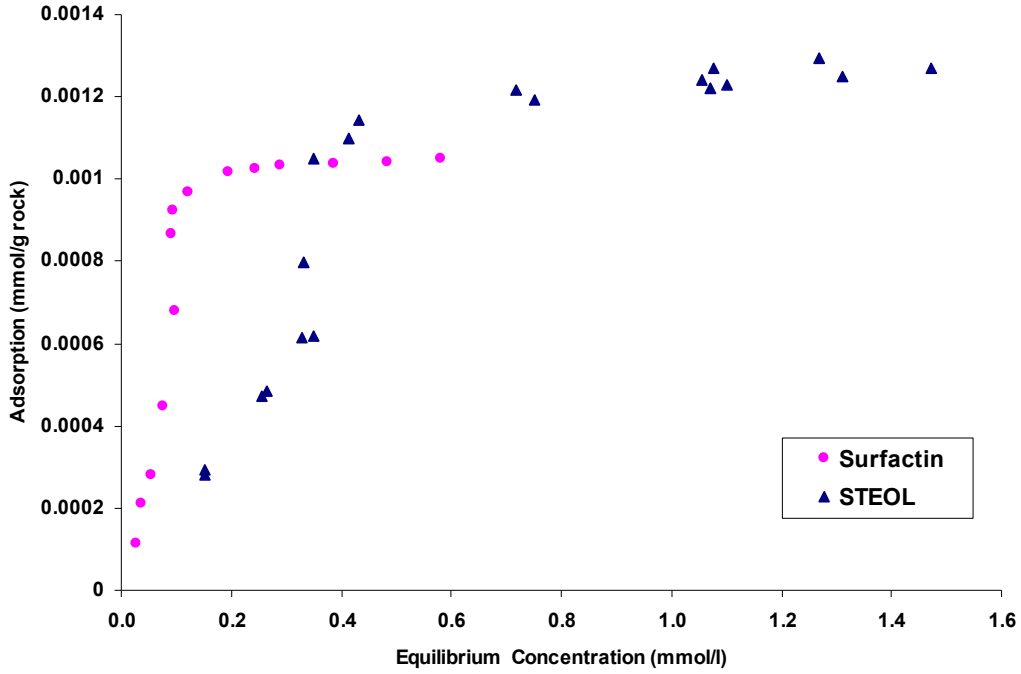

Figure 4-22 Dynamic adsorption isotherms for STEOL CS-330 and surfactin on molar basis on L7B2 LKC core

The adsorption isotherms for surfactin and STEOL CS-330 on L7B2 reservoir core exhibit the same four regions seen in static adsorption isotherms (**Figure 4-19**).

4.2.3 Imbibition

Imbibition tests were performed on cleaned and LKC crude-oil-aged reservoir cores to compare the performance and effectiveness of surfactin against the benchmark

chemical surfactant in accelerating the spontaneous imbibition process under the reservoir conditions of LKC formation.

4.2.3.1 Mixed-wet cores

To establish baselines, spontaneous and forced imbibition tests at reservoir temperature were performed on cleaned field cores using deionized water and Soltrol 130. 1-inch diameter cores L7B2 and L7B3 were cleaned first using our cleaning procedure as discussed in Section 4.1. After cleaning each core was dried in an oven to constant weight. The cores were then saturated with water and pore volume, porosity and permeability values were obtained. Initial water saturations of 38 and 35 % for L7B2 and L7B3 cores respectively were established by flooding them with Soltrol 130 and then both L7B2 and L7B3 cores were placed in imbibition cells at 45 °C in contact with water and oil production was monitored versus time. **Figure 4-23** shows the imbibition profiles for these cores in deionized water at reservoir temperature. The imbibition mechanism into these cores was driven by capillary forces resulting in a countercurrent imbibition of water into these cores; the oil was produced from the sides of the core (**Figure 4-24**). Water imbibition resulted in 12-13 % OOIP recovery from these cores. After reaching their production plateaux, they were flooded with water to residual oil saturation and water wettability indices were calculated. Table 4.3 summarizes the imbibition data for these cores. Even after going through the cleaning procedure, these reservoir cores exhibited a mixed-wet behavior (I_w ~ 0.25-0.27).

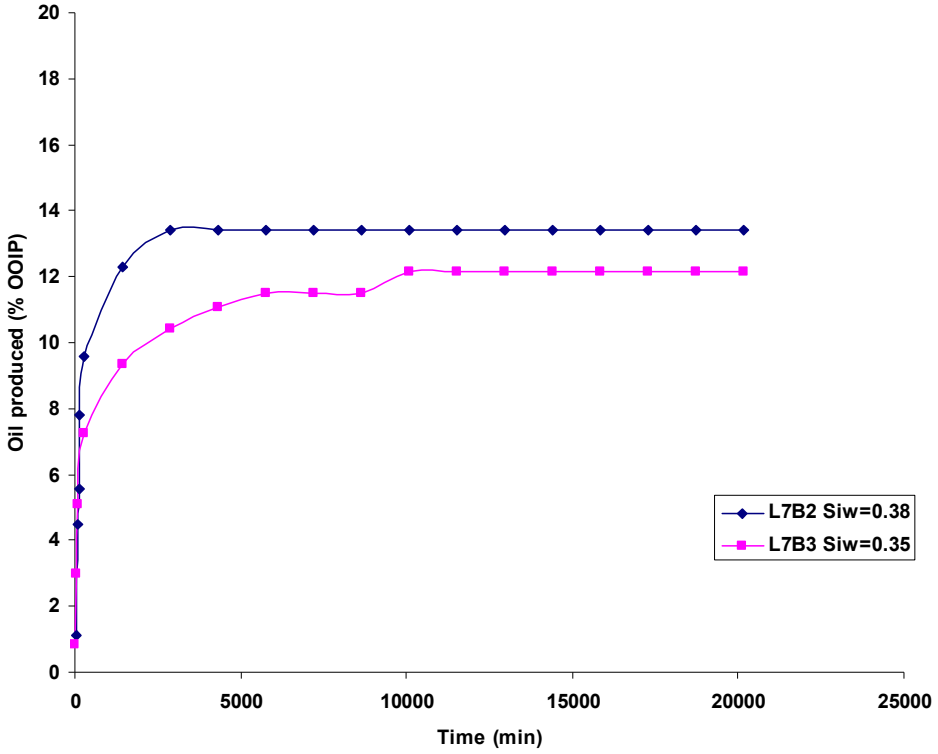

Figure 4-23 Imbibition profiles for L7B2 and L7B3 in deionized water at 45 °C

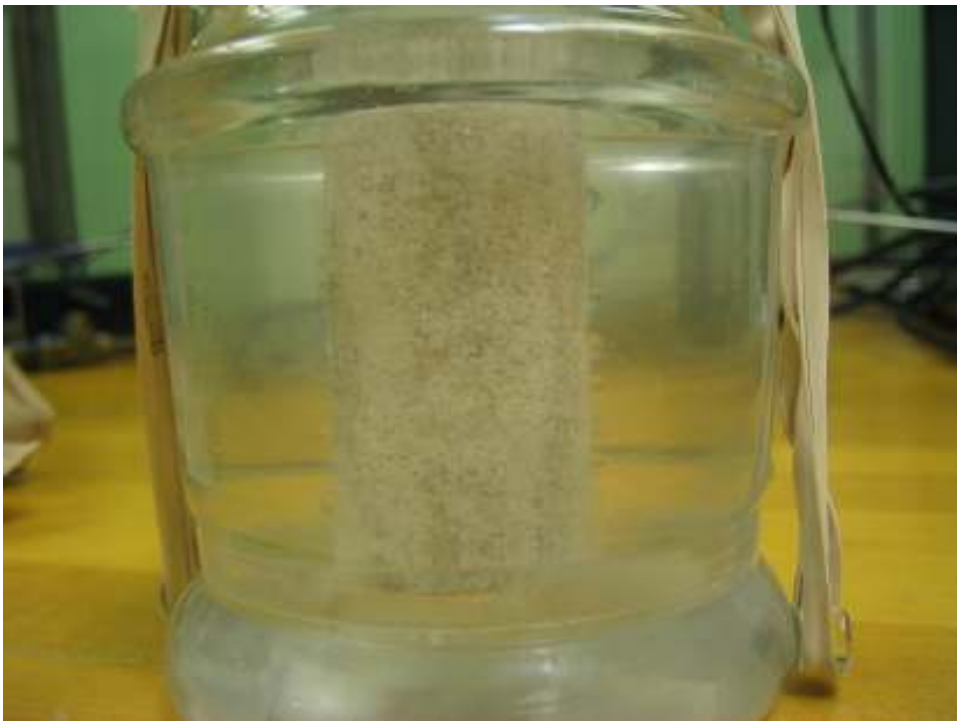

Figure 4-24 Cleaned L7B2 LKC core in water showing the countercurrent imbibition of water into the core at 45 °C

Table 4.3 Baseline imbibition data for cleaned reservoirs cores L7B2 and L7B3

Core	PV (ml)	S_{iw}	S_{ws}	S_{wf}	I_w
L7B2	**7.28**	**0.38**	**0.47**	**0.71**	**0.25**
L7B3	**7.21**	**0.35**	**0.43**	**0.64**	**0.27**

Core L7B2 was chosen to evaluate and compare the effectiveness of surfactin versus benchmark chemical surfactant STEOL CS-330 in mediating wettability change. This core at residual oil saturation was flooded with Soltrol 130 to an initial water saturation of S_{iw}= 0.36 and exposed to a 600 ppm solution of STEOL CS-330 in an imbibition cell at 45 °C. After reaching the production plateau, the core was flooded with water to residual oil saturation and the Amott water wettability index was calculated to be I_w= 0.30. STEOL CS-330 improved the oil recovery over that by

water alone despite a lower IFT values between the surfactant solutions against Soltrol 130. The core was then flooded with Soltrol 130 to an initial water saturation of S_{iw}= 0.27 and exposed to surfactin. **Figure 4-25** shows the baseline imbibition profile along with those for STEOL CS-330 and surfactin imbibition. Surfactin performed poorly compared with STEOL CS-330 in enhancing the imbibition process. It even performed poorly compared with deionized water. Table 4.4 summarizes the imbibition data for this core in contact with water and anionic surfactants. Since the core has a mixed-wet state, with the surface of the rock exhibiting oil and water-wet patches, it is difficult to interpret these results. This poor performance could be due to the lower IFT value for surfactin versus STEOL CS-330. It is also possible that because of having two negative charges on the head group, surfactin will adsorbed more strongly on the cleaned surfaces of reservoir core with the head group attached to the surface and the hydrocarbon tail toward the solution, making the surface appears to be less, rather than more, water-wet.

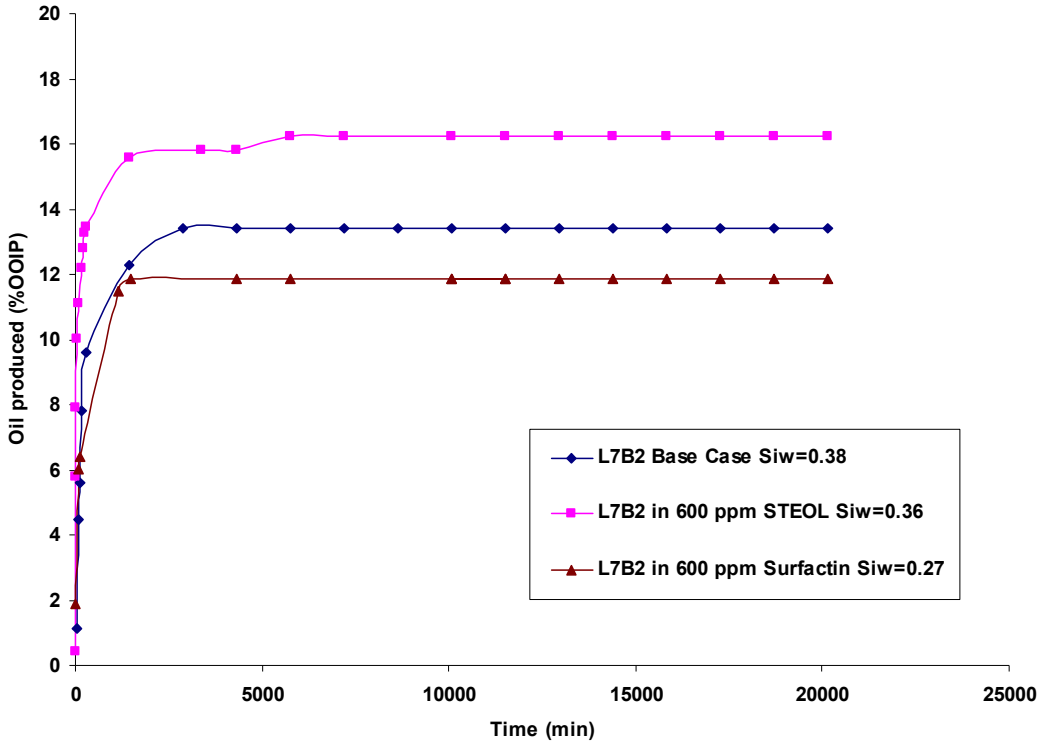

Figure 4-25 L7B2 imbibition profiles in water and anionic surfactants at 45 ºC

Table 4.4 Imbibition data for L7B2 core in water and anionic surfactants at 45 °C

Surfactant	PV (ml)	S_{iw}	S_{ws}	S_{wf}	I_w
Water	7.28	0.38	0.47	0.71	0.25
STEOL CS-330	7.28	0.36	0.46	0.71	0.30
Surfactin	7.28	0.27	0.35	0.68	0.20

There was also the possibility that surfactin performed poorly because of the high test temperature, where there could be surfactant degradation. To make sure that the lower performance of surfactin was not related to the temperature, L7B2 and L7B3 cores were cleaned and imbibition tests at room temperature were performed using both anionic surfactants. These cores were used to compare the performance of surfactin

versus STEOL CS-330 at two different surfactant concentrations of 100 and 500 ppm. After cleaning and drying to constant weight cores L7B2 and L7B3 were flooded and saturated with Soltrol 130 with no initial water saturation and placed in contact with 100 and 500 ppm solutions of STEOL CS-330 respectively. After obtaining the production profiles, these cores were flooded (forced imbibition) with water to residual oil saturation and Amott water wettability indices were calculated. Table 4.5 shows the imbibition data for these cores. Both cores were cleaned and then dried to constant weight. Soltrol 130 was used to saturate both L7B2 and L7B3 cores with no initial water saturation for testing in surfactin solution at concentrations of 100 and 500 ppm respectively. **Figure 4-26** and **Figure 4-27** show the imbibition profiles at room temperature for these cores in 100 and 500 ppm solutions of surfactin and STEOL CS-330 respectively. Table 4.6 summarizes the imbibition data for 500 ppm surfactant solutions. It can be seen from both figures that surfactin performed poorly compared with STEOL CS-300. It can be concluded that temperature has no significant effect on the performance of surfactin and lower performance could be due to the lower IFT value or higher adsorption through the head group for this surfactant as explained before.

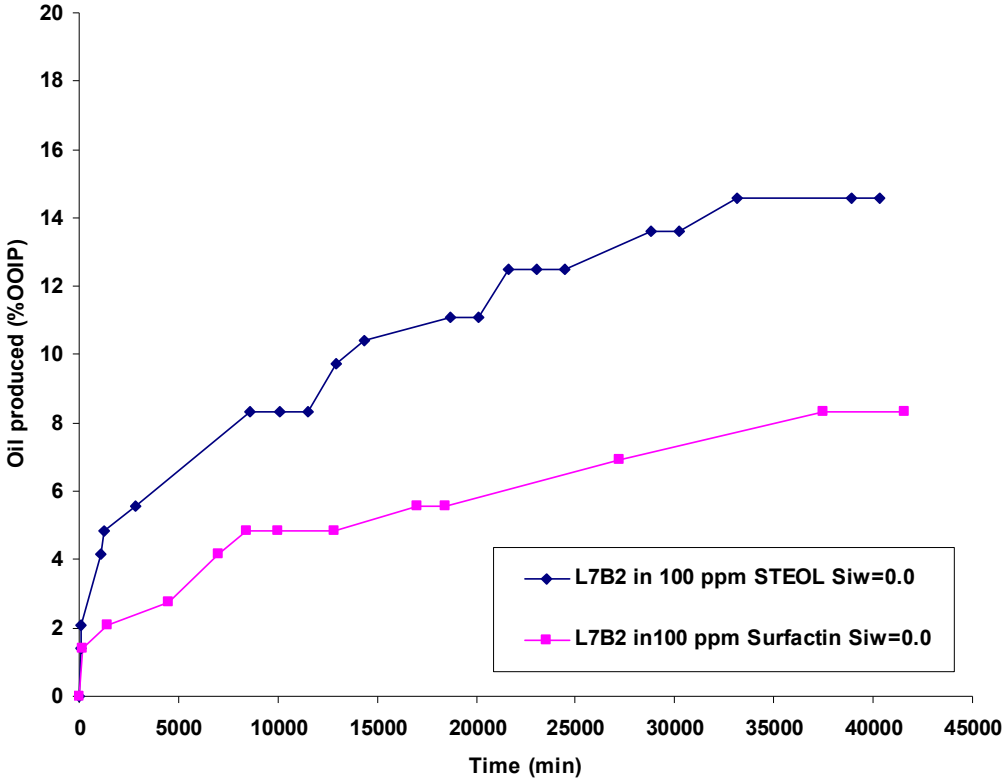

Figure 4-26 L7B2 Imbibition profiles in 100 ppm solution of anionic surfactants at room temperature

Table 4.5 Imbibition data for L7B2 core in 100 ppm solutions of anionic surfactants

Surfactant	S_{iw}	S_{ws}	S_{wf}	I_w
STEOL	0	0.15	0.66	0.22
Surfactin	0	0.08	0.69	0.12

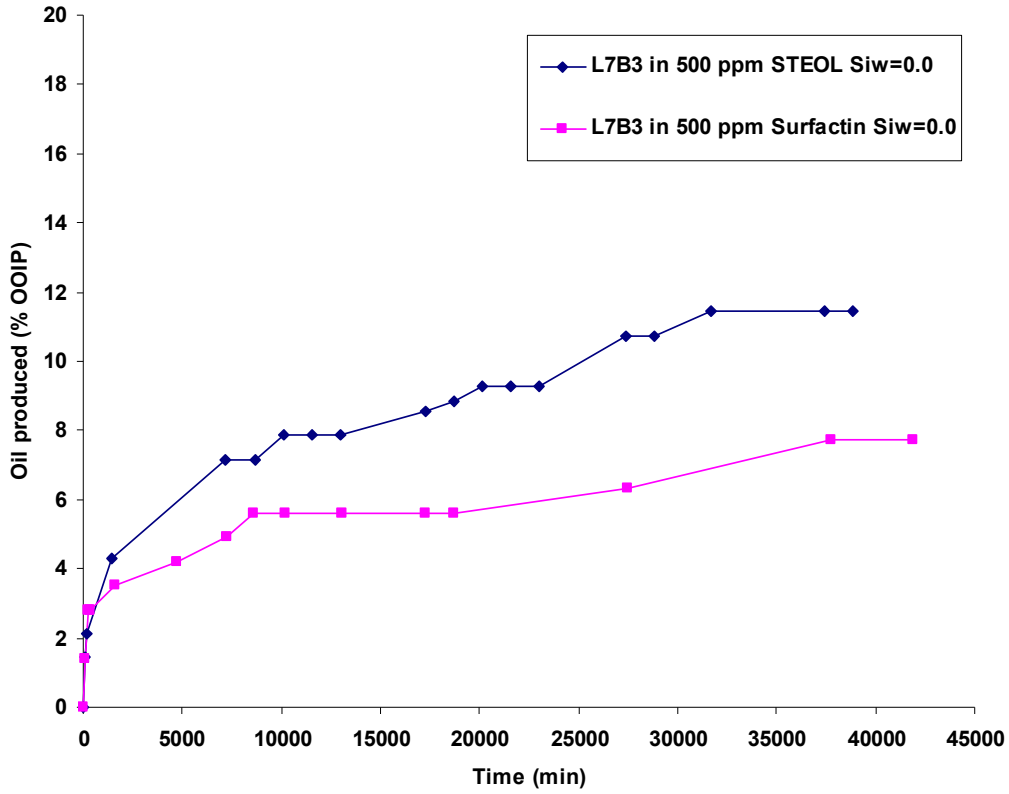

Figure 4-27 Imbibition profiles in 500 ppm solution of anionic surfactants at room temperature

Table 4.6 Imbibition data for L7B3 core in 500 ppm solutions of anionic surfactants

Surfactant	S_{wi}	S_{ws}	S_{wf}	I_w
STEOL	0	0.11	0.65	0.17
Surfactin	0	0.08	0.70	0.11

Having the baseline imbibition profile for L7B3 core, it was decided to look at the case where the core has been flooded and aged with anionic surfactants and then put in imbibition cell in contact with water. The procedure was to use the circulation set up used to obtain the dynamic adsorption data and flood the core which was initially saturated with water, with the desired surfactant solution (STEOL CS-330) and circulate the solution through the core for 24 h. The system was then aged for another

24 h and finally initial water saturation was established by flooding the core with Soltrol 130. The core was then put in imbibition cell in contact with water at 45°C. After the oil production reached its plateau the core was flooded with water to obtain the water wettability index. The core was then cleaned, dried, saturated with water and flooded and aged with the next anionic surfactant (surfactin). After establishing the initial water saturation, the core was placed in an imbibition cell in contact with water and the imbibition profile was obtained. **Figure 4-28** shows the base line imbibition profile along with those for the cases where L7B3 core was flooded and aged with both STEOL CS-330 and surfactin. Table 4.7 summarizes the imbibition data for L7B3 core for all these tests. STEOL CS-330 performed much better than surfactin in changing the wettability of the core to a more water-wet state, it changed the water wettability index from 0.27 to 0.45. Surfactin performance was poor initially and imbibition rate was less than water imbibition case. However, its final recovery was more than the water imbibition case. All these imbibition experiments indicate that for cleaned reservoir cores, where they exhibit a mixed-wet condition, STEOL CS-330 performed better than surfactin. Again because of the mixed-wet state, the interpretations of the results are difficult and differences in performance between STEOL CS-330 and surfactin could be due to the differences in IFT values against Soltrol 130 and the charged head groups on surfactant monomers.

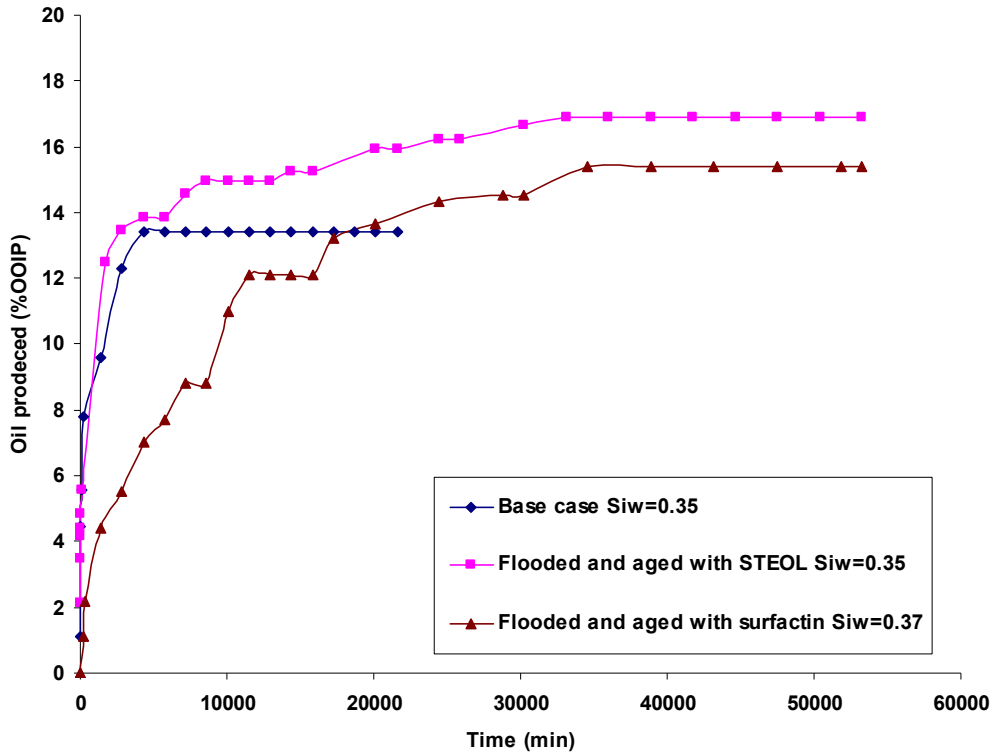

Figure 4-28 L7B3 imbibition profiles in water at 45C. The core was flooded and aged with anionic surfactants and imbibing water

Table 4.7 Imbibition data for L7B3 core flooded and aged with 1.0 mmol/l solutions of anionic surfactants

Surfactant	PV (ml)	S_{iw}	S_{ws}	S_{wf}	I_w
Water	7.21	0.35	0.43	0.64	0.27
STEOL CS-330	7.21	0.35	0.50	0.68	0.45
Surfactin	7.21	0.37	0.46	0.65	0.32

4.2.3.2 Oil-wet Core

Three reservoir core plugs (L701, L702, and L703) were aged in LKC crude oil at 90°C. These cores were previously used to compare the surfactin versus STEOL CS-330 in enhancing the spontaneous imbibition process in oil-wet cores (Eisert 2006).

Surfactin performed much better than STEL CS-330 in imbibing into these crude oil-aged cores (Eisert 2006). Core L702 was used to obtain the water and oil wettability indices needed in calculating the Amott-Harvey wettability index. This core at an initial water saturation of S_{iw}= 0.36 was placed in contact with water in an imbibition cell. No oil was produced from the core and so the core was then flooded with water to residual oil saturation of S_{or} = 0.32. Upon exposing the core to oil (Soltrol 130) it started producing water (**Figure 4-29**) and after reaching the production plateau, it was flooded with Soltrol 130 to initial water saturation. Table contains the imbibition data for this core. The core had a water wettability index of 0.0 and an oil wettability index of 0.4, indicating an oil-wet core. Two other oil-wet cores L701 and L703 at residual oil saturations were flooded and aged with 1.0 mmol/l of STEOL CS-330 and surfactin solutions respectively using the circulation method at a very low flow rate that did not disturb the residual oil saturation. After 24 h of flooding and 24 h of aging, the cores were flooded with Soltrol 130 to initial water saturation and exposed to water in separate imbibition cells. L701 that was flooded and aged with STEOL CS-330 did not produce any oil. However, L703 core flooded and aged with surfactin started producing oil after exposure to water (**Figure 4-30**). The water in both imbibition cells was replaced with the same surfactant solutions used in flooding and aging process and both imbibition profiles showed a jump in oil production after the exposure to surfactant solutions. Surfactin resulted in a total of ~ 6 % OOIP recovery from the strongly oil-wet core L703. STEOL CS-330 only produced ~ 2 % OOIP. This observation could be explained by the fact that in the case of oil-wet cores, the

surfactants would be able to interact with the adsorbed materials from the crude oil on the rock surface through hydrocarbon interaction. In the case of carbonate rock with an initial positive charge, the adsorbed components from crude oil on the rock surface are negatively charged and therefore only hydrophobic interactions between the tails of surfactant molecules and the adsorbed hydrocarbon layer on the rock surface is possible. Since the tail length is the same for both surfactants, both will have the same tendency to interact with the hydrophobic species on the rock surface. By adsorption through the tail, both surfactants have their head group toward the aqueous phase, and since surfactin has two charges on the head group, it interacts more water strongly molecules and enhances the spontaneous imbibition by creating a weakly water-wet layer near the rock surface.

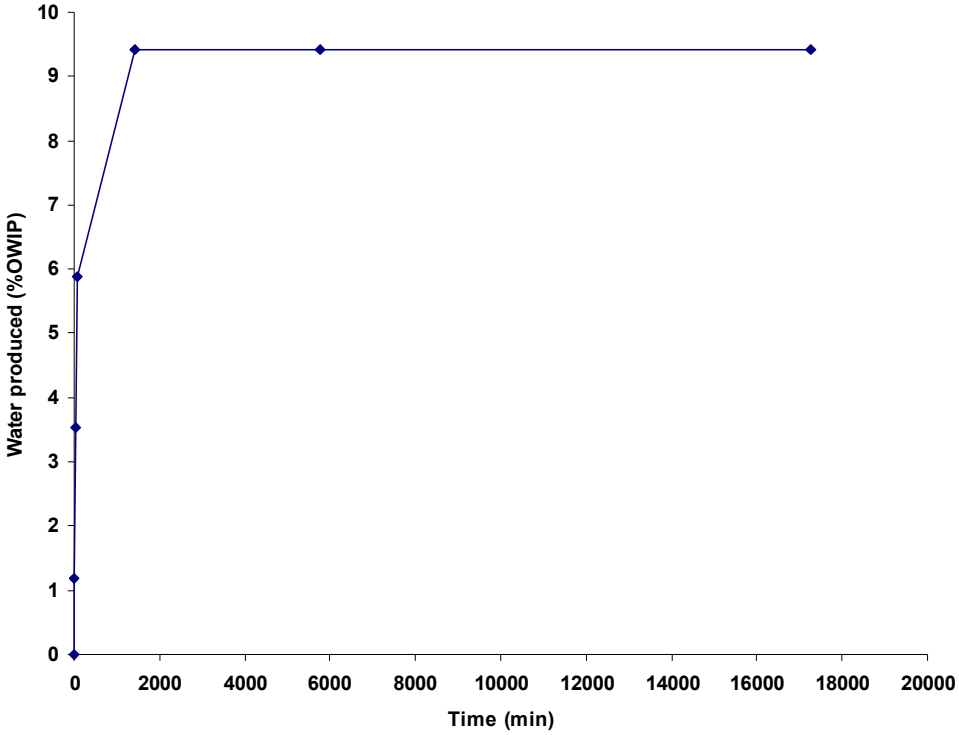

Figure 4-29 Crude oil-aged L702 imbibition profile in Soltrol 130

Table 4.8 Imbibition data for L702 core in water and Soltrol 130

S_{iw}	0.36
S_{ws}	0.36
S_{wf}	0.68
I_w	0.00
S_{or}	0.32
S_{os}	0.49
S_{of}	0.51
I_o	0.40

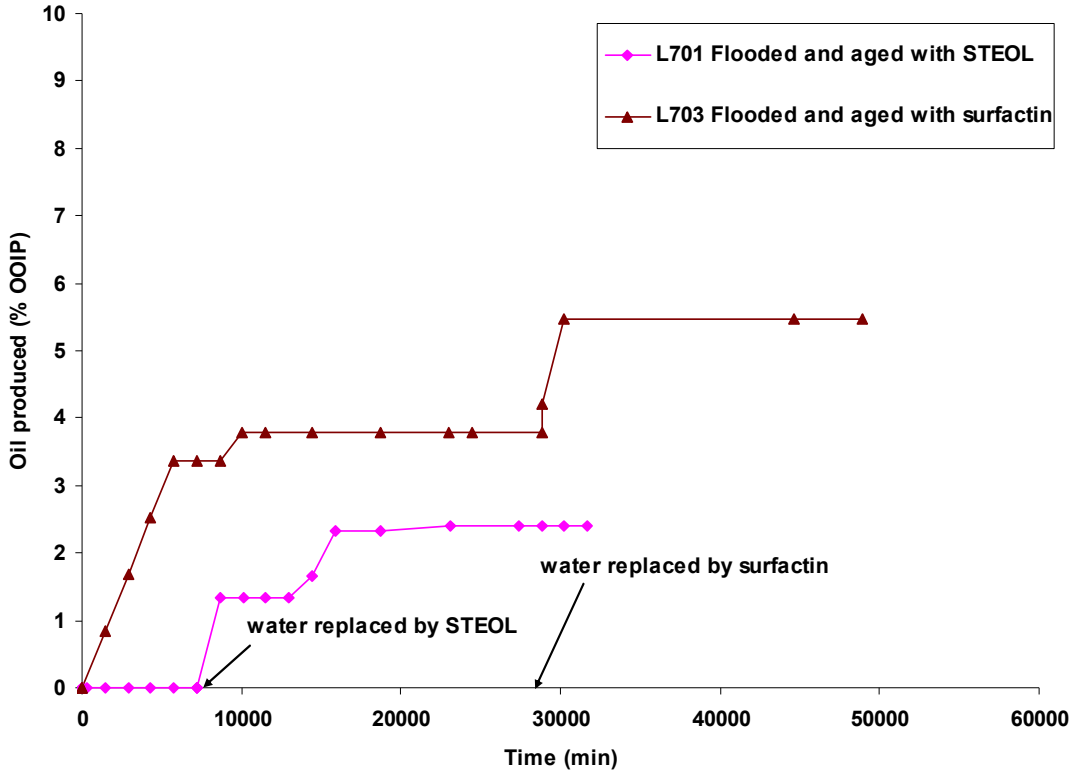

Figure 4-30 Imbibition profiles for oil-wet L701 and L703 cores flooded and aged with anionic surfactants in water and anionic surfactants at 45 °C

Table 4.9 Imbibition data for oil-wet cores L701 and L703 in water and anionic surfactants

Core	S_{iw}	S_{ws}	S_{wf}	I_w
L701	0.25	0.27	0.7	0.04
L703	0.34	0.37	0.77	0.07

4.2.4 Qualitative wettability tests

The effectiveness of surfactants in mediating wettability change was also observed through two qualitative tests: a two-phase separation test and a flotation test. Two-phase separation is a rapid method to test wettability of crushed rock material, adapted from Somasundaran and Zhang (1997). In this method a small quantity (0.2-0.3 g) of the material to be tested is weighed into a test tube in 15-20 ml aqueous

phase (water or a surfactant solution). An equal volume of Soltrol 130 is poured into the tube and the tube is gently agitated to mix the two phases. The tube is left to settle for 10 min and the amount of material in each phase (aqueous, oil) gives a qualitative indication of the wettability of the crushed rocks.

In flotation test, a small quantity (0.2-0.3 g) of the material to be tested is weighed into a test tube containing 15-20 ml aqueous phase (water or a surfactant solution). The system is left for several hours and the wettability of the crushed rock is assessed by the amount of the material that sinks to the bottom of the tube. The greater the amount of rock remaining at the surface, the more oil-wet it is. Cleaned carbonate material was found to be completely water wet (**Figure 4-31**). To alter the wettability of the clean crushed material towards a more oil-wet state, samples were placed in a glass container under crude oil at 90°C and the wettability of samples was determined using two-phase separation at intervals (**Figure 4-32**). To investigate the efficiency of the crude oil in altering the wettability, the samples were dried to constant weight and then either exposed to the crude oil directly, or moistened with water before being added to the crude. It was found that while the wettability of the dry material changed rapidly, the material with water remained hydrophilic for a much longer period (**Figure 4-32**). It was clear that the layer of water on the particle surfaces prevented the oil from coming into direct contact with the rock. This has obvious implications for the alteration of wettability of core materials.

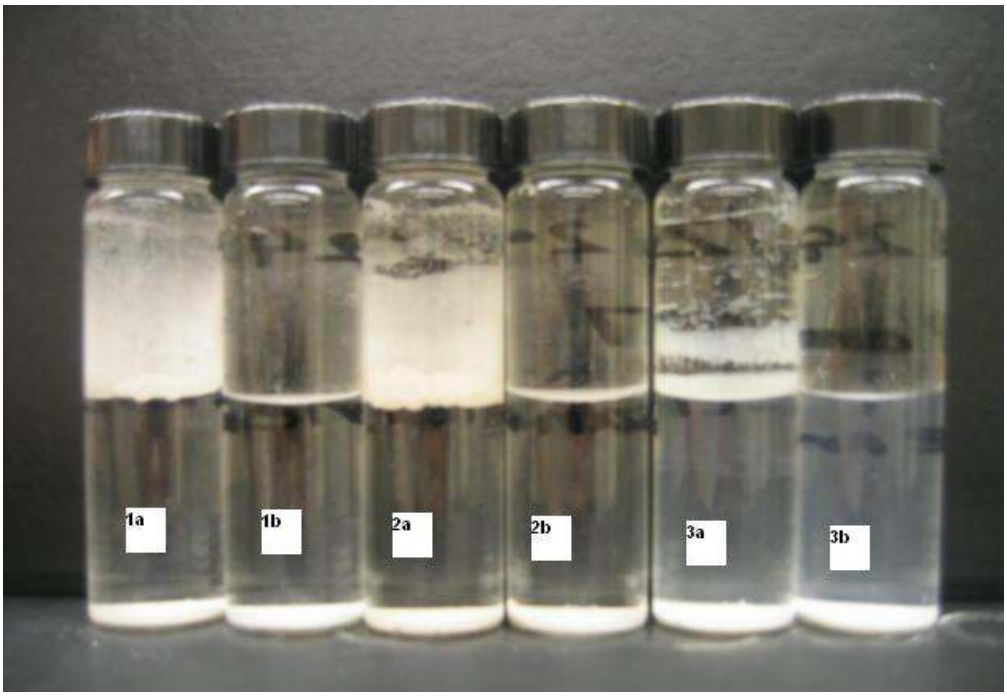

Figure 4-31 Two-phase separation tests on crushed BF, L7 and Miami rocks in water/Soltrol: (1a) fresh un-cleaned BF, (1b) cleaned BF, (2a) fresh un-cleaned L7, (2b) cleaned L7, (3a) fresh un-cleaned Miami, (3b) cleaned Miami

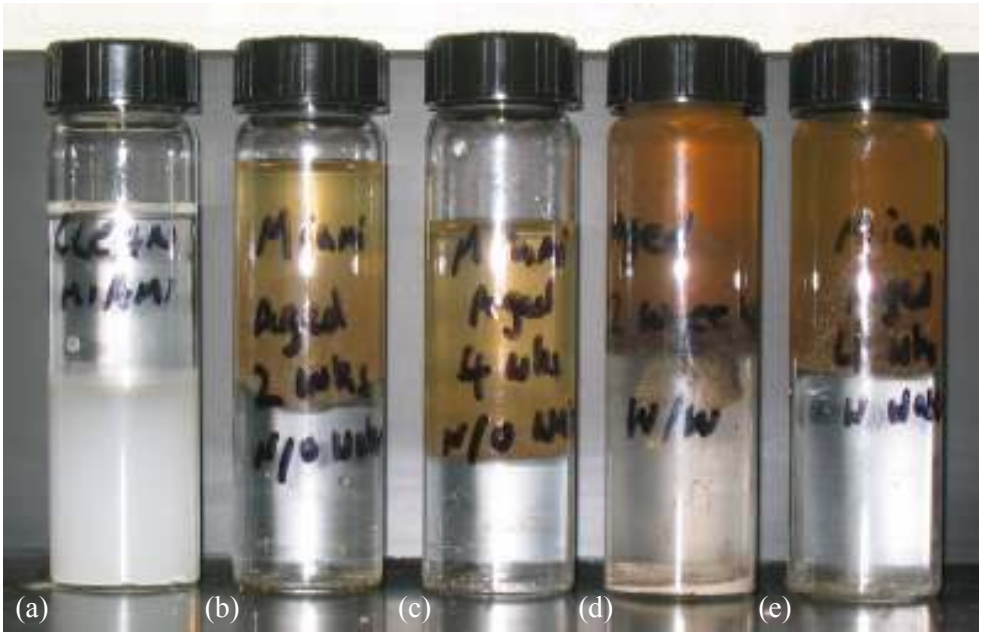

Figure 4-32 Crushed Miami oolite in water/Soltrol: (a) clean, (b) and (c) with no initial water saturation after 2 and 4 weeks under crude oil at 65 °C to show rapid change to oil wet state, (d) and (e) with initial water saturation after 2 and 4 weeks under crude oil at 65 °C

Figure 4-33 shows the result of two-phase separation test on crude-oil aged BF crushed rocks, demonstrating the effectiveness of surfactin compared with STEOL CS-330 in changing the wettability. The same results were obtained using oil-wet L7 crushed rock (**Figure 4-34**). These results were confirmed by performing flotation tests on the oil-wet BF and L7 crushed rock samples in contact with both surfactants (**Figure 4-35** and **Figure 4-36**). A larger proportion of the sample in contact with surfactin sank compared with that in contact with STEOL CS-330 for both rocks.

Figure 4-33 Two-phase tests showing the effectiveness of surfactants in mediating the wettability (1) oil-wet BF, (2) Oil-wet BF in contact with STEOL CS-330 for 24 h. (3) Oil-wet BF in contact with surfactin for 24 h

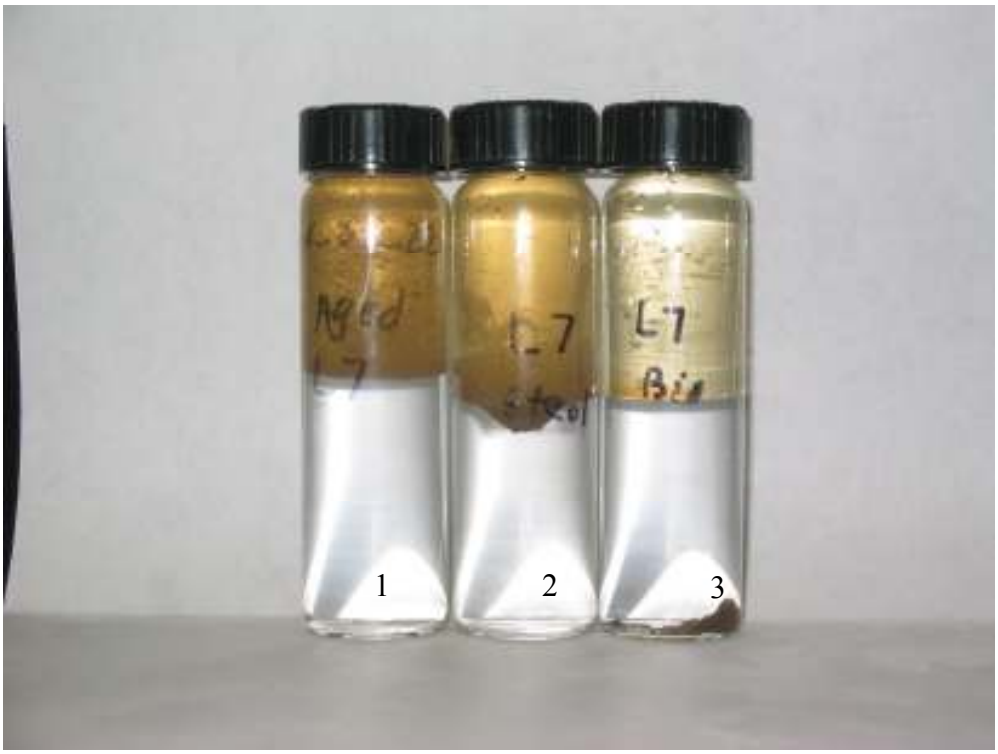

Figure 4-34 Two-phase tests showing the effectiveness of surfactants in mediating the wettability (1) Oil-wet L7 (2) Oil-wet L7 in contact with STEOL CS-330 for 24 h. (3) Oil-wet L7 in contact with surfactin for 24 h

Figure 4-35 Flotation test showing the change in wettability of BF rock after contact with surfactants for 24 h (1) oil-wet BF rock in contact with surfactin, (2) oil-wet L7 rock in contact with STEOL CS-330

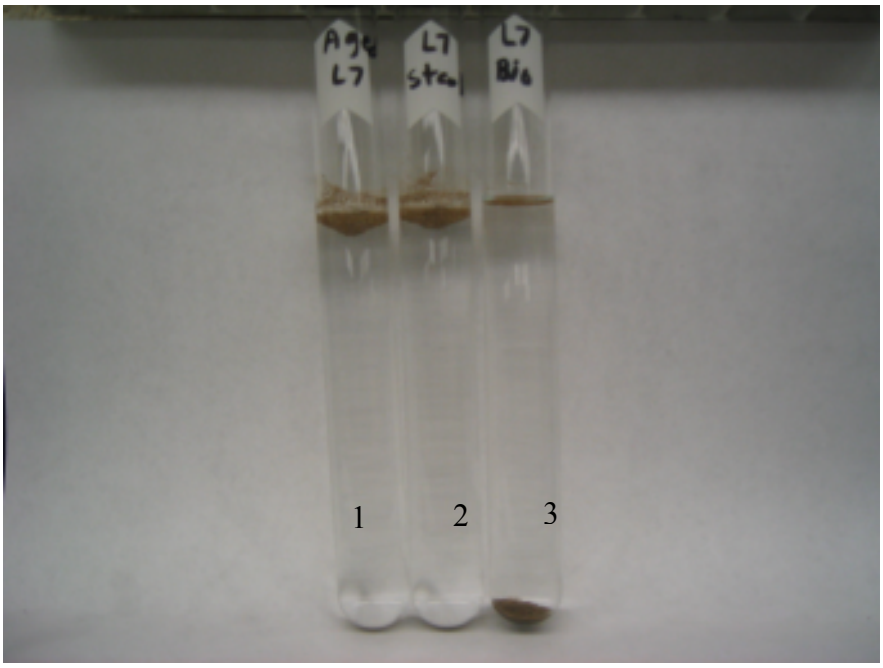

Figure 4-36 Flotation test showing the change in wettability of L7 rock after contact with surfactants for 24 h (1) oil-wet L7 rock in water (2) L7 in contact with surfactin, (2) BF rock in contact with STEOL CS-330

It was concluded from both tests that surfactin is more effective than STEOL CS-330 in reversing the wettability of oil-wet crushed rocks toward a water-wet state.

4.3 Wettability Alteration Mechanisms Study

In this study, we performed mechanistic studies to test the hypotheses proposed in the literature for the mechanisms of wettability alteration by surfactants. Austad *et al.* (Austad, Matre et al. 1998; Standnes and Austad 2000) observed that in oil-wet chalk cores, both cationic and anionic surfactants altered the rock wettability toward a more water-wet state, however, the cationic surfactants were more effective than the

anionic surfactants in the wettability alteration process. In their experiments, chalk cores were first aged in a crude oil at 90 °C. During the process, the adsorption of negatively charged carboxylate groups from crude oil on the positively charged chalk surface changed the rock wettability toward oil-wet. They proposed that cationic surfactants could alter the wettability of the oil-wet chalk surface toward a more water-wet state by forming ion pairs between the cationic head groups and the negatively charged carboxylate groups adsorbed on the rock surface. The ion-pairs resulting from the strong electrostatic interactions are further stabilized by hydrophobic interactions. In the surfactant literature, the product of reaction between carboxylates and organic ammonium compounds is referred to a "cat-anionic surfactant" (Carlson, Backlund et al. 2000). It was suggested that ion-pair formation could strip the adsorbed layer of crude oil components off the rock surface, exposing the originally water-wet carbonate rock. For anionic surfactants, they claimed that the surfactant molecules could form a monolayer on the rock surface through hydrophobic interactions with the adsorbed crude oil components. The layer of adsorbed surfactants with the hydrophilic head groups covering the originally oil-wet rock surface could then change the wetting state of the rock surface toward more water-wet. Since the hydrophobic interactions are much weaker than the ion-pair interactions, they proposed that this could explain why cationic surfactants performed better than the anionic surfactants in altering the wettability of the carbonate rock to a more water-wet state. However, none of the hypotheses for the wettability alteration were verified experimentally. In the following, I discuss results of experiments

designed to test the mechanistic hypotheses proposed by Austad *et al.* (Austad, Matre et al. 1998; Standnes and Austad 2000).

4.3.1 Wettability Alteration by Ion-pair Formation

Standnes and Austad (Standnes and Austad 2000) observed accelerated imbibition rates with the cationic surfactant dodecyltrimethylammonium bromide (C12TAB) present in the aqueous phase for oil-wet chalk cores (made oil-wet by flooding with and aging in crude oil) and related that to the ability of the surfactant to make the chalk surface more water-wet. They proposed that ion-pair formation between the positive head groups of the cationic surfactant molecules and the negatively charged adsorbed material, mostly carboxylic groups from crude oil on the surface of the chalk, was the mechanism responsible for making the core more water-wet.

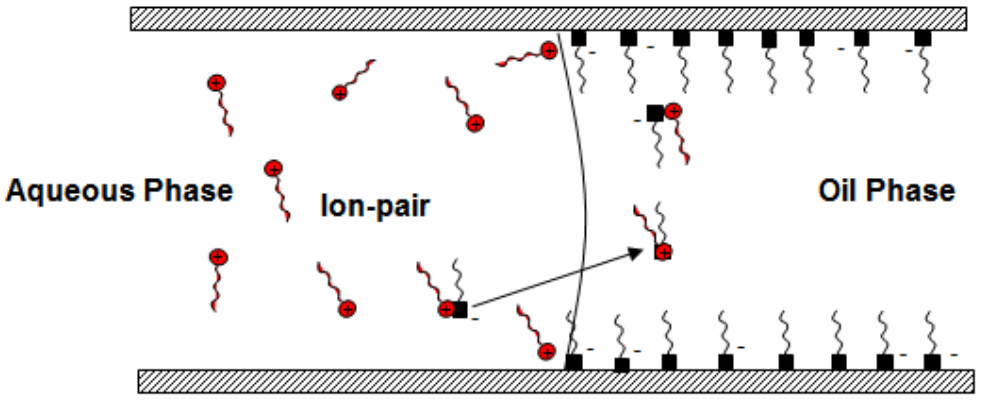

Figure 4-37 Schematic model of suggested wettability alteration mechanism by cationic surfactant C12TAB. Circles are cationic surfactant molecules and squares are anionic organic materials from crude oil (Standnes 2001)

The ion-pair formation is driven by electrostatic interactions between the head groups and stabilized by hydrophobic interactions between the tail sections. As shown in **Figure 4-37**, the formation of ion pairs could strip the adsorbed layer of crude oil components from the rock surface, exposing the originally water-wet rock surface. The ion pairs formed during the process would no longer be water soluble and therefore, would partition into the oil phase leaving the free surfactant molecules in the water phase to associate with the adsorbed crude oil components near the oil/water interface (**Figure 4-37**). In this way, the surfactants could change the wettability of the rock surface successively to a more water-wet state.

If the proposed mechanism is correct, we should expect anionic surfactants to be more effective than cationic surfactants in changing the wettability of oil-wet sandstone rock. Based on this hypothesis, the experimental work shown in **Figure 4-38** was proposed. The wettability of the originally strongly water-wet sandstone rock can be altered toward the oil-wet state by aging it in crude oil at elevated temperatures. Buckley *et al*. (1998) demonstrated that the negatively charged sandstone surface has a higher affinity toward the positively charged basic components in crude oil and therefore crude oils with larger fraction of basic components are more effective in turning the sandstone rock oil-wet (**Figure 4-39**). They observed that when grouped by their API number, crude oils with higher fraction of basic components made the sandstone core less water-wet after the aging process. The LKC crude oil used here is more basic and a good candidate for this study. After the aging process, the surface of the sandstone rock is coated with the

positively charged basic components originally dissolved in the crude oil. If ion-pair formation is indeed the mechanism for wettability alteration, anionic surfactants should be more effective than cationic surfactants in changing the wettability of sandstone rock toward a more water-wet state because in this case, the electrostatic interaction driving the ion-pair formation exists only between the anionic head groups of the surfactant molecules and the positively charged basic components of the crude oil adsorbed on the sandstone surface.

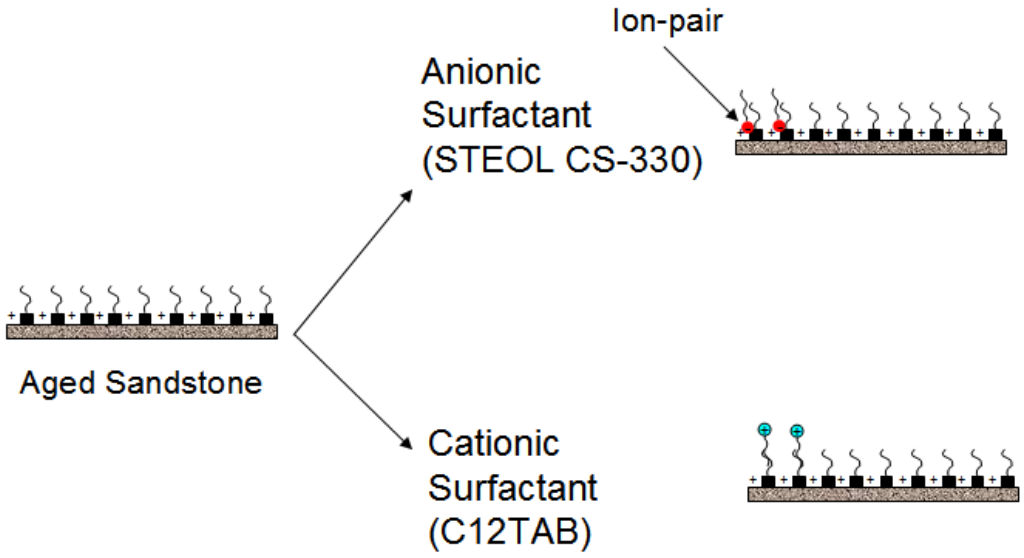

Figure 4-38 Proposed experiments for wettability alteration mechanistic study by ion-pair formation

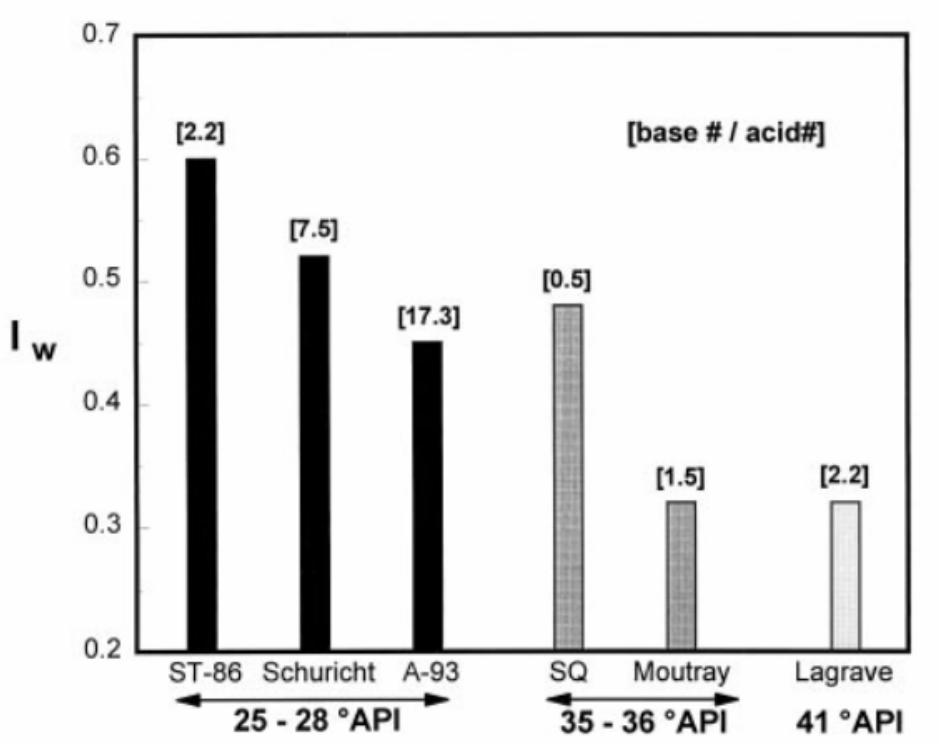

Figure 4-39 Oil-wetness in sandstone rock increase by increasing the basic to acid ratio in crude oil (Buckley, Liu et al. 1998)

To test the hypothesis, we performed imbibition tests in Berea sandstone cores using an anionic surfactant, STEOL CS-330; and a cationic surfactant, C12TAB. The reasons for selecting Berea sandstone as the porous medium were its high permeability, homogeneous properties, and strong water wettability. The properties of the Berea sandstone cores used in this study are summarized in Table 4.10. Core B02 was first saturated and characterized with Soltrol 130. Soltrol 130 was then displaced by crude oil and the core was aged in crude oil in oven at 90 °C for one month. Core B03 was saturated and characterized with 10 g/l NaCl and then the initial water saturation was established by flooding the core with Soltrol 130. To prepare the cores

for the aging process, Soltrol 130 was then displaced by crude oil. After that, the cores were aged in crude oil at a temperature of 90 °C for one month. A separate complete imbibition test on a crude oil-aged sandstone core resulted in an Amott-Harvey index of I_{A-H}= -0.4 indicating the effectiveness of the aging process in making these cores oil-wet. After aging, they were flooded with Soltrol 130 to displace the crude oil. The cores were then placed in imbibition cells in contact with 1% brine solution and oil production was monitored. Core B02 started producing oil within a few hours of contact with brine solution. However, there was a few days delay before oil production from core B03. After two weeks, the brine solutions in contact with cores B02 and B03 were replaced with 1.0 mmol/l solutions of cationic and anionic surfactants (C12TAB and STEOL CS-330) respectively.

Table 4.10 Properties of Berea sandstone cores

Core	Length (cm)	Diameter (cm)	Area (cm^2)	PV (ml)	ϕ (%)	k (md)
B02	6.19	3.76	11.1	14.6	21	490
B03	6.35	3.76	11.1	14.9	21	510
B04	7.17	3.82	11.4	17.8	21	590
B05	7.17	3.81	11.4	17.2	21	560
B06	6.79	3.82	11.4	16.7	21	512
B07	7.05	3.83	11.6	17.3	21	480

The IFT values for all the surfactants used in this work against Soltrol 130 were obtained using a ring tensiometer (Table 4.11). STEOL CS-330 had an IFT of 7 mN/m and that of C12TAB was 19 mN/m.

Table 4.11 IFT values for 1.0 mmol/l surfactants vs. Soltrol 130

Surfactant	IFT vs. Soltrol 130 (mN/m)
STEOL CS-330	7
C12TAB	19
Surfactin	4
Gemini	8

Figure 4-40 shows the results of imbibition tests from these two crude oil-aged sandstone cores in brine and surfactants. It can be seen that over a period of two weeks imbibition in brine, these cores only produced 2 % of original oil in place (OOIP), indicating an initial strong oil-wet state. The oil produced during this period from both cores came from the top surface of the cores, consistent with an imbibition driven by gravity. After replacing the brine with surfactant solutions, in the case of anionic surfactant STEOL CS-330, the core started producing oil from all faces in about 10 minutes, showing a change in production mechanism from gravity to capillary driven, despite the lower IFT value for this surfactant against Soltrol 130. The core in contact with cationic surfactant produced very little extra oil. These results were in agreement with those expected if ion-pair formation is responsible for the wettability alteration. After reaching their production plateau, both cores were flooded with brine at a constant flow rate of 5 ml/min (this was the flow rate in all flow tests). This enables one to calculate the water wettability indices for these cores. Table 4-12 summarizes the imbibition data for these cores. STEOL CS-330 resulted

in a water wettability index of 0.12 versus 0.04 for C12TAB. To investigate the effectiveness of both cationic and anionic surfactants in changing the surface wettability of oil-wet cores when surface is exposed to these surfactants, both B02 and B03 cores at residual oil saturation were flooded (24 h) and aged for 24 h (using the circulation set up) with C12TAB and STEOL CS-330 respectively at a very low flow rate (0.2 ml/min) that did not change the residual oil saturation. Then cores were flooded with Soltrol 130 to initial water saturation and put in imbibition cells in contact with brine. **Figure 4-41** shows the imbibition profiles for these cores in brine at room temperature. B03 core (flooded and aged with STEOL CS-330) started producing oil after exposure to brine and reached its production plateau in about two weeks (2.7 ml oil produced). Core B02 core (flooded and aged with C12TAB) did not produce any oil after contact with brine. After three weeks of imbibition in brine, both cores were flooded with brine to residual oil saturations to calculate their water wettability index. Table 4-13 summarizes the imbibition data for B02 and B03 cores. B03 core exhibited a water wettability index of 0.6 and shows the effectiveness of the anionic surfactant in changing the rock surface toward a water-wet state. B02 imbibed no brine and resulted in a water index of 0.0. These cores at residual oil saturation were then placed in imbibition cells in contact with Soltrol 130 and water production was monitored versus time. **Figure 4-42** shows the imbibition profiles for both cores in Soltrol 130 at room temperature. This time B02 core started producing oil and B03 core only produced a trace amount of water after contact with Soltrol 130. These results indicate that B02 core is still somewhat oil-wet and B03 core is behaving as a

water-wet core. After a week of imbibing Soltrol 130, both cores were flooded with Soltrol 130 to initial water saturation and oil wettability indices were calculated (Table 4-14). It can be concluded that anionic surfactant STEOL CS-330 does perform much better than cationic surfactant C12TAB in changing the wettability of crude oil-aged sandstone cores.

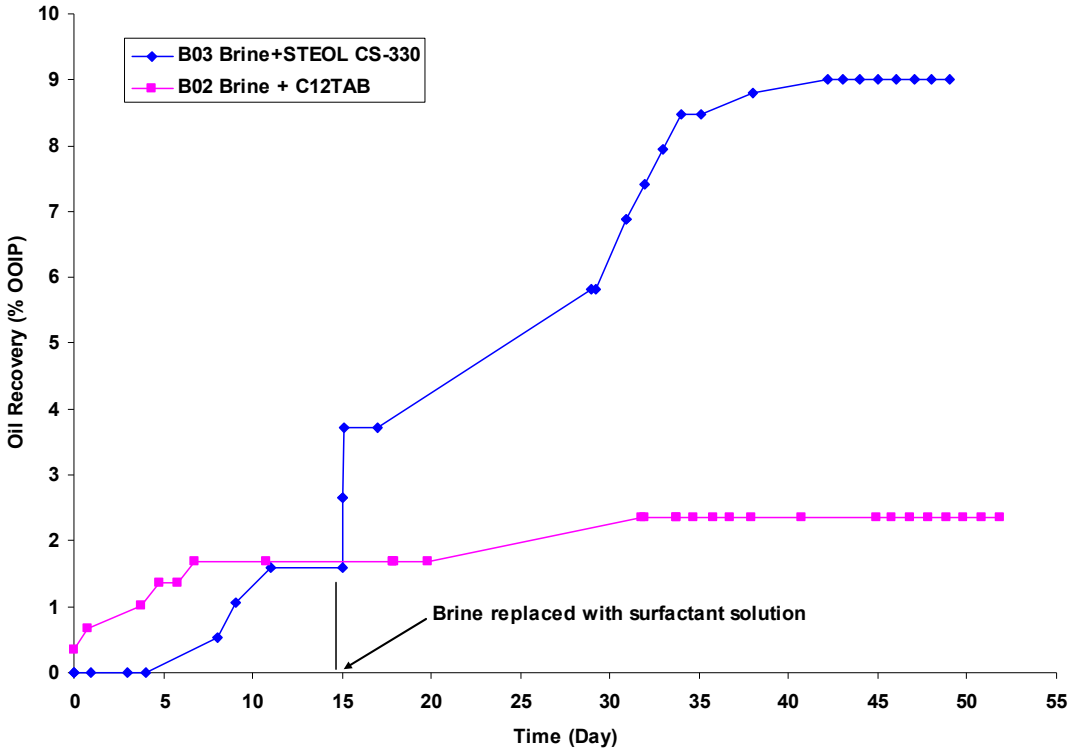

Figure 4-40 Sandstone cores B02 and B03 imbibition profiles in 1% brine solution and in 1.0 mmol/l solutions of cationic and anionic surfactants at room temperature

Table 4.12 B02 and B03 cores imbibition data in brine and surfactant solutions

Core	S_{iw}	$S_{ws(b+s)}$	S_{wf}	I_w
B02	0.0	0.02	0.55	0.04
B03	0.38	0.43	0.92	0.12

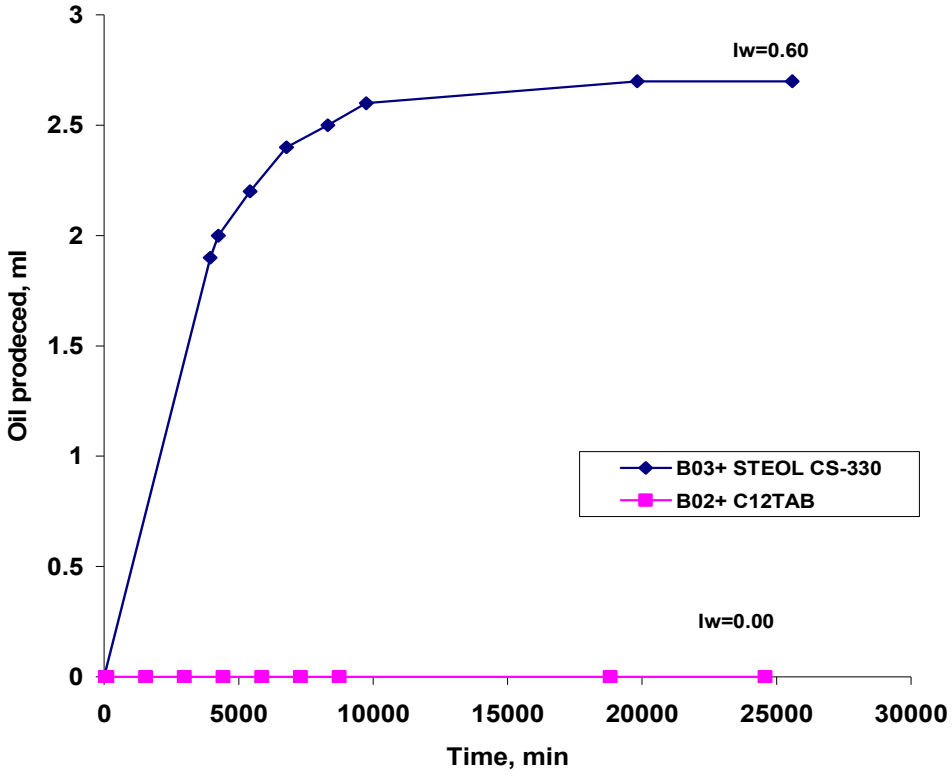

Figure 4-41 B02 and B03 imbibition profiles in brine after flooding and aging with C12TAB and STEOL CS-330 surfactants at room temperature

Table 4.13 Imbibition data for B02 and B03 cores in brine after flooding and aging in surfactants

Core	S_{iw}	S_{ws}	S_{wf}	I_w
B02	0.09	0.09	0.41	0.00
B03	0.48	0.66	0.78	0.60

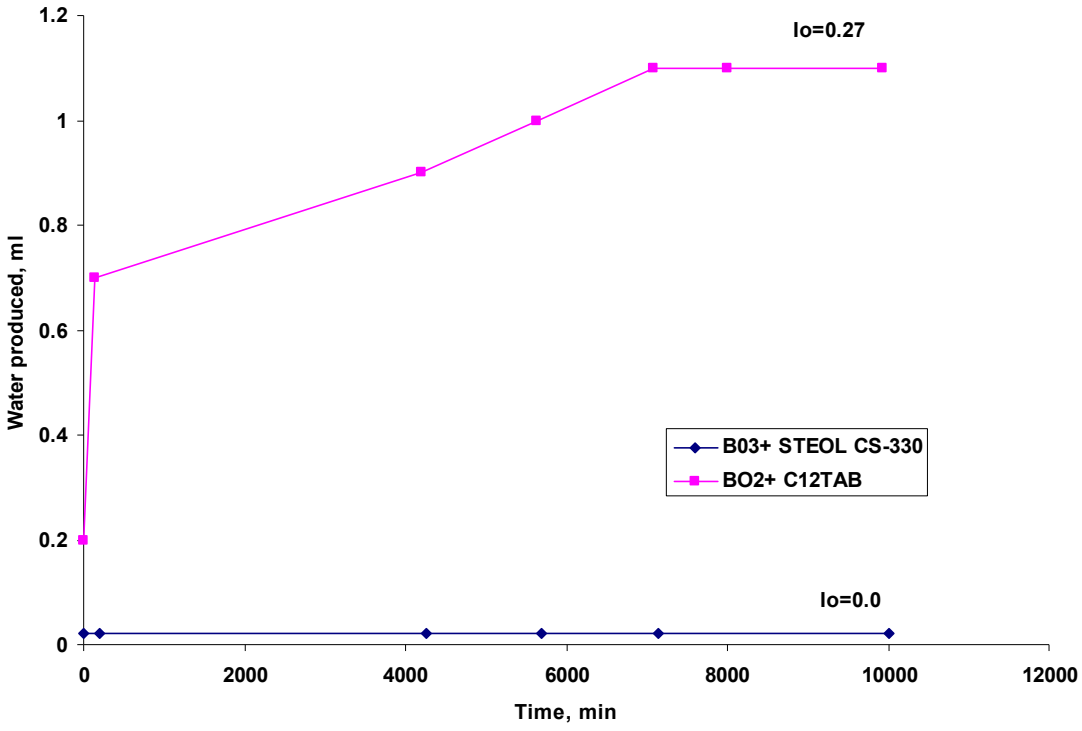

Figure 4-42 B02 and B03 imbibition profiles in Soltrol 130 after flooding and aging with C12TAB and STEOL CS-330 surfactants at room temperature

Table 4.14 Imbibition data for B02 and B03 in Soltrol 130 after flooding and aging in surfactants

Core	S_{or}	S_{os}	S_{of}	I_o
B02	0.59	0.66	0.85	0.27
B03	0.22	0.22	0.50	0.0

To check the reproducibility of the imbibition results obtained with B02 and B03 cores in surfactant solutions, two imbibition tests were repeated using two more crude oil-aged sandstone cores B04 and B05. In this test, both cores were first saturated and characterized by Soltrol 130 and then flooded with crude oil and aged with no initial water saturation for one month at 90°C. The cores first were exposed to brine solution

and then brine was replaced with surfactant solutions. Similar to previous imbibition test on B02 and B03, same results were obtained from B04 and B05 cores. The anionic surfactant STEOL CS-30 performed better than cationic surfactant C12TAB after 170 days of total imbibition time (**Figure 4-43**).

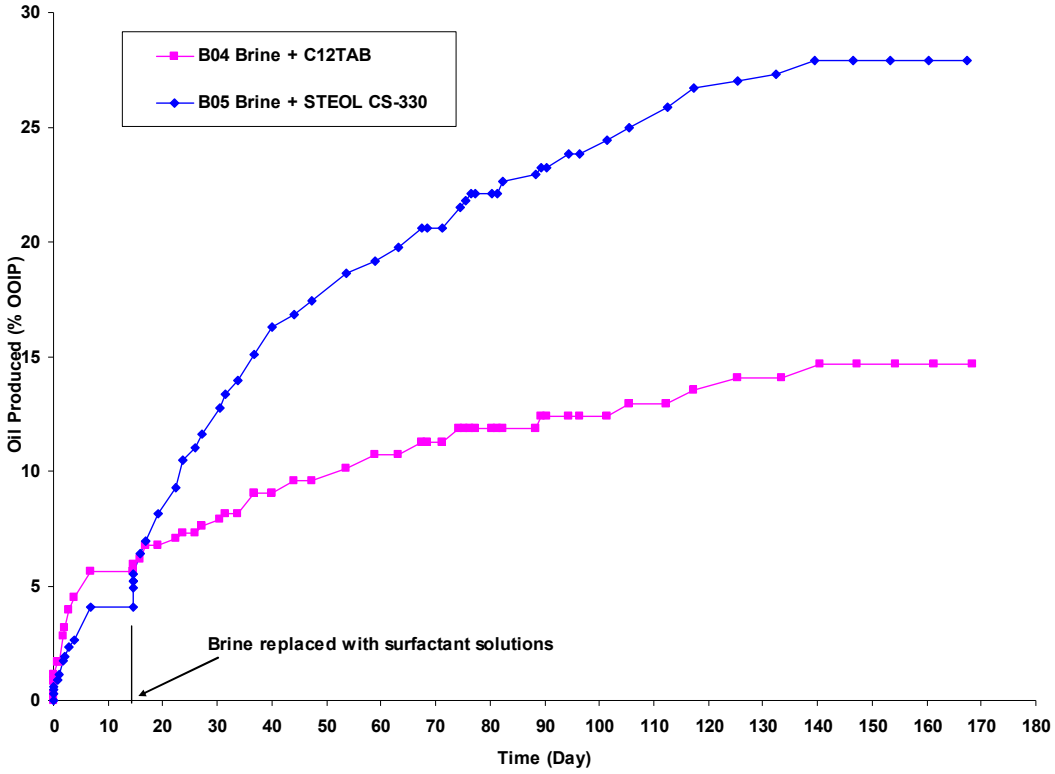

Figure 4-43 Sandstone cores B04 and B05 imbibition profiles in 1% brine solution and in 1.0 mmol/l solutions of cationic and anionic surfactants at room temperature

One may argue that the better performance for STEOL CS-330 is related to the lower IFT value for this surfactant which in turn enhanced the oil production by gravity forces. Inverse Bond number (Equation 12), which is the ratio of capillary to gravity

forces, is used to determine if the imbibition is driven by capillary forces (countercurrent flow) or gravity forces (cocurrent flow):

$$N_B^{-1} = C\frac{\sigma\sqrt{\frac{\phi}{k}}}{\Delta\rho g h} \qquad (4.2)$$

where C is a constant related to the pore geometry (C=0.4 for cylindrical capillaries), σ is the IFT (mN/m), ϕ is the porosity, k is the permeability (cm^2), $\Delta\rho$ is the density difference between the two immiscible phases (g/cm^3), g is the gravitational acceleration (cm/s^2), and h is the length of the core (cm). It is concluded from the work of Schechter *et al.* (Schechter, Zhou et al. 1994) that if $N_B^{-1}>5$, capillary forces are driving the imbibition process. For $N_B^{-1}<<1$, the imbibition is dominated by the gravity forces and the flow will be cocurrent. The imbibition mechanism could be the results of combination of capillary and gravity forces if N_B^{-1} falls in the intermediate range of $1<N_B^{-1}<5$. Table 4-15 lists the calculated inverse Bond numbers for all the imbibition tests in this study. These values show that gravity is not the dominant imbibition mechanism in any of the tests, which was to be expected for the short cores (L ~ 3 inch) used in this work. The inverse Bond number discussed by Schechter *et al*. (Schechter, Zhou et al. 1994) was developed for a well-defined water-wet system and, as suggested by Hognesen *et al.* (Hognesen, Oslen et al. 2006), its use for systems of altered wettability should be used with caution to distinguish between relative contribution of capillary and gravity forces on the spontaneous imbibition process. For the IFT values (4.0 to 19.0 mN/m) encountered for the

systems studied in this study (Table 4.11), the displacement of oil is believed to be dominated mainly by capillary forces at the start, while gravitational forces may come into effect at a later stage in the imbibition process; this is consistent with the surfactants acting as wettability modifying agents.

Table 4.15 Values of the inverse Bond number for the imbibition tests

Imbibition Test		N_B^{-1}
B02 + C12TAB	(Fig.101)	34
B03 + STEOL CS-330	(Fig.101)	12
B04 + C12TAB	(Fig.104)	26
B05 + STEOL CS-330	(Fig.104)	10
B02 + Surfactin	(Fig.105)	7
B03 + STEOL CS-330	(Fig.105)	12

On the other hand, these sandstone cores were aged in crude oil and their surface is no longer carries the initial negative charge. It was assumed in this study that based on the work of Buckley et al. (Buckley, Takamura et al. 1989) the basic components of crude oil (which are the dominant components in LKC crude oil) will adsorb onto the rock surface and the net charge will be positive. So there is no electrostatic attraction between the cationic surfactant and the crude oil-aged sandstone rock surface which could result in low adsorptions values for this surfactant onto oil-wet sandstone rock, which rules out the possibility of lower performance due to higher adsorption for this cationic surfactant. Moreover, this will create an electrostatic interaction between the anionic surfactant and the positively adsorbed components

from crude oil on the surface of the sandstone rock which drives the formation of ion-pair and consequently wettability alteration. It can be seen from the imbibition profiles that by introducing the anionic surfactant, the oil production increased dramatically over the values obtained by brine imbibition. The IFT value for the brine (10 g/l NaCl solution) vs. Soltrol 130 is about 37 mN/m. That for 1.0 mmol/l solution of STEOL CS-330 vs. Soltrol 130 is 7 mN/m. An IFT reduction from 37 to 7 mN/m is expected to result in a decrease in the oil production from a reduction in the IFT contribution to capillary forces. However, in our case, the increase in oil production possibly resulted from wettability alteration of some of the pore surfaces to a more water-wet state by the anionic surfactant through ion-pair formation. If the effect from wettability alteration is greater than that from the IFT reduction, a higher production could result.

Based on these findings, we hypothesized that it may be possible to improve the wettability alteration process by increasing the charge density on the head group of the surfactant molecule, since the ion-pair formation is driven by the electrostatic interactions. To test this hypothesis, we used an anionic biosurfactant (surfactin from *Bacillus subtilis*), which carries two negative charges on the head group. This surfactant can be produced by growing bacteria on agricultural waste streams and could be cost effective for field applications compared with commercially produced surfactants (Salehi, Johnson et al. 2006). Previously used cores B02 and B03 were cleaned by Dean-Stark extraction with toluene, dried and were saturated with Soltrol 130, which was displaced by crude oil again and aged in LKC crude oil at 90 °C for

one month. They were then flooded with Soltrol 130 and placed in imbibition cells in contact with brine for 10 days. No oil was produced from either of the cores, indicating an oil-wet state after the second time of aging in crude oil for these cores. The brine solutions were then replaced by 1.0 mmol/l anionic surfactants (STEOL CS-330 or surfactin). **Figure 4-44** shows the imbibition profiles for both cores. After reaching their production plateaux, both cores were flooded with brine and water wettability indices were obtained (Table 4.16). STEOL CS-300 resulted in a water wettability index of 0.12, similar to that obtained from B03 core exposed to the same solution. Surfactin resulted in a water wettability index of 0.33, showing the effectiveness of this surfactant in changing the wettability of oil-wet surface and hence enhancing the capillary driven imbibition process. The IFT values for these surfactants against Soltrol 130 were obtained using a ring tensiometer. STEOL CS-330 had an IFT of 7 mN/m and that of surfactin was 4 mN/m. It is generally believed that spontaneous imbibition rate decreases when capillary forces are reduced by lowering the IFT, due to increased influence of weaker gravity forces. Despite a lower IFT value, it can be seen that surfactin performed well compared with STEL CS-330, and the same discussion regarding the inverse Bond number as above holds. This is consistent with the hypothesis that the performance could be improved by increasing the charge density on the head group of the surfactant molecule. There also not seen to be documentation of this in the literature, however, these data support this hypothesis and we feel it is worthy of further study. These findings led to the suggestion that wettability alteration processes might be improved through the use of

dimeric surfactants, which have two charged head groups and two hydrophobic tails. Gemini surfactants where the molecules are joined at the head end are likely to be effective when ion-pair formation is the wettability alteration mechanism and Bolaform surfactants, in which molecules are joined by the hydrophobic tails, should be more effective in the case of surfactant monolayer adsorption. This class of surfactants has been studied recently for use in reservoirs with high salinity and temperature (Barnes, Smit et al. 2008).

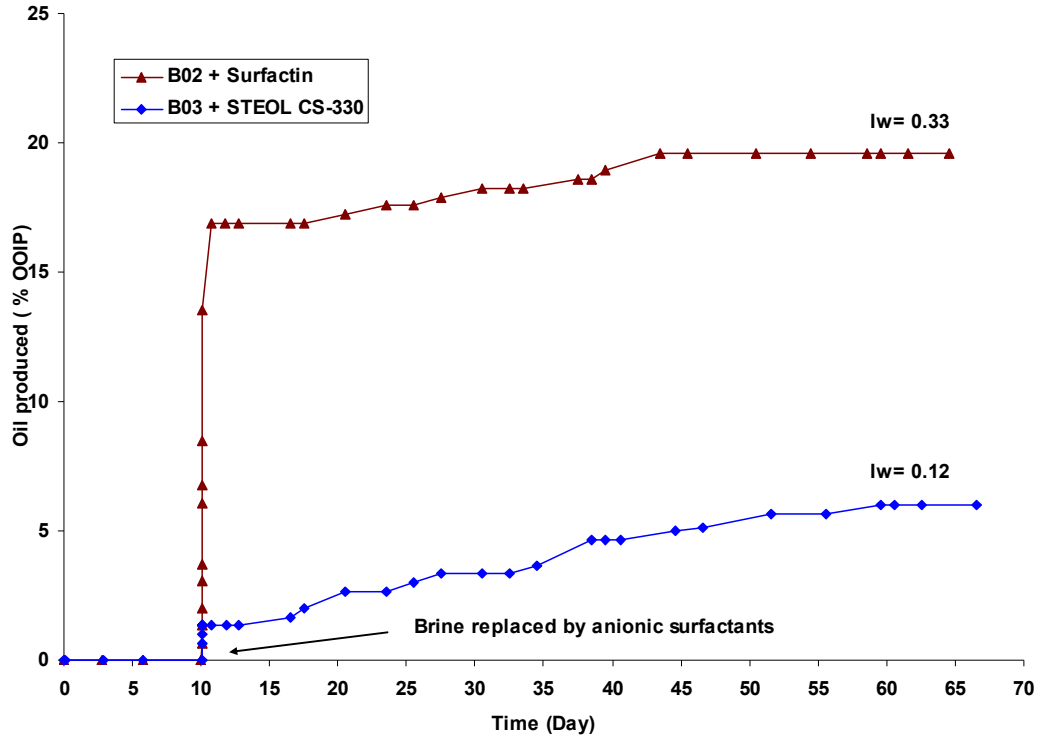

Figure 4-44 B02 and B03 sandstone cores imbibition profiles in 1% brine solution and in 1.0 mmol/l solutions of anionic surfactants

Table 4.16 Imbibition data for B02 and B03 in cationic surfactants at room temperature

Core	S_{iw}	S_{ws}	S_{wf}	I_w
B02	0.0	0.20	0.59	0.33
B03	0.0	0.06	0.51	0.12

To test this hypothesis, a sample of an anionic Gemini surfactant was obtained from Oil Chem Company to be tested against surfactin. This surfactant is a xylene di C14/C16 sulfonate Gemini with a molecular weight of 746. It was supplied in 100 % active acid form and had to be dissolved in water and neutralized with sodium hydroxide to form water soluble salt. The structure of the surfactant is shown in **Figure 4-45**.

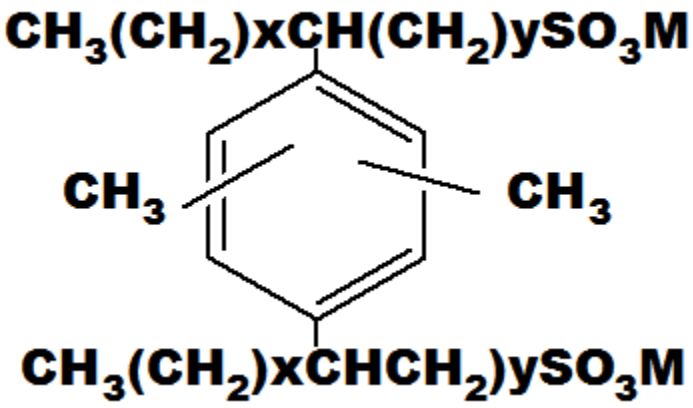

Figure 4-45 Chemical structure of sulfonate Gemini

After neutralization, a 1.0 mmol/l sample of anionic Gemini surfactant was prepared. Two sandstone cores B06 and B07 were chosen to compare the Gemini and surfactin in oil-wet cores. Core B06 was first saturated and characterized with Soltrol 130.

Soltrol 130 was then displaced by crude oil. Core B07 was saturated and characterized with 10 g/l NaCl and then the initial water saturation of S_{iw}= 0.36 was established by flooding the core with Soltrol 130. To prepare the cores for the aging process, Soltrol 130 was then displaced by crude oil. After that, both cores were aged in crude oil at a temperature of 90°C for one month. After aging, they were flooded with Soltrol 130 to displace the crude oil. The cores were then placed in imbibition cells in contact with 1% brine solution and oil production was monitored. Core B06 with no initial water saturation started oil production after 23 h in brine solution. Core B07, on the other hand, started oil production after 3 days of contact with brine. This observation was consistent with those seen for cores B02 and B03. The existence of initial water saturation delayed the imbibition process. After two weeks of brine imbibition, B06 and B07 cores were exposed to surfactin and Gemini surfactants and oil production was monitored versus time. The imbibition profiles for cores B06 and B07 in brine and anionic surfactants are shown in **Figure 4-46**. B06 started producing oil about 3 minutes after exposure to surfactin. It took almost 4 h for B07 to start producing oil. The imbibition profile for B06 core in surfactin was very similar to that of B02 core in surfactin and confirmed the reproducibility of the results obtained using this surfactant on oil-wet sandstone cores. Oil production rate for B07 was less than that for B06 core; however, the final oil recovery was almost double using the Gemini surfactant compared with surfactin after 150 days of imbibition. This higher performance could be due to combined effects of smaller head groups and the presence of two negative charge groups per surfactant molecule and hence higher

packing and interactions with the adsorbed materials on the rock surface. The test was repeated by cleaning and aging the previously used core B05 under LKC crude oil and displacing the crude with Soltrol 130. The test was repeated with no initial water saturation present in the core to investigate the water presence effect. The core was placed in brine and after 5 days, brine was replaced by Gemini surfactant. The initial oil production rate was a little higher for B05 core compared with that of B07 core (**Figure 4-47**); however the final oil recovery was less in the case of zero initial water saturation. **Figure 4-48** shows the imbibition profiles for B05 and B07 cores after the time they were exposed to Gemini surfactant. It can be seen that up to 25 days of imbibition, the imbibition profiles look the same, and after that period the oil production rate decreases for the core with no initial water saturation (B05). It seems that the presence of initial water saturation affects the final oil recovery but the initial phase of imbibition process in not affected by the initial water saturation. The reason could be that the initial water saturation present in the core is not connected to from a continuous phase, so it does not improve the process initially. However, after some time (25 days in this case) in imbibition process they can form a connected film with the imbibed aqueous phase and accelerate the process. The same results obtained for crude oil-aged core B03 in STEOL CS-330 with and without initial water saturation (**Figure 4-49**) confirming the results from B05 and B07 cores.

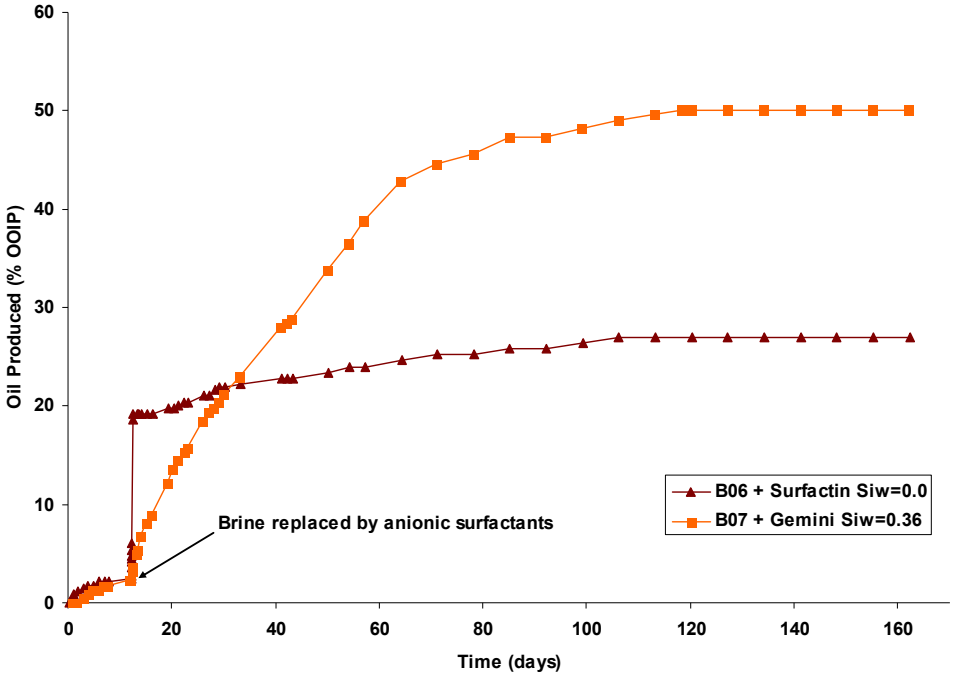

Figure 4-46 Imbibition profile for B06 and B07 core in brine and anionic surfactants at room temperature

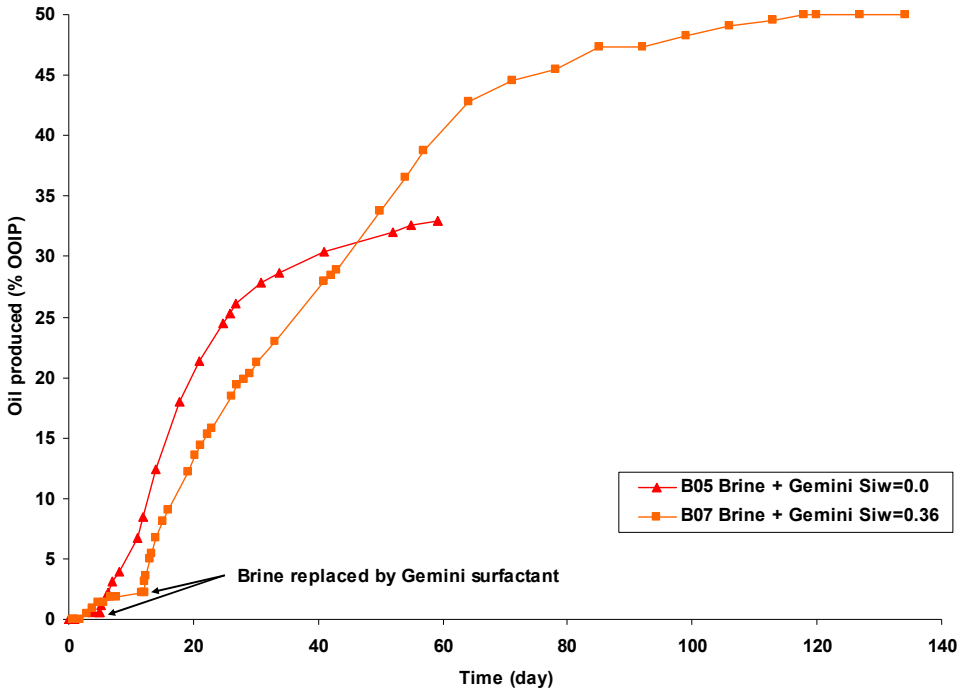

Figure 4-47 Imbibition profiles for oil-wet cores B05 and B07 in brine and Gemini surfactant

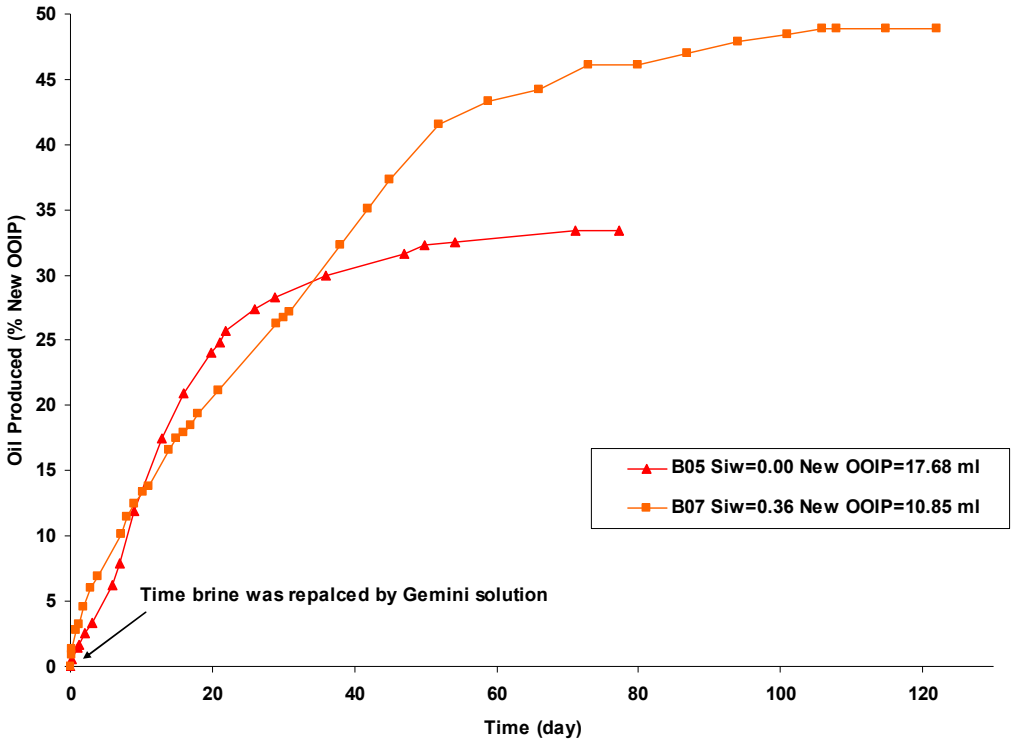

Figure 4-48 Imbibition profiles for oil-wet cores B05 and B07 from the time in Gemini surfactant

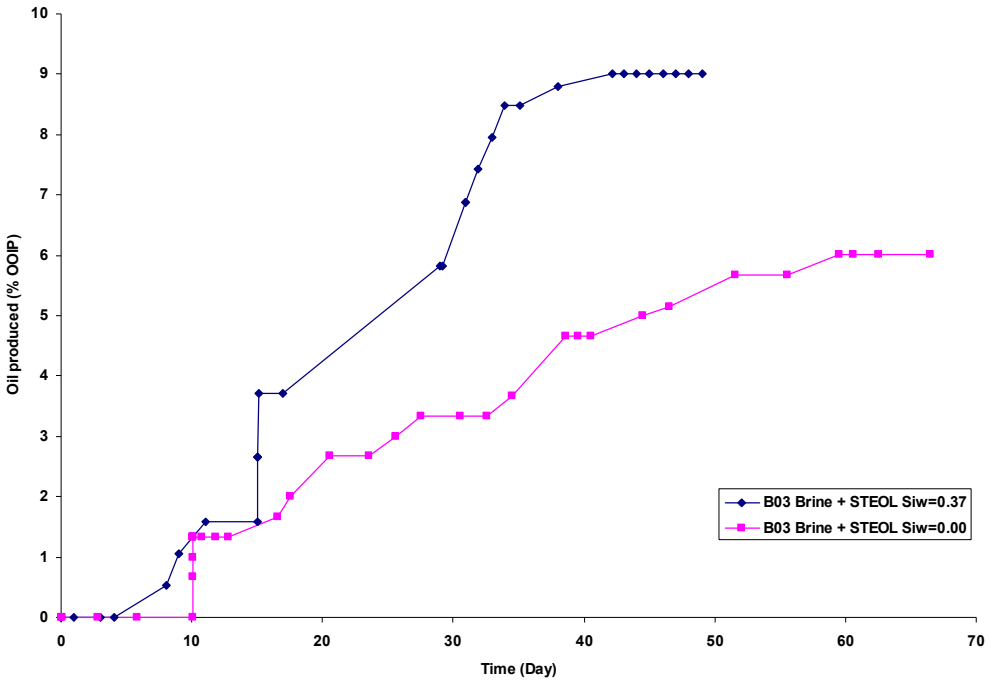

Figure 4-49 Imbibition profiles for B03 core with and without S_{iw} in STEOL CS-330 at room temperature

4.3.2 Wettability Alteration by Surfactant Adsorption

Standnes and Austad (2000) observed that anionic surfactants can also improve the spontaneous imbibition of water into oil-wet chalk cores, albeit not as effectively as cationic surfactants. For the anionic surfactant, the ion-pair formation could not be responsible for the wettability alteration due to the electrostatic repulsion between the anionic head groups and the negatively charged adsorbed crude oil components on the chalk surface. They hypothesized that anionic surfactants could alter the rock wettability by forming a surfactant monolayer on the oil-wet rock surface. They claimed that the surfactant adsorbs via a hydrophobic interaction with the hydrocarbon layer adsorbed on the surface of the chalk as shown in **Figure 4-50**,

leaving the water soluble head-group of the surfactant oriented toward the solution. This would result in the formation of a thin water zone and create weak capillary forces during the imbibition process. This process would occur sequentially at the surfactant/oil/rock interface. Due to the weak hydrophobic interactions, this process should be readily reversible. If this theory is correct, surfactants should be adsorbed only by their hydrophobic tail on a hydrophobic surface, changing the wettability of the surface to a less oil-wet state by having their hydrophilic head-group oriented toward the solution. The adsorption of the surfactant should also be in the form of a monolayer of surfactant molecules and there would be no possibility of forming a bi-layer since the remaining surfactant molecules in solution have the same charge as those adsorbed.

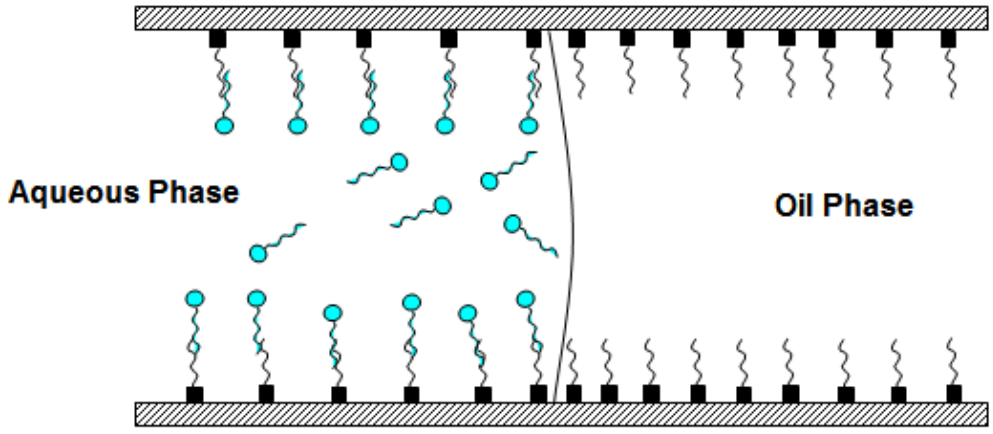

Figure 4-50 Schematic model of suggested wettability alteration mechanism by anionic surfactant and bi-layer formation. Circles are anionic surfactant molecules and squares are anionic organic materials from crude oil (After Standnes 2001)

To test this hypothesis, completely oil-wet synthetic polyethylene cores were selected to perform imbibition and dynamic adsorption tests. This ensures a complete oil-wet surface and eliminates the possibility of having a mixed-wet state as in the case of a real reservoir core. Also, the polyethylene surface is free of any adsorbed charged components and therefore, the only way for the surfactant molecules to adsorb on the polyethylene surface is through the interaction of their hydrophobic tails with the oil-wet surface. To test this hypothesis, the experimental scheme shown in **Figure 4-51** was proposed. The intention was to expose the polyethylene cores to both anionic and cationic surfactants and measure induced wettability alteration through imbibition tests. To distinguish between mono and bi-layer adsorption, the adsorption isotherms for both surfactant needed to be obtained. The shape of the adsorption isotherm would determine the type of the adsorption mechanism (**Figure 4-52**). The properties of the synthetic cores used in this study can also be found in Table 4-17. Results from imbibition tests revealed that, as expected, the polyethylene cores were completely oil-wet with an oil wettability index close to 1 (**Figure 4-53**).

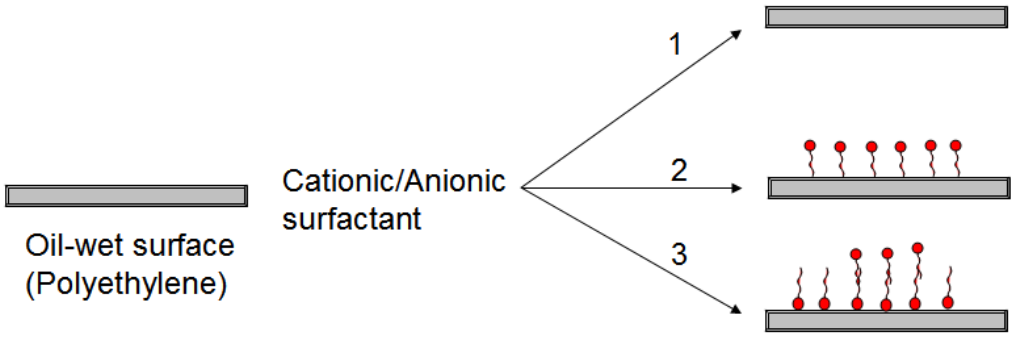

Figure 4-51 Proposed experiments for studying wettability alteration by surfactant adsorption

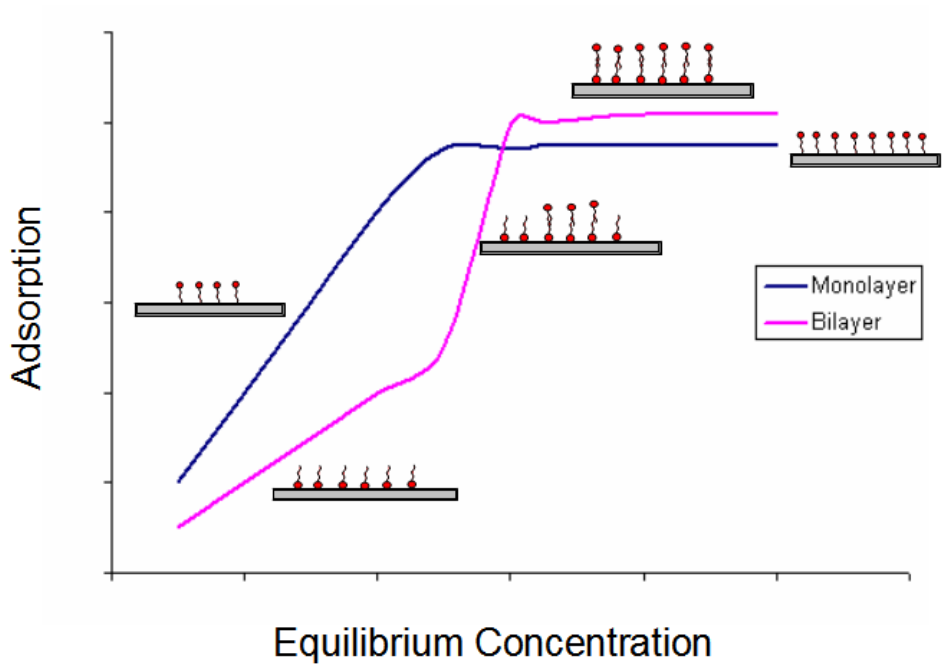

Figure 4-52 Adsorption isotherms showing the difference between mono- and bi-layer adsorption

Table 4.17 Properties of synthetic polyethylene cores

Core	Length (cm)	Diameter (cm)	Area (cm^2)	PV (ml)	ϕ (%)	k (md)
S02	6.62	3.73	11.0	22.4	33	560
S03	6.69	3.74	11.0	21.7	31	550
S04	6.75	3.74	11.0	24.1	32	580

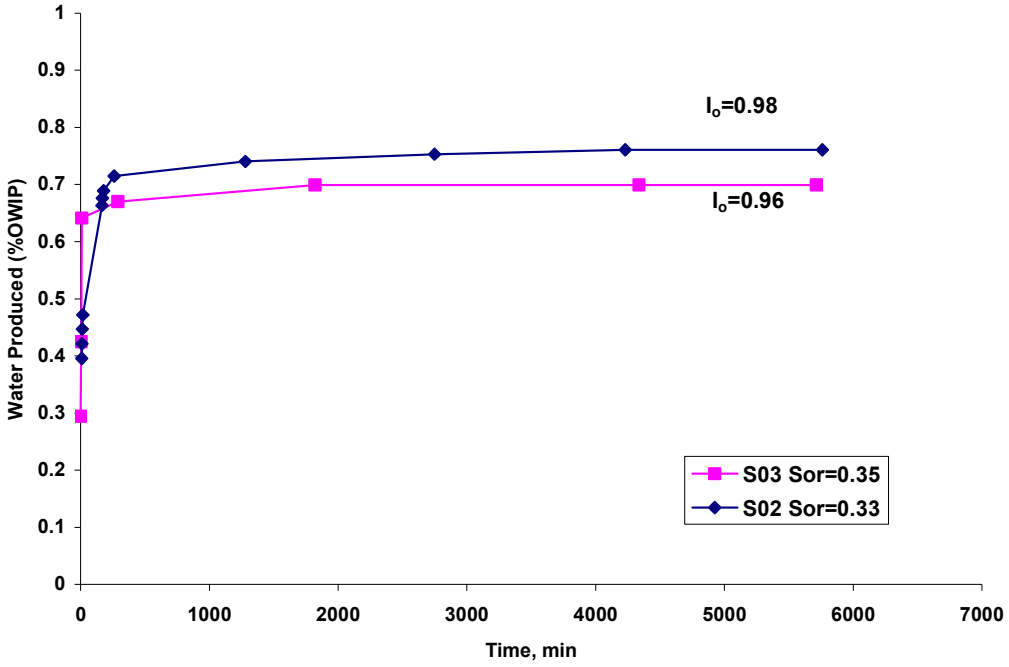

Figure 4-53 Imbibition profiles of synthetic cores in Soltrol 130

To measure the ability of the surfactants to change the wettability of these cores, they were flooded and aged with anionic (STEOL CS-330) and cationic (C12TAB) surfactants at ambient conditions. The procedure was to flood (circulation method)

these cores with a known mass and initial concentration of surfactant solution for 24 h and then age the system for another 24 h. The surfactant solution was then displaced with Soltrol 130 to establish the initial water saturation and then two imbibition cycles were performed on each core. These tests were repeated to confirm reproducibility of the results. For all cores used and both surfactants, the wettability of the cores changed dramatically. The oil index changed from a value of one to zero in the case of STEOL CS-330 and to a value of 0.3 in the case of C12TAB. The wettability of these cores was changed from a strong oil-wet condition to an intermediate wetting state. Going through the second imbibition cycle, the wettability changed to a more oil-wet state (I_o value close to 1). This suggests that the interactions between the surfactant molecules and the oil-wet surface are weak, which is consistent with the surfactant molecules being attached by their hydrophobic tail to the oil-wet surface of the core and forming a monolayer on the surface.

Adsorption isotherms obtained for both surfactants on synthetic cores shown in **Figure 4-54** indicated a Langmuir type adsorption for both surfactants which confirms that surfactant molecules formed a monolayer on the oil-wet surface. It can also be seen from this figure that STEOL CS-330 adsorbed more compared with the C12TAB. This may be due to presence of ethoxyl groups in the molecular structure of STEOL CS-330, which may reduce the charge density of the head group, resulting in a better packing and hence a more compact monolayer.

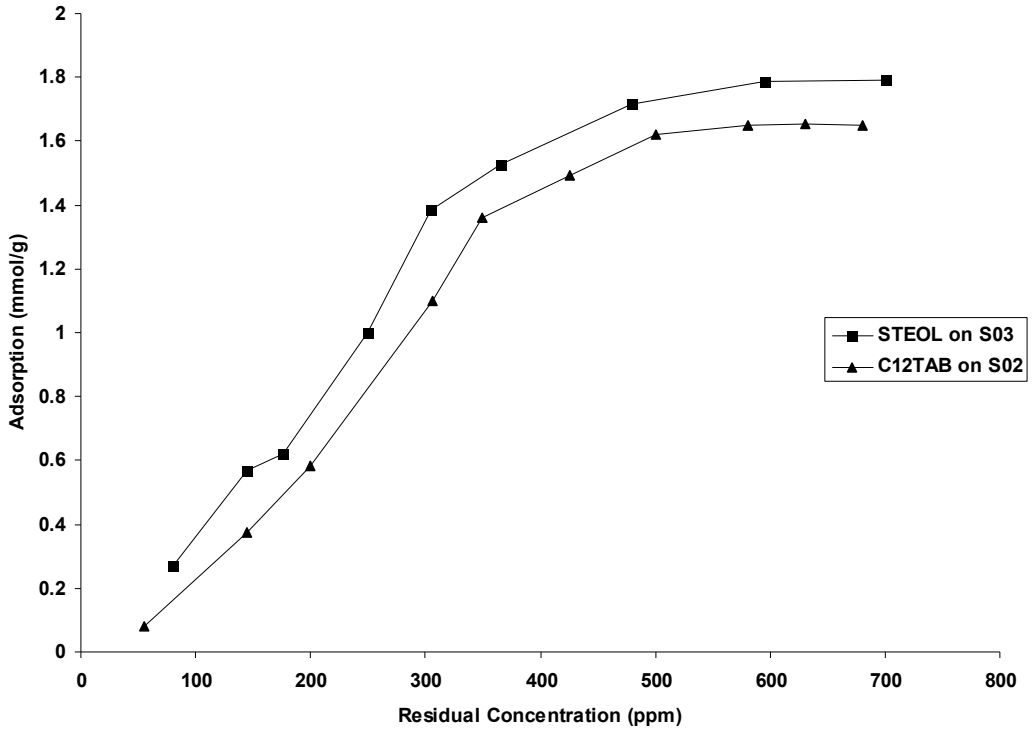

Figure 4-54 STEOL C-330 and C12TAB adsorption isotherms on synthetic cores at room temperature

The change of wettability back toward the more oil-wet state when going through the second imbibition cycle can be explained by the removal of the adsorbed surfactant layer during the water injection displacing the oil. The hydrophilic head group is oriented toward the solution and increases the chance of removal of surfactant molecules adsorbed on the surface during forced imbibition. In one case (Core S04), two aqueous effluent samples from the first and second imbibition cycles were collected and tested for surface tension values. The water has a surface tension of 72.78 mN/m at room temperature. The effluents 1 and 2 showed surface tension values of 34.5 and 46 mN/m, respectively, indicating the presence of surfactants in

effluents with a decreasing trend. These findings confirm that an adsorbed monolayer of surfactant molecules can indeed alter the wettability of an oil-wet surface toward a more water-wet state through hydrophobic interaction of the tail sections of the surfactant molecules with an oil-wet surface. Our findings also show that the hydrophobic interactions are weak and so this process is reversible. Tables 4.18 through 4.21 summarize the imbibition data for all tests performed. Standnes et al. (2002) reported the same observation for a nonionic surfactant in oil-wet carbonate cores. Since there is no electrostatic interaction between the nonionic surfactant molecules and the adsorbed crude oil components, their observation also supports the hypothesis of wettability alteration by surfactant adsorption on rock surface via hydrophobic interactions with adsorbed crude oil components on rock surface.

Table 4.18 Imbibition data for S03 core flooded and aged with STEOL CS-330 at room temperature

Imbibition Cycle	First	Second
S_{iw}	0.17	0.18
Oil produced by SI of water (ml)	0.0	0.0
S_{ws}	0.17	0.18
Oil produced by FI of water (ml)	12	10.7
S_{or}	0.24	0.29
I_w	0.0	0.0
Water produced by SI of oil (ml)	< 0.1	6.7
S_{os}	0.24	0.62
Water produced by FI of oil (ml)	11.8	3.9
S_{of}	0.82	0.81
I_o	0.0	0.63

Table 4.19 Imbibition data for S02 core flooded and aged with C12TAB at room temperature

Imbibition Cycle	First	Second
S_{iw}	0.18	0.20
Oil produced by SI of water (ml)	0.0	0.0
S_{ws}	0.18	0.20
Oil produced by FI of water (ml)	11	11.2
S_{or}	0.34	0.32
I_w	0.0	0.0
Water produced by SI of oil (ml)	3.2	8.2
S_{os}	0.49	0.65
Water produced by FI of oil (ml)	7.1	3.1
S_{of}	0.8	0.79
I_o	0.33	0.73

Table 4.20 Imbibition data for S04 core flooded and aged with STEOL CS-330 at room temperature

Imbibition Cycle	First	Second
S_{iw}	0.12	0.13
Oil produced by SI of water (ml)	0.0	0.0
S_{ws}	0.12	0.13
Oil produced by FI of water (ml)	12.8	13.0
S_{or}	0.38	0.36
I_w	0.0	0.0
Water produced by SI of oil (ml)	0.0	12.4
S_{os}	0.38	0.85
Water produced by FI of oil (ml)	11.8	0.4
S_{of}	0.87	0.87
I_o	0.0	0.96

Table 4.21 Imbibition data for S02 core flooded and aged with C12TAB at room temperature

Imbibition Cycle	First	Second
S_{iw}	0.19	0.20
Oil produced by SI of water (ml)	0.0	0.0
S_{ws}	0.19	0.20
Oil produced by FI of water (ml)	11	11.2
S_{or}	0.33	0.32
I_w	0.0	0.0
Water produced by SI of oil (ml)	3.4	8.2
S_{os}	0.51	0.65
Water produced by FI of oil (ml)	7.3	3.1
S_{of}	0.80	0.79
I_o	0.31	0.76

5 Conclusions and Recommendations

5.1 Core cleaning and characterization of core materials

During the core cleaning process it was observed that reservoir and outcrop core materials contained organic compounds that where dissolved in the injected oil (dodecane or Soltrol 130) and gave a yellowish color to the effluents. The effluent oil also adsorbed strongly in the ultraviolet region. The presence of these UV-absorbing, oil-soluble material was problematic and they were likely to be active in determining the wettability of the materials. They also interfered with the detection of stilbene tracer. These cores were previously cleaned by Dean-Stark extraction method using toluene/methanol azeotrope and these observations shows that this method is not an effective method for core restoration process. So, an aggressive cleaning procedure was adapted where core materials were flooded with a series of solvents (tetrahydrofuran (THF), chloroform, and methanol) until the effluents were colorless. Even after this aggressive cleaning procedure, reservoir core materials exhibited a mixed-wet state. However, crushed core materials became strongly water-wet after being cleaned by the above solvent series.

5.2 Surfactin performance versus benchmark chemical surfactant

5.2.1 Static and Dynamic Adsorption Tests

Based on the results of the static adsorption tests, it is important to standardize and report the mass of rock, and concentration and volume of surfactant solution used to develop adsorption isotherms. It was observed that specific adsorption decreases with the mass of adsorbent.

Both STEOL CS-330 and surfactin exhibit typical adsorption isotherms with four distinct regions. Adsorption isotherms of STEOL CS-330 and surfactin on crushed Lansing-Kansas City outcrop and reservoir material showed that surfactin has higher specific adsorption on these oomoldic carbonates. Dynamic adsorption tests on LKC core plug showed than on a molar basis, surfactin adsorbed less than STEOL CS-300.

5.2.2 Qualitative wettability Tests

Qualitative wettability tests (two-phase separation and flotation tests) showed that surfactin is more effective than STEOL CS-330 at changing wettability of oil-wet crushed LKC material to a more water-wet state on both molar and weight bases.

5.2.3 Enhancing the Spontaneous Imbibition Process

It can be concluded from the static spontaneous imbibition tests that STEOL CS-330 is more effective than surfactin in enhancing the spontaneous imbibition process in cleaned mixed-wet LKC core plugs. This may be due to the larger IFT value for this surfactant against Soltrol 130. However, surfactin performs much better than STEOL

CS-330 in interacting with crude oil-aged LKC core material and results in higher oil recovery from oil-wet reservoir cores.

5.3 Mechanistic study

Results from this study are consistent with the hypotheses that ion-pair formation and adsorption of surfactant molecules through interactions with the adsorbed crude oil components on the rock surface are the two main mechanisms responsible for changing the rock wettability toward a more water-wet state. There were some problem in reproducing the experimental data, but the trends are consistent and support the hypotheses.

When electrostatic interactions exist between the charged head groups of the surfactant molecules and the adsorbed crude oil components on the rock surface, ion-pair formation is the mechanism responsible for the wettability alteration. However, in the absence of electrostatic interactions, surfactant adsorption driven by hydrophobic interactions between the tail sections of the surfactant molecules and the adsorbed crude oil components on the rock surface is the main mechanism responsible for the wettability alteration.

Ion-pair formation between the charged head groups of surfactant molecules and the adsorbed crude oil components on rock surface is more effective in changing the rock wettability toward a more water-wet state than the adsorption of surfactant molecules as a monolayer on the rock surface through hydrophobic interaction with the adsorbed crude oil components. It is shown further that surfactants with higher charge density

on the head groups are more effective in changing the rock wettability toward a more water-wet state if ion-pair formation is the mechanism responsible for the wettability alteration.

The presence of initial water saturation does not affect the initial imbibition rate, but as process continues, the disconnected water can form a continuous phase and affect the total recovery from the core.

5.4 Recommendations

These are still lots of research work than can be done related to the study of wettability alteration using surfactants. Further work on the subject could include more fundamental studies such as characterization of the organic components in the crude oil which adsorb on the rock surface and are responsible for changing the wettability of rock surface to an oil-wet state. In addition, performing imbibition tests using the specific reservoir crude oil sample is very important to see the real interaction of the surfactant with rock surface in presence of crude oil sample. Also, one can investigate the effectiveness of Bolafrom surfactants in the case that wettability alteration is through the surfactant adsorption. Finding the optimum surfactant concentration for specific field conditions (reservoir type) can be done by performing imbibition tests at surfactant concentrations below and above CMC of the specific surfactant.

6 References

(2007). Standard Test Method for Acid Number of Petroleum Products by Potentiometric Titration. West Conshohocken, PA.

(2007). Standard Test Method for Base Number of Petroleum Products by Potentiometric Perchloric Acid Titration West Conshohocken, PA.

Amott, E. (1959). "Observations relating to the wettability of porous rock." Petroleum Transactions, AIME: 156-162.

Anderson, W. G. (1986a). "Wettability Literature Survey- Part 1: Rock/Oil/Brine Interactions and the Effects of Core Handling on Wettability " Journal of Petroleum Technology **281**: 1125-1144.

Anderson, W. G. (1986b). "Wettability Literature Survey- Part 2: Wettability Measurements." Journal of Petroleum Technology **281**: 1246-1262.

Anderson, W. G. (1987a). "Wettability Literature Survey- Part 4: Effects of Wettability on Capillary Pressure." Journal of Petroleum Technology (October): 1283-1300.

Anderson, W. G. (1987b). "Wettability Literature Survey- Part 5: The Effect of Wettability on Relative Permeability." Journal of Petroleum Technology (November): 1453-1468.

Anderson, W. G. (1987c). "Wettability Literature Survey- Part 6: The Effects of Wettability on Waterflooding." Journal of Petroleum Technology (December): 1605-1622.

Austad, T., B. Matre, et al. (1998). "Chemical Flooding of Oil Reservoirs 8. Spontaneous Oil Expulsion from Oil-and Water-wet Low Permeable Chalk Material by Imbibition of Aqueous Surfactant Solutions." Colloids and Surfaces A: Physicochemical and Engineering Aspects **137**: 117-129.

Austad, T. and J. Milter (1997). Spontaneous Imbibition of Water into Low Permeable Chalk at Different Wettabilities Using Surfactants. Paper SPE 37236 presented at the International Symposium on Oilfield Chemistry held in. Houston, TX, USA.

Babadagli, T. (2000). Scaling of Co-current and Counter-current Capillary Imbibition for Surfactant and Polymer Injection in Naturally Fractures Reservoirs. Paper SPE 62848 presented at the SPE/AAPG Western Meeting held in Long Beach, CA, USA.

Barnes, J. R., J. P. Smit, et al. (2008). Development of Surfactants for Chemical Flooding at Difficult Reservoir Conditions. Paper SPE 113313 presented at the 16th Symposium on Improved Oil Recovery, Tulsa, Oklahoma.

Benner, F. C. and F. E. Bartell (1942). The Effect of Polar Impurities Upon Capillary and Surface Phenomena in Petroleum Production. Drilling and Production Practices. New York, API**:** 341-348.

Bobek, J. E., C. C. Mattax, et al. (1958). "Reservoir Rock Wettability: Its Significance and Evaluation." Petroleum Transactions AIME **213**: 155-160.

Bourbiaux, B. J. and F. J. Kalaydjian (1990). "Experimental Study of Co-current and Counter-current flows in natural porous media." SPE Reservoir Engineering: 361-368.

Buckley, J. S., C. Bousseau, et al. (1995). Wettability Alteration by Brine and Crude Oil: From Contact Angles to Cores. Paper SPE 30765 presented at the SPE Annual Technical Conference and Exhibition held in Dallas, TS, USA.

Buckley, J. S., G. J. Hirasaki, et al. (1998). "Asphaltene Precipitation and Solvent Properties of Crude Oils " Journal of Petroleum Science and Engineering **16**(3 & 4): 251-285.

Buckley, J. S. and Y. Liu (1998). "Some Mechanisms of Crude Oil/Brine/Solid Interactions." Journal of Petroleum Science and Engineering **20**: 155-160.

Buckley, J. S., Y. Liu, et al. (1998). "Mechanisms of Wetting Alteration by Crude Oils." SPE Journal: 54-61.

Buckley, J. S. and N. R. Morrow (1990). Characterization of Crude Oil Wetting Behavior by Adhesion Tests. Paper SPE 20263 presented at the SPE/DOE Improved Oil Recovery Symposium held in. Tulsa, OK, USA.

Buckley, J. S., K. Takamura, et al. (1989). "Influence of Electrical Surface Charges on the Wetting Properties of Crude oils." SPE Reservoir Engineering: 332-340.

Butt, H. J., M. Graf, et al. (2006). Physics and Chemistry of Interfaces. Weinheim, Germany, Wiley-VCH.

Chauveteau, G. and K. S. Sorbie (1991). Mobility Control by Polymers Critical Reports on Applied Chemistry. Basic Concepts in Enhanced Oil Recovery Processes. M. Baviere. New York, Elsevier Applied Science. **33:** 43-87.

Chen, H. L., L. R. Lucas, et al. (2000). Laboratory Monitoring of Surfactant Imbibition Using Computerized Tomography. Paper SPE 59006 presented at the SPE International Petroleum Conference held in. Villahermosa, Mexico.

Chernicoff, S. (1999). Geology. Boston, Houghton Mifflin Company.

Chilingar, G. V. and T. F. Yen (1983). "Some Notes on Wettability and Relative Permeabilities of Carbonate Reservoir Rock, II." Energy Sources **7**(1): 67-75.

Clementz, D. M. (1982). Alteration of Rock Properties by Adsorption of Petroleum Heavy Ends: Implications for Enhanced Oil Recovery. Paper SPE/DOE 10683 presented at the SPE/DOE third joint Symposium on EOR Tulsa, OK, USA.

Collins, S. H. and J. C. Melrose (1983). Adsorption of Asphaltenes and Water on Reservoir Rock Minerals. Paper SPE 11800 presented at the International Symposium on Oilfield and Geothermal Chemistry held in Denver, CO, USA.

Collins, S. H. and J. C. Melrose (1983). Adsorption of Asphaltene and Water on Reservoir Rock Minerals. Paper SPE 11800 presented at the International Symposium on Oilfield and Geothermal Chemistry Denver, CO, USA.

Cooper, D. G., C. R. MacDonald, et al. (1981). "Enhanced Production of Surfactin from Bacillus subtilis by Continuous Product Removal and Metal Cation Additions." Applied and Environmental Microbiology **42**: 408-412.

Crocker, M. E. and L. M. Marchin (1988). "Wettability and Adsorption Characteristics of Crude-Oil Asphaltene and Polar Fractions." Journal of Petroleum Technology (April): 470-474.

Cuiec, L. (1977). "Study of Problems Related to the Restoration of the Natural State of Core Samples" The Journal of Canadian Petroleum Technology: 68-80.

Cuiec, L. (1984). Rock/Crude-Oil Interactions and Wettability: An Attempt to Understand Their Interaction Paper SPE 13211 presented at the SPE 59th Annual Technical Conference and Exhibition Houston, TX, USA.

Cuiec, L., B. J. Bourbiaux, et al. (1994). "Oil Recovery by Imbibition in Lowe Permeability Chalk." SPE Formation Evaluation **9**: 200-208.

Cuiec, L. E. (1991). "Evaluation of Reservoir Wettability and Its Effect on Oil Recovery." Surfactant Science series. Interfacial Phenomena in Petroleum Recovery **36** (New York and Basel).

Denekas, M. O., C. C. Mattax, et al. (1959). "Effects of Crude Oil Components on Rock Wettability." Petroleum Transactions AIME **216**: 330-333.

Denekas, M. O., C. C. Mattax, et al. (1959). "Effects of Crude Oil Components on Rock Wettability." Trans. AIME **216**: 330-333.

Donaldson, E. C., R. D. Thomas, et al. (1969). "Wettability Determination and Its Effect on Recovery Efficiency." SPE Journal: 13-20.

Dubey, S. T. and M. H. Waxman (1989). Asphaltene Adsorption and Desorption from Mineral Surfaces. Paper SPE 18462 presented at the SPE International Symposium on Oilfield Chemistry Houston, TX, USA.

Dubey, S. T. and M. H. Waxman (1989). "Base Number and Wetting Properties of Crude Oils." SPE Reservoir Engineering: 195-200.

Dukhin, S. S., G. Kretzschmar, et al. (1995). Dynamics of Adsorption at Liquid Interfaces. Theory, Experiment and Application Studies in Interface Science D. Mobius and R. Miller, Elsevier Science **1**.

Dworkin, M. (1991). The Prokaryotes: An Evolving Electronic Resource for the Microbiological Community, http://141.150.157.117:8080/prokPUB/index.htm.

Eisert, K. (2006). Using Biosurfactants Produced from Agriculture Process Waste Streams to Improve Oil Recovery in Fractured Carbonate Reservoirs. Department of Chemical and Petroleum Engineering. Lawrence, KS, The University of Kansas. **M.S. Thesis**.

Erbil, H. Y. (2006). Surface Chemistry of Solid and Liquid Interfaces, Blackwell Publishing.

Farouq-Ali, S. M. and C. D. Stahl (1970). "Increased Oil Recovery by Improved Waterflooding." Earth and Mineral Sciences **39**(4): 25-28.

Fisher Scientific, C. (Undated). Instruction Manual: Fisher Tensiometer Model 20. Pittsburgh, PA, Fisher Scientific Company.

Gallet, X., M. Deleu, et al. (1999). "Computer Simulation of Surfactin Conformation at a Hydrophobic/Hydrophilic Interface " Langmuir **15**: 2409-2413.

Grangemard, I., J. Wallach, et al. (2001). "Lichenysin: A More Efficient Cation Chelator than Surfactin " Applied Biochemistry and Biotechnology **90**: 199-210.

Green, D. and P. Willhite (1998). Enhanced Oil Recovery.

Grigg, R. B. (2003). Improving CO_2 Efficiency for Recovering Oil in Heterogeneous Reservoirs. Socorro, New Mexico Petroleum Recovery Research Center**:** Chapter 2 (4-22).

Heerklotz, H. and J. Seelig (2001). "Detergent-like action of the antibiotic peptide surfactin on lipid membranes." Biophysical Journal **81**: 1547-1554.

Hirasaki, G. J. (1991). "Wettability: Fundamentals and Surface Forces." SPE Formation Evaluation: 217-226.

Hirasaki, G. J., J. A. Rohan, et al. (1990). Wettability evaluation during restored state core analysis. Paper Presented at 65th Annual Technical Conference and Exhibition of the Society of Petroleum Engineers. New Orleans, LA, Society of Petroleum Engineers.

Hirasaki, G. J., Rohan, J. A.; Dubey, S.T.; Niko, H. (1990). SPE paper 20506 Wettability Evaluation During Restored State Core Analysis. 65th ATCE of Society of Petroleum Engineers, New Orleans, LA.

Hirasaki, G. J. and D. L. Zhang (2004). "Surface Chemistry of Oil Recovery from Fractured, Oil-wet carbonate formations." SPE Journal: 151-162.

Hirasaki, G. J. and D. L. Zhang (2004). "Surface Chemistry of Oil Recovery From Fractured, Oil-wet Carbonate Formations." SPE Journal.

Hognesen, E. J., M. Oslen, et al. (2006). "Capillary and Gravity Dominated Flow Regimes in Displacement of Oil from an Oil-Wet Chalk Using Cationic Surfactants " Energy & Fuels **20**(3): 1118-1122.

Huang, A. Y. (1985). The Surface Excess Concept in Modeling Adsorption in Porous Media, University of Calgary. **Master Thesis**.

Huang, A. Y. and J. J. Novosad (1986). "Modeling of Adsorption of Foam-Forming Surfactants in Porous Media." Fundamentals of Adsorption.

Hunag, Y. H. (1985). The Surface Excess Concept in Modeling Adsorption in Porous Media, University of Calgary. **Master Thesis**.

Instrument Division Fisher Surface Tensiometer Model 20 Instruction Manual.

Ishigami, Y., M. Osman, et al. (1995). "Significance of Beta-Sheet Formation for Micellization and Surface Adsorption of Surfactin." Colloids and Surfactants B **4**: 341-348.

Kaminsky, R. and C. J. Radke (1998). Water Films, Asphaltenes, and Wettability Alteration. Paper SPE 39087 presented at the SPE Improved Oil Recovery Symposium held in. Tulsa, OK, USA.

Carlson, S., S. Backlund, et al. (2000). "Complexation in the heptanoic acid–heptylamine system." Colloid & Polymer Science **278**(1): 8-14.

Legens, C., T. Palermo, et al. (1998a). "Carbonate Rock Wettability Changes Induced by Organic Compound Adsorption." Journal of Petroleum Science and Engineering **20**: 277-282.

Madsen, L., C. Gron, et al. (1996). "Adsorption of Polar Aromatic Hydrocarbons on Synthetic Calcite." Organic Geochemistry **24**(12): 1151-1155.

Mannhardt, K. and J. J. Novodas (1988). "Modeling Adsorption of Foam-Forming Surfactants." Revue de l'Institut Francais de Petrole **45**(5).

Mannhardt, K., L. L. Schramm, et al. (1990). "Effect of Rock Type and Brine Composition on Adsorption of two Foam-Forming Surfactants." SPE ATSM **1**(1).

Marle, C. M. (1991). Oil Entrapment and Mobilization. Critical Reports on Applied Chemistry. Basic Concepts in Enhanced Oil Recovery Processes. M. Baviere. New York, Elsevier Applied Science. **33:** 3-39.

Marsden, S. S. and P. A. Nikias (1962). "The Wettability of the Bradford Sand " Producers Monthly **26**(5): 2-5.

Mattax, C. C. and J. R. Kyte (1962). "Imbibition Oil Recovery From Fractured, water-drive Reservoir." SPE Journal(177-184).

Melrose, J. C. (1982). Interpretation of Mixed Wettability States in Reservoir Rocks. Paper SPE 10971 presented at the SPE Annual Technical Conference and Exhibition held in. New Orleans, LA,USA.

Milter, J. (1996). Improved Oil Recovery in Chalk: Spontaneous Imbibition Affected by Wettability, Rock Framework and Interfacial Tension. Department of Chemistry. Bergen, Norway, University of Bergen. **Dr. Sc.** .

Morikawa, M., Y. Hirata, et al. (2000). "A Study on the Structure-function Relationship of Lipopeptide Biosurfactants." Biochimica et Biophysica Acta **1488**: 211-218.

Morrow, N. R. (1970). "Physics and Thermodynamics of Capillary." Industrial and Engineering Chemistry **62**(6): 32-56.

Morrow, N. R. (1976). "Capillary Pressure Correlations For Uniformly Wetted Porous Media " Journal of Canadian Petroleum Technology **15**(4): 49-69.

Morrow, N. R. (1990). "Wettability and Its Effect on Oil Recovery." Journal of Petroleum Technology: 1476-1484.

Morrow, N. R. (1990). "Wettability and its Effects on Oil Recovery." Journal of Petroleum Technology(December): 1476-1484.

Morrow, N. R. (1991). Introduction to Interfacial Phenomena in Oil Recovery. In: Surfactants Science Series . Interfacial Phenomena in Petroleum Recovery. N. R. Morrow. New York, Marcel Dekker Inc. . **36:** 1-22.

Morrow, N. R. (1991). "Introduction to Surface Phenomena in Oil Recovery " Surfactant Science series. Interfacial Phenomena in Petroleum Recovery **36**(New York): 1-21.

Mukerjee, P. and K. J. Mysels (1971). Critical Micelle Concentrations of Aqueous Surfactant Systems. Washington DC, US Department of Commerce.

Myers, D. (1999). Surfaces, Interfaces, and Colloids: Principle and Applications. New York, Wiley-Vch.

Novosad, J. (1981). Adsorption of Pure Surfactant and Petroleum Sulfonate at the Solid-Liquid Interface. in Surface Phenomena in Enhanced Oil Recovery. D. O. Shah. New York, Plenum Publishing**:** 675-694.

Parsons, R. W. and P. R. Chaney (1966). "Imbibition Model Studies on Water-wet Carbonate Rocks." SPE Journal: 26-34.

pHOENIX ELECTRODE COMPANY (April 17, 2006). Surfactant Electrode Instruction Manual.

Ramirez, W. F., P. J. Shuler, et al. (1980). "Convection, Dispersion, and Adsorption of Surfactants in Porous Media." SPE Journal.

Reisberg, J. and T. M. Doscher (1956). "Interfacial Phenomena in Crude Oil-Water Systems." Producers Monthly(November): 43-50.

Rosen, M. J. (1986). Surfactants and Interfacial Phenomena, John Wiley & Sons, Inc.

Salathiel, R. A. (1973). "Oil Recovery by Surface Film Drainage in Mixed-Wettability Rocks." Journal of Petroleum Technology(October): 1216-1224.

Salehi, M., S. J. Johnson, et al. (2006). Wettability alteration of carbonate rock mediated by biosurfactant produced from high-starch agricultural effluents. 9th International Wettability Symposium. Bergen, Norway.

Salehi, M., Johnson, S.; Liang, J.; Bala, G.; Fox, S. (2006). Wettability Alteration of Carbonate Rock Mediated by Biosurfactant Produced from High-Starch Agricultural Effluents. 9th International Wettability Symposium, Bergen, Norway.

Schechter, D. S., D. Zhou, et al. (1991). Capillary Imbibition and Gravity Segregation in Low IFT Systems. Paper SPE 22594 presented at the SPE Annual Technical Conference and Exhibition held in. Dallas, TX, UAS.

Schechter, D. S., D. Zhou, et al. (1994). "Low IFT Drainage and Imbibition." Journal of Petroleum Science and Engineering **11**: 283-300.

Seright, R. S. and J. T. Liang (1994). A Survey of Field Application of Gel Treatments for Water Shut-off. Paper SPE 26991 presented at the III Latin American/Caribbean Petroleum Engineering Conference Buenos Aires, Argentina.

Sharma, R. (1995). Surfactants Adsorption and Surface Solubilization. Washington DC, American Chemical Society.

Skauge, A., S. Standal, et al. (1999). Effects of Organic Acids and Bases, and Oil Composition on Wettability. Paper SPE 56673 presented at the SPE Annual Technical Conference and Exhibition held in. Houston, TX, USA.

Somasundaran, P. and L. Zhang (1997). "Adsorption of Surfactants on Minerals for Wettability Control in Improved Oil Recovery Processes." Journal of Colloid and Interface Science **191**: 202-208.

Song, F. Y. and M. R. Islam (1994). A New Mathematical Model and Experimental Validation of Multicomponent Adsorption. Paper SPE 27838 presented at the SPE Annual Technical Conference and Exhibition

Spinler, E. A., D. R. Zornes, et al. (2000B). Enhancement of Oil Recovery Using a Low Concentration of Surfactant to Improve Spontaneous and Forced

Imbibition in Chalk. Paper SPE 59290 presented at the SPE Improved Oil Recovery Symposium held in Tulsa, OK, USA.

Standal, S. (1999). Wettability of Solid Surfaces Induced by Adsorption of Polar Organic Components in Crude Oil. Department of Chemistry. Bergen, Norway, University of Bergen. **Dr. Sc.** .

Standnes, D. C. (2000). Enhanced Oil Recovery from Oil-wet Carbonate Rocks by Spontaneous Imbibition of Aqueous Surfactant Solutions. Department of Petroleum Technology. Stavanger, Norway, Stavanger University. **Ph.D. Thesis**.

Standnes, D. C. (2001). Enhanced Oil Recovery from Oil-Wet Carbonate Rock by Spontaneous Imbibition of Aqueous Surfactant Solutions. Department for Petroleum Technology. Stavanger, Stavanger College. **PhD:** 115.

Standnes, D. C. and T. Austad (2000). "Wettability Alteration in Chalk 2. Mechanism for Wettability Alteration from Oil-wet to Water-wet using Surfactants." Journal of Petroleum Science and Engineering **28**: 123-143.

Standnes, D. C., L. A. D. Nogaret, et al. (2002). "An Evaluation of Spontaneous Imbibition of Water into Oil-wet Carbonate Reservoir Cores Using a Nonionic and Cationic Surfactant." Energy & Fuels **16**(6): 1557-1564.

Sydansk, R. D. and G. P. Southwell (1998). More than 12 Years of Experience with a Successful conformance-control Polymer-gel Technology. Paper SPE 49315 presented at the SPE Annual Technical Conference and Exhibition New Orleans, LA.

Tabatabai, A., M. V. Gonzalez, et al. (1993). "Reducing Surfactant Adsorption in Carbonate Reservoirs." SPE Reservoir Engineering Journal: 117-122.

Thomas, M. M., J. A. Clouse, et al. (1993a). "Adsorption of Organic Compounds on Carbonate Minerals 1. Model Compounds and Their Influence on Mineral Wettability." Chemical Geology **109**: 201-213.

Torsaeter, O. (1984). An Experimental Study of Water Imbibition in Chalk From the Ekofisk Field. Paper SPE 12688 presented at the SPE Improved Oil Recovery Symposium held in Tulsa, OK, USA.

Treiber, L. E., D. L. Archer, et al. (1972). "A Laboratory Evaluation of the Wettability of Fifty Oil Producing Reservoirs." SPE Journal **253**: 531-540.

Treiber, L. E., D. L. Archer, et al. (1972). "A Laboratory Evaluation of the Wettability of Fifty Oil Producing Reservoirs." SPE Journal **253**(December): 531-540.

Trogus, F. J., R. S. Schechter, et al. (1979). "A New Interpretation of Adsorption Maxima and Minima." Journal of Colloid and Interface Science **70**: 293-305.

Wagner, O. R. and R. O. Leach (1959). "Improved Oil Displacement Efficiency by Wettability Adjustment." Petroleum Transactions AIME **216**: 65-72.

Wardlaw, N. C., M. S. J. Chilingarian, et al. (1996). Factors affecting oil recovery from carbonate reservoirs and prediction of recovery. New York, Elsevier.

Watney, L. (2006). Location map of Hall-Gurney Field on map of Lansing-Kansas City oil production in Kansas. http://www.searchanddiscovery.net/documents/06093watney/images/01.htm.

Web Page. "www.jimseven.com/2006/06/13/foams/." Retrieved October 2008, 2008.

Xie, X. and N. R. Morrow (2000). "Contact Angles on Quartz Induced by Adsorption of Heteropolar Hydrocarbons." Journal of Adhesion and Science Technology **13**(10): 1119-1135.

Xie, X., N. R. Morrow, et al. (2000). Contact Angles Hysteresis and the Stability of Wetting Changes Induced by the Adsorption from Crude Oil Paper presented at the 6th International Symposium on Reservoir Wettability and Its Effect on Oil Recovery held in Socorro, NM,USA.

Young, T. (1805). Philosophical Transactions, Royal Society London.

Zhou, X., O. Torsaeter, et al. (1993). The Effect of Crude-oil Aging Time and Temperature on the Rate of Water Imbibition and Long-term Recovery by Imbibition. Paper SPE 26674 presented at the SPE Annual Technical Conference and Exhibition held in Houston, TX, USA.

Ziegler, V. M. and L. L. Handy (1981). "Effect of Temperature on Surfactant Adsorption in Porous Media." SPE Journal.